

**ANALYSIS OF YTTRIA-STABILISED ZIRCONIA AND
ALUMINIUM SILICATE COATED PISTON CROWN ON THE
ENGINE PERFORMANCE WITH PALM BIODIESEL**

NAVIN A/L RAMASAMY

**FACULTY OF ENGINEERING
UNIVERSITI MALAYA
KUALA LUMPUR
2022**

ANALYSIS OF YTTRIA-STABILISED ZIRCONIA AND
ALUMINIUM SILICATE COATED PISTON CROWN ON THE
ENGINE PERFORMANCE WITH PALM BIODIESEL

NAVIN A/L RAMASAMY

THESIS SUBMITTED IN FULFILMENT OF THE
REQUIREMENT FOR THE DEGREE OF
DOCTOR OF PHILOSOPHY

FACULTY OF ENGINEERING
UNIVERSITI MALAYA
KUALA LUMPUR

2022

UNIVERSITY OF MALAYA

ORIGINAL LITERARY WORK DECLARATION

Name of Candidate: **Navin A/L Ramasamy**

Registration/Matric No: **KHA130122**

Name of Degree: **Doctor of Philosophy**

Title of Thesis: **ANALYSIS OF YTTRIA-STABILISED ZIRCONIA AND ALUMINIUM SILICATE COATED PISTON CROWN ON THE ENGINE PERFORMANCE WITH PALM BIODIESEL**

Field of Study: **Energy**

I do solemnly and sincerely declare that:

- (1) I am the sole author/writer of this work;
- (2) This work is original;
- (3) Any use of any work in which copyright exists was done by way of fair dealing and for permitted purposes and any excerpt or extract from, or reference to or reproduction of any copyrighted work has been disclosed expressly and sufficiently and the title of the Work and its authorship have been acknowledged in this work;
- (4) I do not have any actual knowledge, nor do I ought reasonably to know that the making of this work constitutes an infringement of any copyrighted work;
- (5) I hereby assign all and every right in the copyright to this Work to the University of Malaya (UM), who henceforth shall be owner of the copyright in this Work and that any reproduction or use in any form or by any means whatsoever is prohibited without the written consent of UM having been first had and obtained;
- (6) I am fully aware that if in the course of making this work, I have infringed any copyright whether intentionally or otherwise, I may be subject to legal action or any other action as may be determined by UM.

Candidate's Signature

Date:

Subscribed and solemnly declared before,

Witness's Signature

Date:

Name:

Designation:

ABSTRACT

In this study, the effects of thermal barrier coatings (TBC) with yttria-stabilised zirconia ($Y_2O_3.ZrO_2$) and aluminium silicate ($Al_2O_3.SiO_2$) with NiCrAl bond coatings on the engine performance and emission were evaluated using conventional diesel and pure palm oil biodiesel. These materials were coated on the piston crown using plasma spray coating. The findings demonstrated that $Y_2O_3.ZrO_2$ coatings presented better engine performances in terms of brake thermal efficiency (BTE), and brake specific fuel consumption (BSFC) for both fuels, which was much better than $Al_2O_3.SiO_2$ coatings. The piston with $Y_2O_3.ZrO_2$ -coated materials (P2D & P2B) achieved the highest BTE (15.94% for P2D, 14.55% for P2B), and lowest BSFC (498.96 g/kWh for P2D, 619.81 g/kWh for P2B). However, $Al_2O_3.SiO_2$ coatings indicated better emissions with the lower NO, CO, and CO_2 emissions for both fuel. It recorded the lowest HC emission due to complete combustion of the fuel in the engine. Hence, it was concluded that the $Y_2O_3.ZrO_2$ coating could lead to better engine performance. At the same time, $Al_2O_3.SiO_2$ showed promising low emissions in the first phase. TBC was prepared using a series of mixtures consisting of different blend ratios of $Y_2O_3.ZrO_2$ and $Al_2O_3.SiO_2$ via plasma spray coating. The experimental results showed that a TBC mixture with 60% $Y_2O_3.ZrO_2$ + 40% $Al_2O_3.SiO_2$ had excellent NO and CO reductions compared to the other blend coated pistons. The findings also indicated that the coating mixture with 50% $Y_2O_3.ZrO_2$ + 50% $Al_2O_3.SiO_2$ had the highest BTE and lowest BSFC compared to all other blend coatings. Blends coated with 50% $Y_2O_3.ZrO_2$ + 50% $Al_2O_3.SiO_2$ had the highest performance, lowest emission, and highest durability for the diesel engine application. These encouraging findings further proved the significance of TBCs in terms of enhancing the engine performance and emission reductions operated with different types of fuels.

Keyword: TBC, $Y_2O_3.ZrO_2$, $Al_2O_3.SiO_2$.

ABSTRAK

Dalam kajian ini, kesan salutan penebat termal (TBC) dengan zirkonia stabil yttria ($Y_2O_3.ZrO_2$), dan aluminium silikat ($Al_2O_3.SiO_2$) bersama dengan salutan ikatan NiCrAl terhadap prestasi enjin, dan pelepasan kandungan asap dinilai dengan menggunakan diesel konvensional dan biodiesel minyak sawit tulen. Bahan-bahan ini disalut pada aloi ombok melalui salutan penyembur plasma. Hasil kajian menunjukkan bahawa salutan $Y_2O_3.ZrO_2$ menghasilkan prestasi enjin yang lebih baik, dari segi BTE dan BSFC, berbanding dengan $Al_2O_3.SiO_2$. Piston bersalut $Y_2O_3.ZrO_2$ (P2D & P2B) mencapai BTE tertinggi (15.94% untuk P2D, 14.55% untuk P2B), dan BSFC mencapai angka yang terendah (498.96 g/kWh untuk P2D, 619.81 g/kWh untuk P2B). Justeru, salutan $Al_2O_3.SiO_2$ menunjukkan pelepasan NO, HC dan CO yang terendah untuk diesel dan biodiesel. Justifikasinya, salutan $Y_2O_3.ZrO_2$ menghasilkan prestasi enjin yang baik, sementara $Al_2O_3.SiO_2$ menunjukkan pengurangan dari segi pelepasan gas. Dalam fasa kedua eksperimen, TBC dihasilkan dengan menggunakan nisbah campuran $Y_2O_3.ZrO_2$ dan $Al_2O_3.SiO_2$ yang berbeza. Hasil eksperimen menunjukkan campuran TBC yang disalut dengan 60% $Y_2O_3.ZrO_2$ + 40% $Al_2O_3.SiO_2$ mempunyai kurang NO dan CO. Ini merupakan aspek yang sangat baik berbanding dengan TBC yang lain. Selain itu, kajian menunjukkan bahawa campuran salutan 50% $Y_2O_3.ZrO_2$ + 50% $Al_2O_3.SiO_2$ mempunyai BTE tertinggi, dan BSFC terendah, berbanding dengan semua salutan campuran yang lain. Salutan 50% $Y_2O_3.ZrO_2$ + 50% $Al_2O_3.SiO_2$ dipilih sebagai salutan yang optimum untuk penggunaan dalam injin diesel, untuk prestasi injin yang tinggi, pelepasan gas yang rendah, dan untuk penggunaan yang tahan lasak. Penemuan ini telah membuktikan betapa pentingnya TBC dalam usaha untuk meningkatkan prestasi injin, dan pengurangan pelepasan gas dengan pelbagai jenis bahan bakar.

Kata kunci: TBC, $Y_2O_3.ZrO_2$, $Al_2O_3.SiO_2$.

ACKNOWLEDGEMENT

I'm very grateful to God for the completion of this project. Firstly, I would like to express my highest gratitude to Prof. Dr Md. Abul Kalam and Dr Mahendra Varman as my project supervisors for their guidance, advice, and support, which enabled me to complete this project. I sincerely appreciate their support, bright ideas, professional guidance, encouragement, and valuable suggestions, which helped me complete this project.

I would also like to express my appreciation to all who contributed toward this research project, as well as the Faculty of Engineering and the Department of Graduate Studies, for supporting me with the required information and guidance necessary to write the thesis.

Last, but not least, I would like to thank my wife, Revathi Kaliappan for supporting this project. She never gave up and pushed me to stay motivated during my toughest moments.

Thank you, I love all of you.

TABLE OF CONTENT

Abstract	iii
Abstrak	iv
Acknowledgements	v
Table of contents	vi
List of figures	x
List of tables	xiii
Nomenclatures	xv
Abbreviations	xvi
CHAPTER 1: INTRODUCTION	
1.1 Overview	1
1.2 Research gaps	9
1.3 Research objective	11
1.4 Research novelty and contribution	11
1.5 Scope of study	13
1.6 Limitation of study	13

CHAPTER 2: LITERATURE REVIEW

2.1	Introduction	14
2.2	Piston geometry	15
2.3	Plasma spray method	16
2.4	Durability TBC	17
2.5	Coating thickness	18
2.6	Conventional & commercialize TBC	20
2.7	Blend and mix TBC	36
2.8	Palm oil methyl ester as biodiesel	44
2.9	Summary	47

CHAPTER 3: RESEARCH METHODOLOGY

3.1	Introduction	48
3.2	Research flow chart	49
3.3	Morphological characteristic of TBC	50
3.4	Equipment setup	56

3.5	Engine performance analysis	66
3.5.1	BSFC and BTE	66
3.5.2	Brake power	67
3.5.3	BTE	67
3.5.4	Exhaust emission analysis	68
3.5.5	Exhaust gas analyser	68
3.6	Statistically significance value	69
CHAPTER 4: RESULTS AND DISCUSSION		
4.1	Introduction	71
4.2	First phase: conventional TBC	71
4.2.1	Exhaust emission analysis	72
4.2.2	Engine performance analysis	84
4.2.3	Condition of piston crown after 6 hours engine operation	93
4.2.4	Summary	96

4.3	Second phase: blend TBC	99
4.3.1	Exhaust emission analysis	100
4.3.2	Engine performance analysis	110
4.3.3	Condition of piston crown after 6 hours engine operation	119
4.3.4	Summary	125
4.4	Cost compression analysis	131
CHAPTER 5: CONCLUSIONS AND RECOMMENDATION		
5.1	Conclusion	133
5.2	Recommendation	135
	References	136
	List of publications	153

LIST OF FIGURES

Figure 1.1	Energy transition maturity curve (Monzon et al., 2018)	2
Figure 1.2	Global primary energy demand by fuel (Cloete, 2019)	3
Figure 1.3	World oil demand by region (International; Energy Agency (IEA), 2019)	4
Figure 1.4	World energy demand, 2019 and 2030 (World Energy Outlook, 2020)	5
Figure 1.5	Better batteries (BloombergNEF (BNEF), 2019)	6
Figure 1.6	The energy trilemma (World Energy Council (WEC), 2019)	9
Figure 2.1	Basic process of thermal spray coating (Manoj et al., 2021)	16
Figure 2.2	Number of cycles for first and second architecture of topcoat samples flame rig test	17
Figure 2.3	Coating thickness (Manoj et al., 2021)	19
Figure 2.4	Layers of TBC (Godiganur, 2021)	20
Figure 2.5	Production of annona oil methyl ester	25
Figure 2.6	Variation in power and torque of baseline engine and TBC engine under different load conditions (Sivakumar & Senthil Kumar, 2014)	27
Figure 2.7	Silicon carbide metal foam (Saravanan, et al., 2020)	40

Figure 3.1	Schematic representation of the research methodology	49
Figure 3.2	SEM photomicrographs (1000X of magnification) of $\text{Al}_2\text{O}_3\cdot\text{SiO}_2$ powder morphology	51
Figure 3.3	SEM photomicrographs (1000X of magnification) of $\text{Y}_2\text{O}_3\cdot\text{ZrO}_2$ powder morphology	52
Figure 3.4	Plasma spray coating	53
Figure 3.5	TBC layer on piston	54
Figure 3.6	Piston crown configuration with specific coating mixture	54
Figure 3.7	Piston coated with (a) $\text{Y}_2\text{O}_3\cdot\text{ZrO}_2$ and (b) $\text{Al}_2\text{O}_3\cdot\text{SiO}_2$	55
Figure 3.8	Complete setup of experiment	57
Figure 3.9	Dynamometer setup of experiment (Focus Applied Technologies, 2017)	58
Figure 3.10	Engine setup for the experiment	59
Figure 3.11	Kubota RT-125 diesel engine	60
Figure 3.12	Controller setup & data collection	61
Figure 3.13	BOSCH BEA-350 exhaust gas analyser	69
Figure 4.1	HC emission at the variable engine speed	72
Figure 4.2	NO emission at the variable speed	75

Figure 4.3	Staged combustion concept	79
Figure 4.4	CO emission at variable speed	80
Figure 4.5	CO ₂ emission at variable speed	83
Figure 4.6	Power (kW) produced at variable speed	85
Figure 4.7	Torque (Nm) produced at variable speed	87
Figure 4.8	BSFC at variable speed	89
Figure 4.9	BTE at variable speed	91
Figure 4.10	HC emission for blended coat	100
Figure 4.11	NO emission for blended coat at the variable speed	103
Figure 4.12	CO emission	105
Figure 4.13	CO ₂ emission	108
Figure 4.14	Power (kW) produced at various engine speed	111
Figure 4.15	Engine torque at various engine speed	113
Figure 4.16	BSFC at various engine speed	115
Figure 4.17	BTE percentage at various engine speed	117

LIST OF TABLES

Table 1.1	List of GHGs and their global warming potential. Intergovernmental panel on climate changes	7
Table 2.1	TBC thermal characteristic	21
Table 2.2	Summary of TBC performance and emission characteristic	34
Table 2.3	Coating layer properties	42
Table 3.1	$\text{Al}_2\text{O}_3\cdot\text{SiO}_2$ material characteristic	51
Table 3.2	$\text{Y}_2\text{O}_3\cdot\text{ZrO}_2$ material characteristic	52
Table 3.3	TBC working parameters	53
Table 3.4	List of the TBC	56
Table 3.5	Specification of a single cylinder Kubota RT125 diesel engine in heat engine laboratory, department of mechanical engineering, University of Malaya	59
Table 3.6	Physicochemical properties of the tested fuels, diesel	63
Table 3.7	Physicochemical properties of the tested fuels, palm oil methyl ester	64
Table 3.8	Fatty acid composition of palm oil methyl ester	65
Table 3.9	List of measurement accuracy and percentage uncertainties	70

Table 4.1	Comparison between conditions of piston crown after running 6 hours	94
Table 4.2	Summary of the first phase of the engine performance	96
Table 4.3	Summary of the first phase of the emission analysis	97
Table 4.4	Summary of the first phase of the durability studies	98
Table 4.5	Piston selection for the first phase of the research work	98
Table 4.6	Comparison between conditions of piston crown after running 6 hours	120
Table 4.7	Summary of the second phase of the engine performance	125
Table 4.8	Summary of the second phase of the emission analysis	127
Table 4.9	Summary of the second phase of the durability studies	129
Table 4.10	Piston selection of the second phase of the research work	130
Table 4.11	Comparison between uncoated and selected blend coated piston	130
Table 4.12	Raw material cost of $\text{Al}_2\text{O}_3\cdot\text{SiO}_2$ and $\text{Y}_2\text{O}_3\cdot\text{ZrO}_2$	131

NOMECLATURES

BMEP	Brake Mean Effective Pressure	MPa
BSFC	Brake Specific Fuel Consumption	g/kWhr
BTE	Brake Thermal Efficiency	%
CA	Crank Angle	-
EGR	Exhaust Gas Recirculation	%
EGT	Exhaust Gas Temperature	°C
HRR	Heat Release Rate	J/°CA
Hz	Hertz	s ⁻¹
ID	Ignition Delay	°CA
IMEP	Indicated Mean Effective Pressure	MPa
IT	Injection Timing	°CA

Universiti Malaysia

ABBREVIATIONS

ASTM	American Society for Testing and Materials
ATDC	After Top Dead Center
Al ₂ O ₃ .SiO ₂	Aluminium Silicate
CFD	Computational Fluid Dynamics
CI	Compression Ignition
CN	Cetane Number
CO	Carbon Monoxide
CO ₂	Carbon Dioxide
COV	Coefficient of Variance
CR	Compression Ratio
DI	Direct Injection
ECU	Engine Controller Unit
EGR	Exhaust Gas Recirculation
EGT	Exhaust Gas Temperature
EN	European Standards
EU	European Union
FAME	Fatty Acid Methyl Ester
GDP	Gross Domestic Product
GHG	Greenhouse Gas
HC	Hydrocarbon
HCCI	Homogenous Charge Compression Ignition
HCDC	Homogenous Charge Diesel Combustion
HRR	Heat Release Rate
ID	Ignition Delay
IEA	International Energy Agency
IT	Injection Timing
LPG	Liquefied Petroleum Gas
NO	Nitrogen Oxide
O ₂	Oxygen
Pa	Pascal
PAH	Polycyclic Aromatic Hydrocarbon
PI	Port Injection
PM	Particulate Matter
POME	Palm Oil Methyl Ester
RCCI	Reactivity Controlled Compression Ignition
RON	Research Octane Number
rpm	Revolution per Minute

SI	Spark Ignition
SO ₂	Sulfur Dioxide
TDC	Top Dead Center
TBC	Thermal Barrier Coating
VCR	Variation of Compression Ratio
VVT	Variable Valve Timing
WOT	Wide Open Throttle
Y ₂ O ₃ .ZrO ₂	Yttria Stabilized Zirconia

Universiti Malaya

CHAPTER 1

INTRODUCTION

1.1 Overview

The depletion of natural fuel sources have become a major concern, as drilling technologies have become more challenging and costly. From conventional drilling to ultra-high deep-water drilling technologies, the exploration efforts have branched out from shallow water to arctic deep-water drilling. The supply and demand scenario however has been moving in the opposite direction; when the supply is higher than the demand, the oil prices hit rock bottom. The impact is favourable to the consumers. Still, on the other hand, the adverse effects include retracement of employees, downsizing of businesses, and lay off of small oil producers. Oil producers need to be more agile and compete much better to survive. Figure 1.1 depicts the recovery of oil prices from the pre-1900s discovery era, and the mandatory enforcement of electric vehicles in 2050.

Energy Transition Maturity Curve⁷



Figure 1.1: Energy Transition Maturity Curve (Monzon, et al., 2018)

But this storm should not be taken for granted, because it deals with a continuous supply for the next generation. Petroleum or natural resources such as crude oil, natural gases, and coal will not be replenished, as the consumption rate is higher. This will deplete the reserves. Without any effort for preserving or finding an alternative source of energy, this may result in a difficulty to meet energy demands, as depicted in Figure 1.1.

Global Primary Energy Demand by Fuel

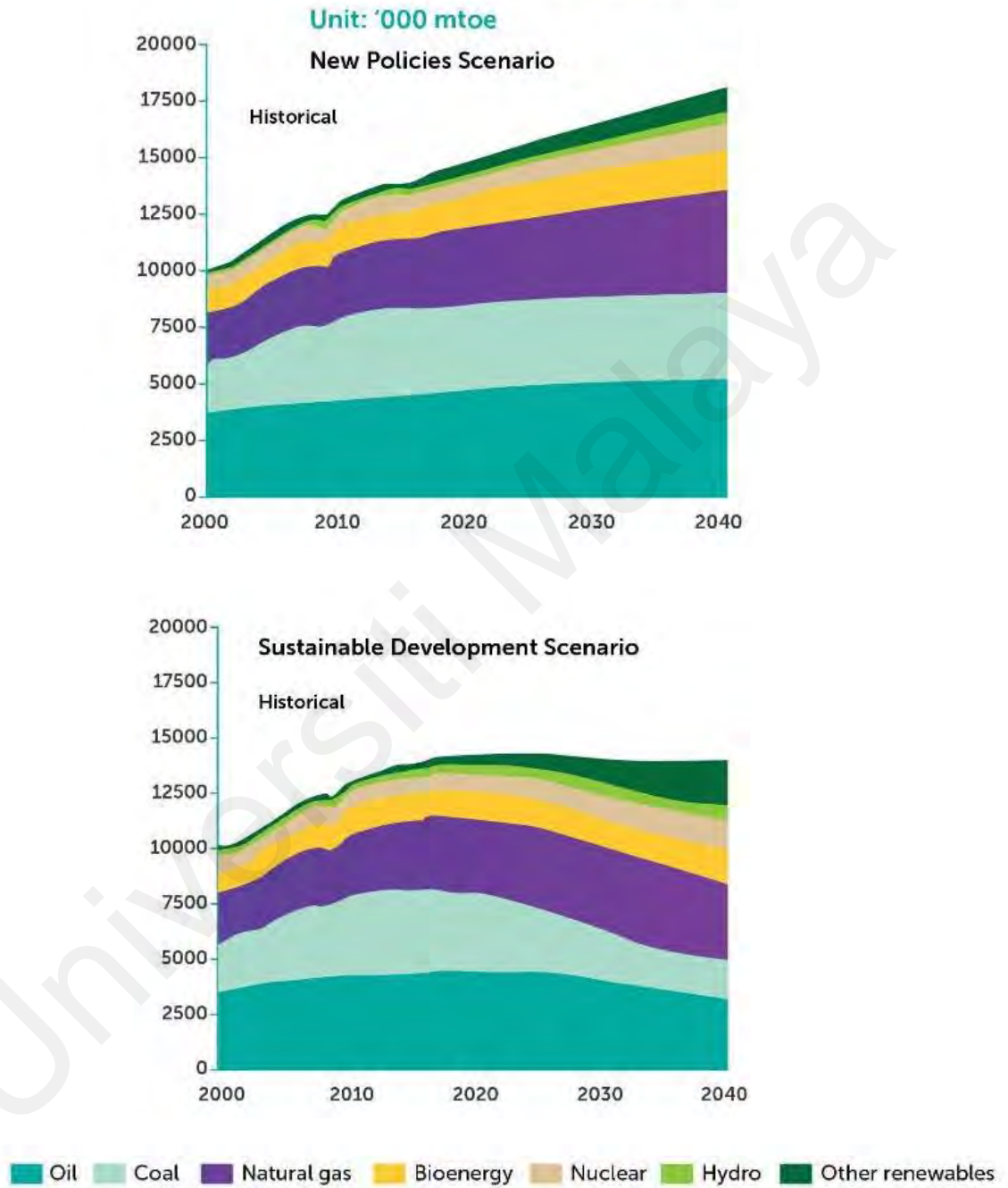


Figure 1.2: Global Primary Energy Demand by Fuel (Cloete, 2019)

Biodiesel, vegetable oil, cottonseed oil, and various other blending technologies need to be further explored. This will help to improve and enhance green energy production, provide better performances, enhance cost-saving, and most importantly, deliver safety to human beings. Collaborative discoveries are crucial in this research area. Figure 1.2 illustrates that the reduction of conventional fuel consumption for vehicles will not end the oil and gas business. However, traditional resources such as coal and oil will significantly impact the rise in renewable energy. Oil is still required beyond the energy utilization cut off point, as oil is needed as feedstock for petrochemical processing plants, with a 4-5% yearly growth.

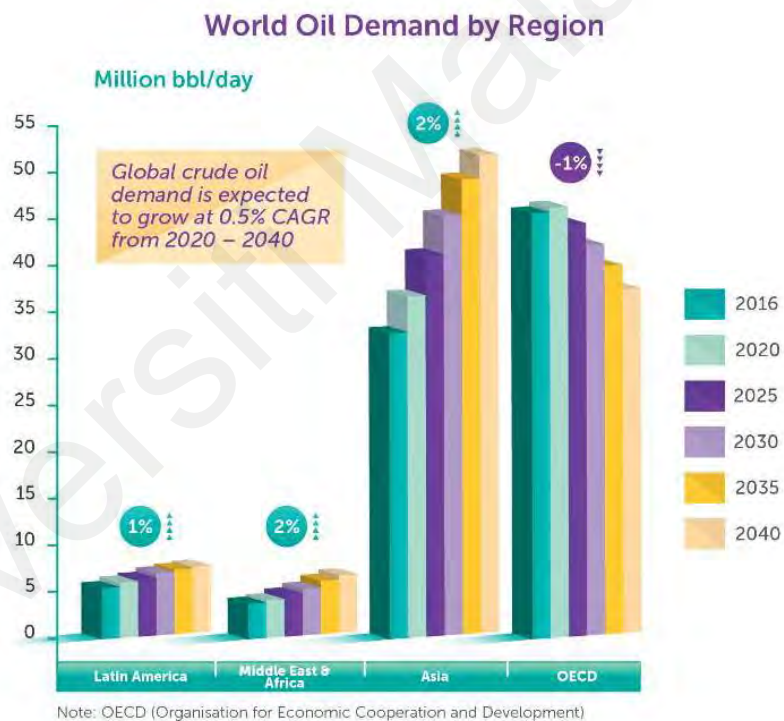


Figure 1.3: World Oil Demand by Region (International; Energy Agency (IEA), 2019)

Oil and gas will continue to be a major supply element for the next 10 years, supporting almost 50% of the global energy demand, as shown in Figure 1.3. However, renewable energy will be the fastest growing energy source which will be able to meet the low carbon requirements.

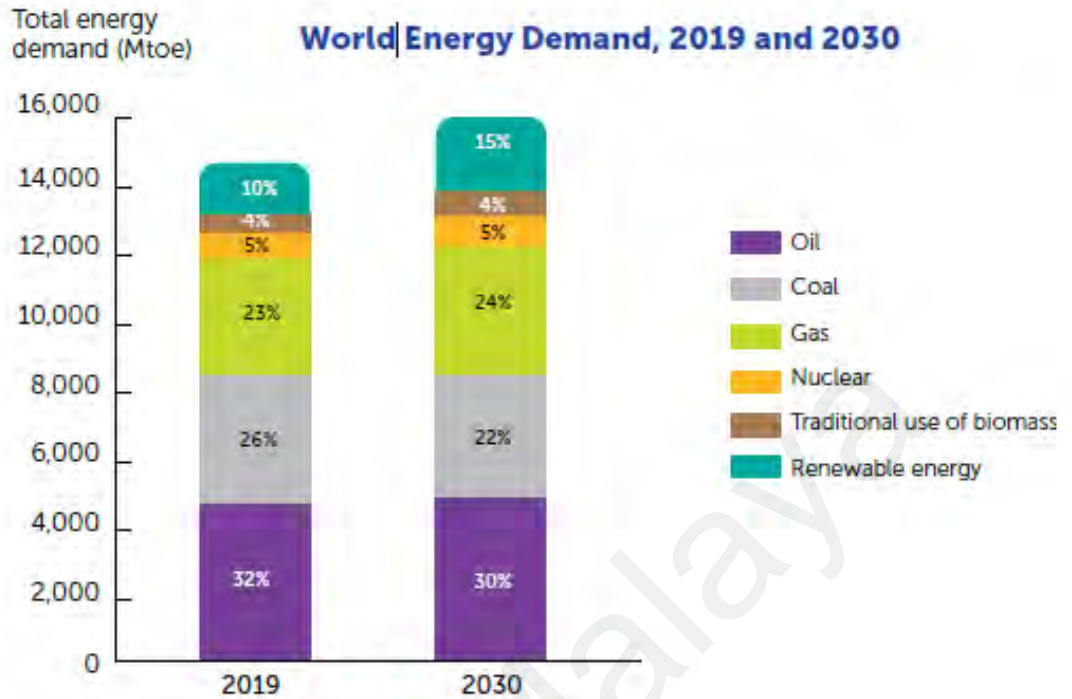


Figure 1.4: World Energy Demand, 2019 and 2030 (World Energy Outlook, 2020)

The increase in an electric vehicle production and use is correlated to the reduction in the cost of batteries, and increased energy density trends over the past decade, as shown in Figure 1.4, which shows signs of meeting the ambitious targets set by car manufacturers such as Tesla, and GM. However, renewable and alternative energy will remain relevant to support heavy machinery and vehicle operations in the future. Furthermore, the application of TBC can be used in large pistons such as in Ship, bunkers, barges, and so on.

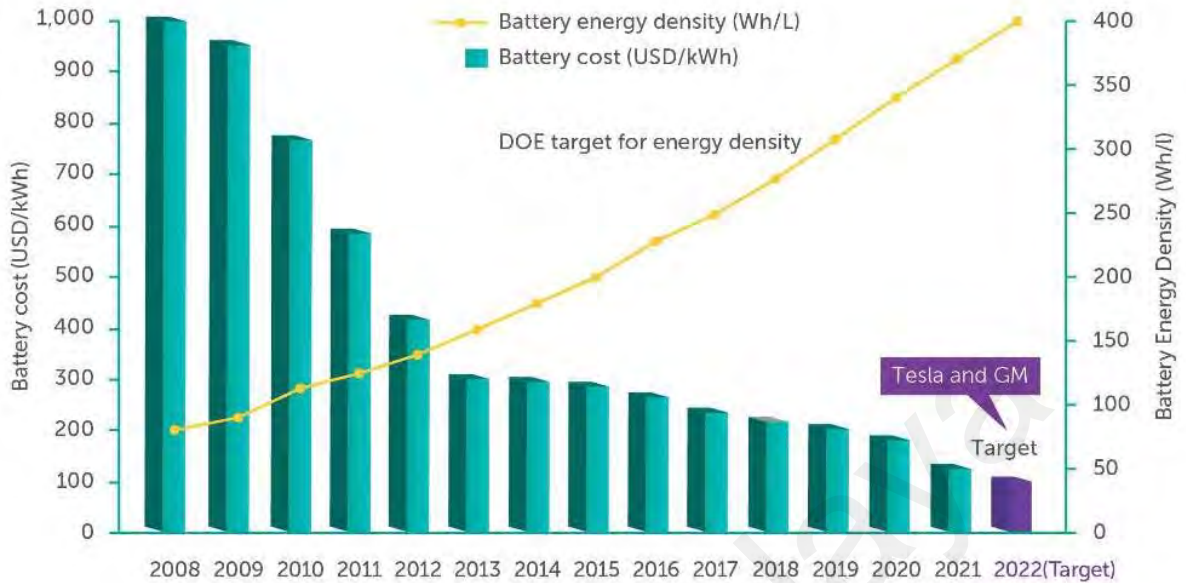


Figure 1.5: Better Batteries (BloombergNEF (BNEF), 2019)

One of the most common problems for vegetable oil is its lower calorie value, which leads to a higher demand in the combustion chamber to be able to achieve the same power as that of the diesel fuel. The oxygen content in the biofuel tends to increase the amount of NO_x produced compared to conventional fuels. Biodiesel has a downside, with its higher viscosity and lower calorie values, where more fuel is required to be burned to achieve the same performance as that of conventional fuels. Furthermore, higher oxygen content in vegetable oils typically contributes to higher NO_x numbers. Generally, the reduction of NO_x may be achieved by introducing TBC, modifying the geometry of the piston's crown, the mixture of fuels, and so on. Ultimately the reduction of NO_x will reduce the GHG elements, as shown in Table 1.1.

Table 1.1: List of GHGs and their global warming potential. Intergovernmental Panel on Climate Changes)

GHG	Chemical Formula	GWP ₁₀₀
Carbon Dioxide	CO ₂	1
Methane	CH ₄	25
Nitrous Oxide	N ₂ O	298
Hydrofluorocarbons	HFC ₅	12 - 14,800
Perfluorocarbons	PFC ₅	7,390 - 12,200
Sulphur Hexafluoride	SF ₆	22,800
Nitrogen Trifluoride	NF ₃	17,200

Blended fuel has the limitation of quantum to blends with petroleum fuel. To achieve greater heights, the effort should be different from the traditional means, whereby instead of adding additives in the fuel, one needs to explore the improvements in the geometry of an engine, or the coating technology in the combustion engine, as part of the relationship between the mechanical parts and the fuel, which can be defined as “liquid to the metal”, as themed by the PETRONAS AMG Mercedes Formula One car.

The piston bowl plays an essential role in facilitating the mixing of air and fuel within the combustion chamber, hereby increasing the thermal efficiency in the combustion chamber. The bowl of the piston provides better mixing between fuel and air. For direct injection, the Deep Toroidal Bowl Piston Type is fabricated to have a better and faster swirl of air intake with proper mixture ratios, better firing, complete burns, and an improvement of 3-5% in the torque value.

Coating technologies can improve green technologies with improvements in the BSFC and reducing some of the emission and smoke opacity. TBC is a common term given in the industry to describe coating advantages in terms of improving the thermal efficiency. The target area should be the combustion chamber, including the piston, piston ring, the intake, and exhaust valves, to be able to marry the fuel performance and coating. The coating has its advantages, and this depends on the target area of the coating and the material itself. Typically, the coating is divided into two functions; reducing the wear and friction, or improving the thermal efficiency. The results of the coated engines were better than the uncoated ones in terms of the cylinder's gas pressure, heat release rate, and heat release itself. The TBC for the piston crown is commonly made of ceramic material. Lots of attention has been given to stabilized zirconia with various components, such as Yttria-partially-stabilized zirconia (YPSZ), partially stabilized zirconium (PSZ), Yttria stabilized zirconia ($Y_2O_3.ZrO_2$), magnesia-stabilized zirconia (MSZ), PEO ($Al_2O_3.ZrO_2.SiO_2$). These ceramic coatings were tested in a diesel engine with Pongamia oil, cottonseed oil, blend of crude Jatropha oil, carburate oil, and diesel oil, which led to significant improvements in the thermal efficiency.

Optimum green fuel compositions, with highly engineered geometries of the piston crown, and excellent candidates of TBC coatings, could contribute toward better thermal efficiency, lower emissions, and lower fuel consumption, than conventional fuels in the market. The benchmark for research can be consider by referring to the approach of The Energy Trilemma (Energy Affordability), as shown in figure 1.6. The Energy Trilemma illustrates what a country needs to consider towards avoiding potential environmental harm. The three dimensions provide valuable insights on the energy transition using The Energy Trilemma,

which acts as a compass to navigate across different policies, political goals, and new alternative energies, and so on. All resources have supply insecurity issues, needs to be continuous, and needs to be sustainable in terms of supplying in the long run. It should also be affordable to ensure it meets the market requirements.



Figure 1.6: The Energy Trilemma (World Energy Council (WEC), 2019)

1.2 Research Gaps

Typically, the TBC of $Y_2O_3.ZrO_2$ is most used in industry for its proven engine performance and low emission for the diesel engine. However, this TBC is too expensive, and it is rare. It is also rare that a commercially available single cylinder diesel engine would be equipped with a TBC of $Y_2O_3.ZrO_2$ due to the high cost of the application. Additionally, the TBC of $Al_2O_3.SiO_2$ offers many advantages, including in terms of improvement in the thermal efficiency, fuel economy, and cleanliness of the exhaust emissions, compared to an uncoated piston, as a substitute to the TBC of the $Y_2O_3.ZrO_2$.

Thus, its introduction in a single-cylinder diesel engine should be an interesting idea, as it is a much cheaper alternative than TBCs of the $Y_2O_3.ZrO_2$. Furthermore, the TBC of $Al_2O_3.SiO_2$ offers the possibility to reduce smoke and NO_x emissions. Therefore, this study focuses on the investigation of TBC parameters against the baseline diesel on a single-cylinder engine test. It is known that the TBC of the $Y_2O_3.ZrO_2$ performs better than the TBC of the $Al_2O_3.SiO_2$. However, the TBC of the $Al_2O_3.SiO_2$ is much more commercially cheaper and a much more attractive solution.

This would involve the development of a blend of TBCs from $Al_2O_3.SiO_2$ and $Y_2O_3.ZrO_2$ whereby the performance of the existing $Al_2O_3.SiO_2$ will be enhanced by adding more blended percentages of $Y_2O_3.ZrO_2$ to match 100% of the TBC of the $Y_2O_3.ZrO_2$ to obtain a performance with cheaper solution for research studies. The developed blend of TBC must be able to provide flexible installation and an application to meet the desired outcome. Theoretically, NO values will increase with the increase of heat in combustion chamber. Hence, for this experiment, the coating needs to be done on the piston crown to reduce the NO emission, as the heat will be contained partially to reduce the temperature in the combustion chamber. In global markets, alternative fuels explored and analysed in the context of coating are Pongamia oil, cottonseed oil, crude jatropha oil, frying oil, and so on. Since Malaysia is one of the biggest producers of crude palm oil globally, the intention is to leverage a crude palm oil base, and adopt it as a palm oil methyl ester, to be applied in the diesel engine. Despite biodiesels having a downside with its higher viscosity, lower calorie values, and higher oxygen content which contributes toward a higher NO, the TBC is expected to reduce the NO with an improved thermal efficiency.

Hence, this study would help establish a good starting point for the B100 palm biodiesel used in the diesel engine research in Malaysia, specifically dealing with the newest and most promising approach of the TBC blend coat. Likewise, the B100 palm biodiesel has been established as a renewed interest due to its low pollution and renewable resources, in contrast to the petroleum resources. Therefore, this research study focuses on the application of the B100 palm biodiesel as an alternative energy source for engines operating in the selected blend of the TBC coated piston.

1.3 Research objectives

The objective of this experiment is defined as follows:

- i. To characterize the piston's surface coating using the thermal barrier $Y_2O_3.ZrO_2$ and $Al_2O_3.SiO_2$.
- ii. To evaluate the engine's thermal efficiency and emission characteristics using the Palm Biodiesel with uncoated and coated $Y_2O_3.ZrO_2$ and $Al_2O_3.SiO_2$ materials, with different percentages.
- iii. To analyse the cost-effectiveness for the industrial commercial CI Engine application using coating materials.

1.4 Research novelty and contribution

The original contribution of the present study includes the development of various key experimental setups, engine performance, emissions, and combustion characteristics of the diesel and biodiesels fuels in the diesel combustion engine using TBCs.

Furthermore, this study also offers a better understanding of the performance of the TBC in an engine with various promising NO_x reduction strategies, such as a blend of TBC and palm biodiesel fuelled engine. The summary for contributions of the present research are as follows:

1. Develop a pioneer experimental setup using the Kubota RT 125 diesel engine research in the University of Malaya.
2. Explore the impact of the TBC Y₂O₃.ZrO₂ and Al₂O₃.SiO₂ on the diesel and biodiesel engine performance, emissions, and combustion characteristics.
3. Explore the impact of the blend coated between the TBC of Y₂O₃.ZrO₂ and Al₂O₃.SiO₂ on the diesel and biodiesel engine performance, emissions, and combustion characteristics.
4. Establish a good starting point for the blend of TBC research in Malaysia, especially dealing with the newest and most promising approaches of blended TBC, which has the potential to generate savings.

From the outcome of this study, two numbers of research papers have been published in a high impact international journal. The publication list is presented in Appendix A.

1.5 Scope of study

- i. The fuel used for these studies were Palm Biodiesel (100%) and Diesel.
- ii. Preparation of 8 samples of pistons starting with the uncoated piston (P1D & P1B), 100% $Y_2O_3.ZrO_2$ coated piston (P2D & P2B), 100% $Al_2O_3.SiO_2$ (P3D & P3B) coated piston, coated 90% $Y_2O_3.ZrO_2$ + 10% $Al_2O_3.SiO_2$ (P4D & P4B), coated 80% $Y_2O_3.ZrO_2$ + 20% $Al_2O_3.SiO_2$ (P5D & P5B), coated 70% $Y_2O_3.ZrO_2$ + 30% $Al_2O_3.SiO_2$ (P6D & P6B), coated 60% $Y_2O_3.ZrO_2$ + 40% $Al_2O_3.SiO_2$ (P7D & P7B) and coated 50% $Y_2O_3.ZrO_2$ + 50% $Al_2O_3.SiO_2$ (P8D & P8B).
- iii. The exhaust emission gases which were investigated were CO, CO₂, NO and HC.

1.6 Limitation of study

- i. The maximum load that the engine can run with an acceptable vibration is at the lowest speed of 1200 rpm. Due to safety reasons, operating lower than 1200 rpm was not recommended. The maximum speed tested was up to 2400 rpm as per the OEM recommendation.
- ii. The lubricity characteristics for the coating material was not evaluated. The durability test was not performed. The studies were limited to the effects of the TBC in the engine's performance & emissions.

CHAPTER 2

LITERATURE REVIEW

2.1 Introduction

There has been continuous improvement in the combustion chemistry and desired combustion products over the years. For instance, discovering alternative liquid fuels has been one of the optimum solutions to improve combustion. The combustion chamber's geometrical or mechanical (metal) aspects should be critically considered to achieve a better performance and less emission. Based on the literature, better combustion chemistry can be achieved through the perfect bonding between the metal and liquid. Malaysia is generally regarded as one of the world's primary producers of palm oil. Palm oil has been identified as one of Malaysia's most reliable sources of alternative fuels. Numerous matured palm oil biodiesel factories in Malaysia have been operating successfully, and have managed to sell their products to local and global users (Oguma *et al.*, 2011; Johari *et al.*, 2015). The use of palm biodiesel in the compression ignition (CI) engine typically reduces thermal efficiency, unburnt HC, and CO. It increases specific fuel consumption and NO (Gad *et al.*, 2018). In the CI engine, a piston bowl significantly influences the mixing of fuel and air. In the direct injection CI engine, pistons of deep toroidal bowl types provide a better and faster swirl of air intake with a proper mixing ratio, better firing, and complete burns. It improves the torque value by 3% to 5%. Based on the simulation results, the toroidal bowl piston was found to reduce the engine's BSFC (da Silva *et al.*, 2017). Coating technologies have a way of enhancing green technologies with proven results in terms of improvement in the BSFC and lower emissions, as well as the smoke opacity (Sivakumar *et al.*, 2014). The TBC is a

common term in the industry that describes the coating advantages for improved thermal efficiencies. The coating advantages depend on the target coating areas and the materials. Two typical coating functions are to reduce wear or improve the thermal efficiency.

The TBC of the piston crown is commonly made of ceramic material. Still, most studies have focused on stabilised zirconia with various compositions, such as zirconia oxide (ZrO_2) (Bahatin, 2016), partially stabilised zirconium (PSZ), yttria-stabilised zirconia (YSZ) (Sivakumar et al., 2014), magnesia-stabilised zirconia (MSZ) (Cerit and Coban, 2014), and PEO ($Al_2O_3-ZrO_2-SiO_2$) (Traon et al., 2014; Wang et al., 2016). YSZ is considered a good choice for TBC. This coating material offers several advantages, such as high thermal expansion coefficients, low thermal conductivity, and high thermal shock resistance (Krishnamoorthi and Vinayagasundram, 2019). YSZ is commonly used in the industry to coat blades in gas turbine engines to achieve better thermal efficiencies (Clarke et al., 2012; Abbas et al., 2016). Some of these ceramic coatings for diesel engines were tested using Pongamia oil, cottonseed oil (Wang et al., 2016), blend of crude Jatropha oil, carburate oil, and diesel fuel, which revealed significant improvements in the thermal efficiency.

2.2 Piston Geometry

The engine performance and emission reduction can be achieved through high turbulent kinetic energies with a large swirl. The variation in the initial swirl effects the in-cylinder pressure, temperature, and emission pointedly for the piston geometries with a high bowl to piston diameter ratio, rather than with low diameter ratios. Numerical simulations performed on a single-cylinder diesel engine across two scenarios with a 70% diameter ratio and a 0.5 initial swirl ratio, and a 55% diameter ratio, with a 2.5 initial swirl ratio, were reported to

have optimal emission and performance features. Hence, pistons with cavities and a wide range of initial swirl ratios are considered much better for combustion purposes. (Abdul Gafoor & Rajesh, 2015)

2.3 Plasma Spray Method

An alternative is the APS (Atmospheric Plasma Spray) technology which has been identified successfully, and applied in gas turbines in industries known as the SPS (Suspension Plasma Spraying) process, but has not been tested in the automotive engineering field.

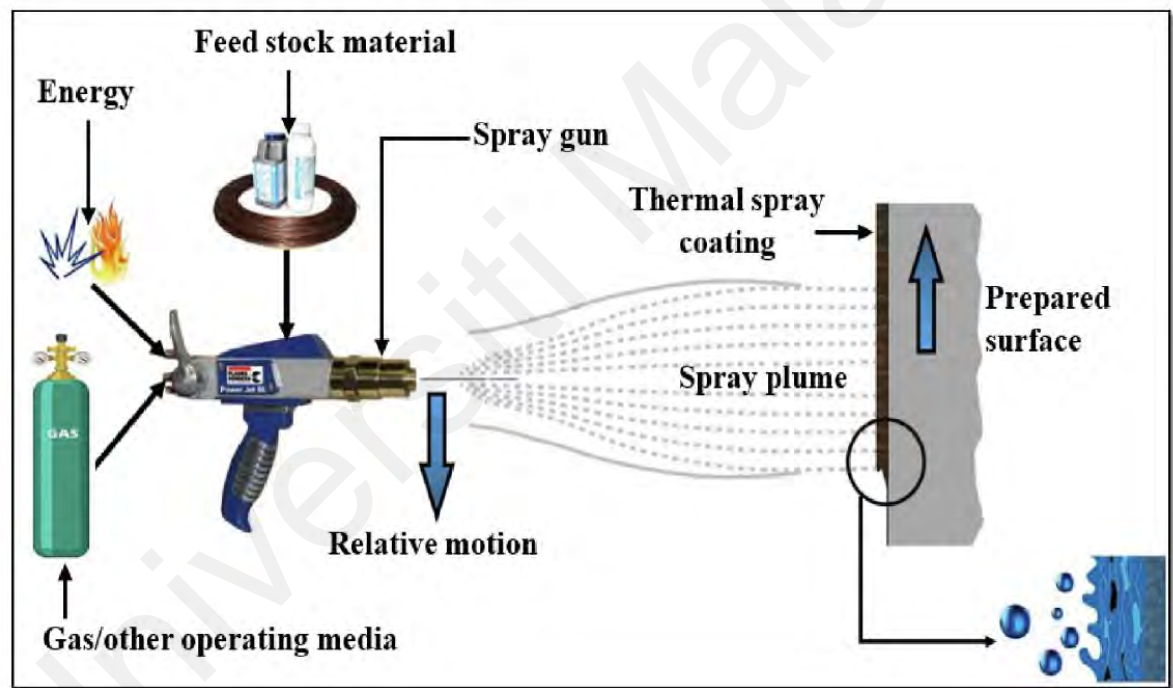


Figure 2.1: Basic process of thermal spray coating (Manoj, et al., 2021)

Three types of coating methodologies were embedded for this experimental work. The first was YSZ with APS, the second was YSZ/GZO (Gadolinium Zirconate) with SPS, and the third was a SPS columnar sealed with a metallic or a ceramic dense sealing agent on the topcoat. Two different thermal cyclic tests were used to test the TBC behaviour, and were associated with the coating's microstructure properties. It was concluded that the columnar

coatings produced by SPS boosted the service life in the cyclic thermal tests compared to the APS coatings. However, further studies needed to be performed on the diesel engine performance testing, and the emission analysis for the columnar SPS technology (Wellington et al., 2020).

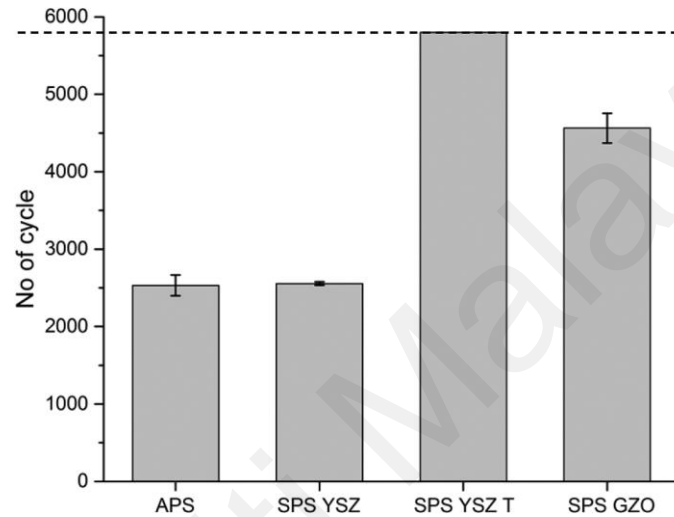


Figure 2.2: Number of cycles for first and second architecture of top coat samples flame rig test.

2.4 Durability TBC

Flat specimens (1 in x 1 in) were removed through the machining process from the piston of a 4-stroke diesel engine. These samples had been coated with a base coat nickel chromium aluminium yttrium of a 10 μm TBC zirconium dioxide 250 μm , and a 350 μm sample using the plasma spray deposit method. One (1) sample has not been coated, and was maintained as a reference for this experiment. From the SEM analysis, the porosity of the coated specimen was reduced. The result from the Brinell test indicated that the increase in the hardness of the coating correlated with an increase in thickness of the coated sample. Furthermore, the Brinell test confirmed that the coated specimen's hardness was higher than the uncoated specimen. From observations of the thermal stability tests, the physical

characteristics of the coated specimens did not deteriorate at 1200°C, and the uncoated samples melted at 650°C. Based on the corrosion tests using the sodium sulphate (V_2O_5) and vanadium pentoxide (Na_2SO_4) salts, the coated samples did not show any chemical changes compared to the uncoated samples. (Kalyana & Sudersanan, 2021).

A novel thermal-protective coating $Al_2O_3.ZrO_2$ with an addition of SiO_2 was prepared using the novel plasma electrolytic oxidation (PEO) process on a cast Al-12Si piston alloy. The crack formation reduced with the addition of the Zirconia sol. The primary Si and SiO_2 phases stopped the aluminium from oxidizing and significantly impacting the morphology and structure of the PEO coating. After a durability test of 1000 cycles of thermal shock, no cracks were found on the coating surface, which showed that the PEO coating increased in the zirconia and had an excellent thermal shock resistance (Ping Wang et al., 2016).

2.5 Coating thickness

The piston in a diesel engine may suffer from heat damage, and it can be solved using TBCs. The simulation analysis of the temperature showed that the TBC piston design effectively reduced the temperature and thermal load capacity on the piston's crown. The temperature of the substrate decreased as the thickness of the TBC was added. The engine will perform at ignition depending on the properties of the fuel. Hence, the optimum thickness of the TBC was set at 1.0 mm for the natural gas engine application. The natural gas was evaluated with a Nanoceramic layer (PYSZ) TBC (Zhimin et al., 2018).

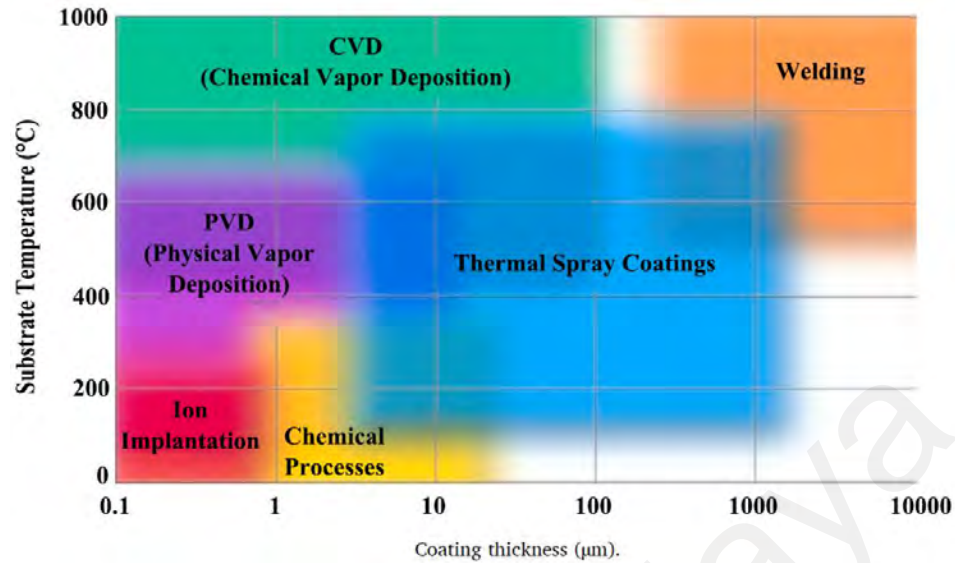


Figure 2.3: Coating thickness (Manoj, et al., 2021)

The steady-state temperature of a coated diesel engine piston has been defined using finite element method (FEM) using the ANSYS software. The Al-Si piston was used with a coating crown of Lanthanum Cerate ($\text{La}_2\text{Ce}_2\text{O}_7$) as the TBC. Temperature tabulations were compared with that of an uncoated piston. The piston model created in the ANSYS and boundaries of the convection were defined. The TBC thickness was set at 0.4 mm, 0.8 mm, 1.2 mm, and 1.6 mm, with a difference of 0.4 mm for the temperature profile. Based on the analysis, the maximum temperature for the thickness ranged from 0.4 mm to 1.6 mm, and was 45.5%, 69.3%, 84.1%, and 94.1%. The 0.4 mm value was accepted as the ideal case for practical engine application practices. The $\text{La}_2\text{Ce}_2\text{O}_7$ was considered as a TBC with low thermal conductivity, and enhanced corrosion resistance capabilities, versus Magnesium Zirconate. (Jai et al., 2021).

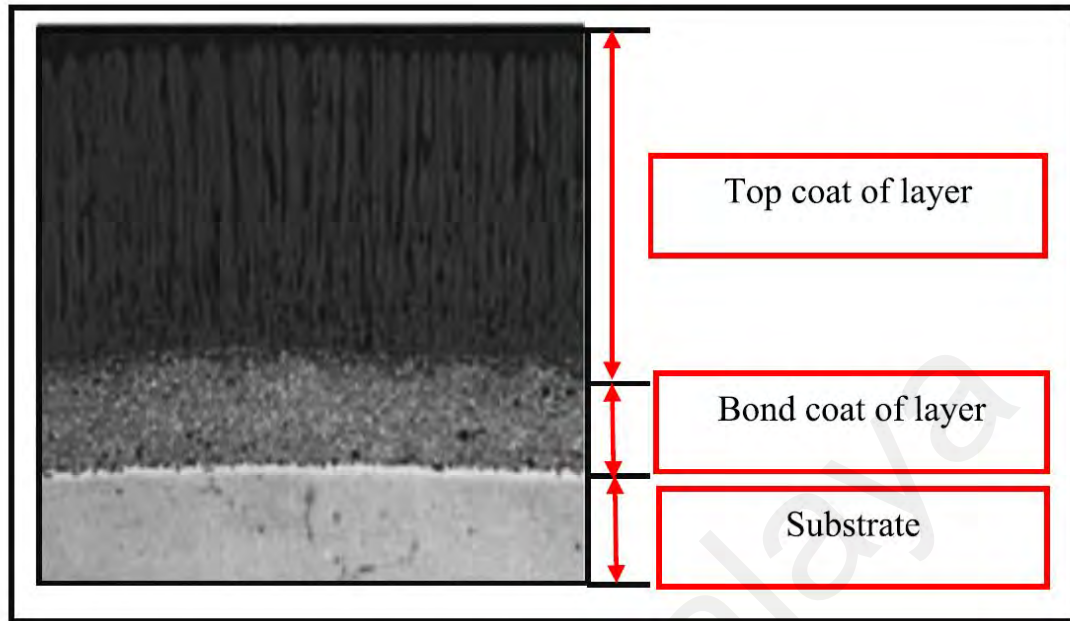


Figure 2.4: Layers of TBC (Godiganur, 2021)

2.6 Conventional & Commercialized TBC

A 4-stroke CI engine was coated with 100 μm base coat NiCrAl and 400 μm TBC, which was made up of a blend of 88% of ZrO_2 , 8% of Al_2O_3 and 4% of MgO. The target coating area was the piston crown and valve. The primary test fuel used for this experimental work was residual frying oil fuel (B100). Based on the engine test performance, the power output increased slightly when coated using residual frying oil fuel (B100). No changes were noticed for B5 and diesel fuels. The BSFC was lower for coated diesel fuels (4.15%), and highest for the uncoated B100 BSFC. It was also reported that the coating lowered the BSFC compared to the uncoated test engine. The coating positively reduced noise with the shortening of the ignition delay due to the ceramic material of the TBC, which lowered the heat transfer in the combustion chamber. The emission analysis for CO, HC, and smoke opacity reported a reduction for the coating and biofuels. However, the emission analysis for the NO_x increased with the coated engines and biofuels (Selman et al., 2015).

Table 2.1: TBC Thermal Characteristic

No	TBC	Thermal Conductivity W/m-K	Coefficient Of Thermal Expansion $10^{-6}/K$	Maximum Service Temperature ($^{\circ}C$)	References
1	La ₂ Zr ₂ O ₇	1.5	9.1	2300	Fukuchi et al., 2013.
2	YSZ	2.2	10.7	1200	Fukuchi et al., 2013 and Gok & Goller, 2016.
3	CYSZ	1.7	13.0	1300	Ahmaniemi et al., 2004.
4	Gd ₂ Zr ₂ O ₇	1.1	10.4	1530	Gok & Goller, 2019.
5	Sm ₂ Zr ₂ O ₇	1.5	10.8	2000	Dokur & Goller, 2014.
6	Al ₂ O ₃	5.8	9.6	2050	Gok & Goller, 2016.

The direct injection, turbocharged, and inter-cooled diesel 4-stroke engine was coated with a 150 μm base coat NiCrAl and 350 μm TBC with CaZrO₃ on the cylinder head and valves. The piston was also coated with a 150 μm base coat NiCrAl and TBC with 350 μm of MgZrO₃. The experiment was conducted using conventional diesel fuels. The BSFC reported a lower coated diesel fuel range between 2% ~ 7% for the various loads. The insulated engine parts of the turbo-charged and inter-cooled diesel engines displayed substantial improvements in terms of the fuel consumption over a conventional type cooling engine. The effective efficiency was slightly higher for the ceramic-coated engine with increases of about 2% at low loads, 5% at medium loads, and 3% at full loads. The coating material positively prevented excessive heat losses during the combustion, reduced the heat loss to the engine's cooling system, grounded the cylinder walls to sustain the heat, and increased the effective efficiency. The reduction in the volumetric efficiency due to the high temperatures on the combustion chamber can be resolved by using turbo-charging to enhance the pressure in the system (Imdat, 2007).

The 4-stroke CI engine was coated with a TBC of 450 μm , a blend composition of PSZ (Partially Stabilized Zirconia) included, which was made up of 8 mol% (2.77 wt%) of MgO, 8 mol% (3.81 wt%) of CaO, or 3–4 mol% (5.4–7.1 wt%) of Y_2O_3 . The target coating area were pistons, valves, and cylinder heads. The coating thickness exceeded 450 μm , and decreased the thermal efficiency, because of the decreased volumetric efficiency. PSZ had been chosen as a TBC material due to its higher coefficient of thermal expansion, and lower thermal conductivity. Furthermore, the PSZ with a tetragonal phase is much more stable and avoids the formation of cracks at high temperatures. The primary test fuel used was a low-cost feedstock, CNSL (cashew nut shell liquid), as a foundation for making biodiesel. The BTE was increased by 6% CNSLME (CNSL diesel - 75% and biodiesel - 25%) in the coated engine compared to the uncoated engine. Additionally, emissions such as CO, HC, and smoke opacity were reduced by 27.7%, 7.2%, and 14.3%, with a complete load condition, whereas the NO_x emission was increased. Lastly, based on the FEA simulation (finite element analysis), the thermal stress and heat fluxes were lower for the coated piston, confirming the significant improvement in the thermal efficiency (Vedharai et al., 2014).

A 4-stroke direct injection engine with a single-cylinder was coated with 100 μm base coat NiCrAl and TBC with a 200 μm 100% ZrO_2 . The target coating areas were the piston crown, valves, and cylinder head. The primary test fuel used for this experimental work was a series of volumetrically blended waste cottonseed oil with conventional diesel fuels, ranging from B15 (15 % waste cottonseed oil), B35 (35 % waste cottonseed oil), and B65 (65 % waste cottonseed oil). The coating process decreased the BSFC of the engine which was running on diesel fuel. The comparison across all the test results showed that the coating process improved the engine's performance.

Furthermore, the emissions such as CO, HC, and smoke opacity were reduced for all the test fuels with TBC and CO, HC, and smoke opacity of the blended fuels of the cottonseed oil, which were lower than those for diesel fuel coated, and non-coated engine parts. However, the NO_x emissions were increased when the engine was coated, and the NO_x emissions rose when using blended fuels of waste cottonseed oil. No abnormalities were reported on the coating layer, except for minor acceptable cracks on the coated diesel engine parts after a durability running test for 100 hours of engine operation (İŞCAN, 2016).

A 4-stroke CI direct injection, water-cooled, naturally aspirated diesel engine was coated with a 100 µm base coat NiCrAl and TBC with 200 µm of YPSZ (Yttria Partially Stabilized Zirconia). The target coating area was the piston crown and valve. The primary test fuel used for this experimental work was Annona oil methyl ester (B100). To promote the reduction of NO_x, aqueous ammonia was introduced as an antioxidant agent in the test fuels. The combustion chemistry of the aqueous ammonia as a NO_x reduction agent is as follows:

The overall combustion chemistry of the aqueous ammonia equation is,



Diesel scored a higher performance characteristic than A100 due to its higher fuel properties. The antioxidant addition to the blended fuels exhibited higher performance characteristics than other fuel blends. The emissions such as CO, HC, and smoke opacity were reduced for the A100+PG+CE (Annona seed oil methyl ester with antioxidant and TBC) as it boosted the combustion efficiency. Finally, the A100+PG+CE was able to deliver lower NO_x than

previous fuel samples and, at maximum loads, showing high combustion characteristics (Karthickeyan et al., 2021).

A 4-stroke direct injection engine with a single-cylinder was coated with a 100 μm base coat NiCrAl and TBC of 400 μm made up of 100% TiO_2 using a plasma spray deposition method. The target coating area was the piston crown and the combustion chamber. The primary test fuel used for this experimental work was a series of blended Pongamia Pinnata biodiesel with conventional diesel fuels, ranging from 20BD (20 % Pongamia Biodiesel), 50BD (50 % Pongamia Biodiesel), and 100BD (100 % Pongamia Biodiesel). The coating process decreased the specific fuel consumption (SFC) of the engine running on diesel fuel. The SFC of the TBC 20BD was 10.6% lower and 4.25% higher in the TBC 50BD compared to the uncoated diesel engines. The BTE of the TBC 20BD was 4.7% higher and 2.7% lower in the TBC 50BD compared to the uncoated diesel engines. The mechanical efficiency of the TBC 20BD was 2.6% higher and 2.0% lower in the TBC 50BD compared to the uncoated diesel engines. The TBC of the 20BD can be used in a diesel engine with its enhanced properties in terms of engine performance (Amriya et al., 2021).



Figure 2.5: Production of annona oil methyl ester

A 4-stroke direct injection engine with a single-cylinder was coated with a 50 μm base coat and 100 μm TBC made up of 100% stellite - 6 using a plasma spray method. This TBC was a wear-resistant cobalt-based alloy. The target coating area was the piston crown. The primary test fuel used for this experimental work were a series of volumetrically blended Pongamia oil methyl esters with conventional diesel fuel ranging from B10 (10 % Pongamia Biodiesel), B20 (20 % Pongamia Biodiesel), and B30 (30 % Pongamia Biodiesel). The BSFC of the TBC B30 was 28.5% lower, and the BTE was 12% higher compared to the diesel fuels. Furthermore, the emissions for B30 such as CO, were reduced by 17.3%, and the HC was reduced by 5%, whereas the NO_x emission was increased by 10.94% compared to the diesel fuels (Hemanandh et al., 2018).

A 4-stroke direct injection engine with three cylinders was coated with a thin TBC layer of 100 μm (YSZ (8 mol% of Yttria (Y_2O_3) and the remaining mol % of a fully stabilized zirconia (ZrO_2)) using a plasma spray deposition method. The target coating area was the piston crown. The experiment was conducted using conventional diesel fuels. In general, the emissions such as CO by 2.7%, CO_2 by 5.27%, and HC by 35.27%, were reduced for the diesel fuel with the TBC. However, NO_x emissions were increased by 19% when the engine was coated, and Smoke opacity rose by 12% when coated with YSZ. However, the BSFC of the TBC was 3.38% lower at full load, and the BTE was 8.84 % higher at 50% of the full load compared to the diesel fuels. The TBC coated engine showed better BTE and better BSFC than the uncoated piston. Exhaust gas temperatures increased at all loading settings, which increased the NO_x emissions of the YSZ coated engine. The power and torque developed in the TBC engine were reduced for all load settings compared to the uncoated piston engine, as shown in Figure 2.6. Although the TBC was expected to reduce the heat loss transferred to the cooling medium, in reality, it affected the engine's compression ratio, which decreases the power and torque in the diesel engine (Sivakumar & Senthil Kumar, 2014).

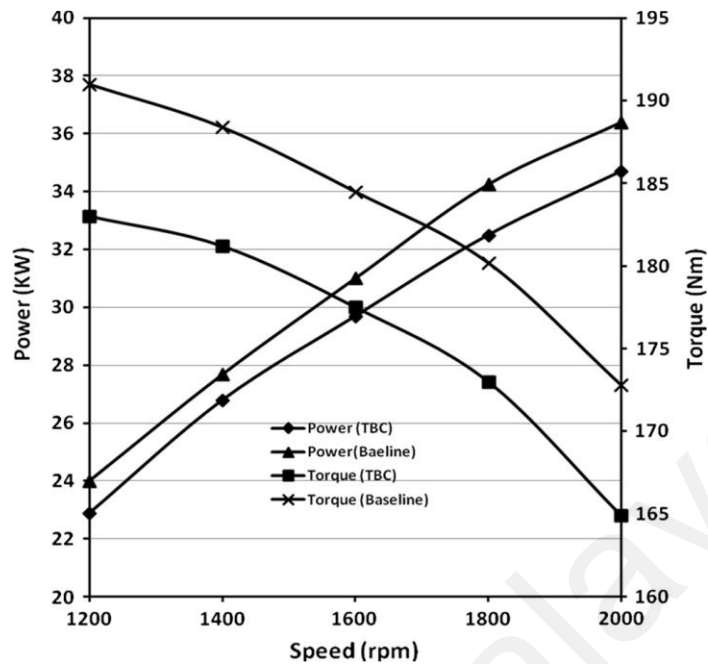


Figure 2.6: Variation in power and torque of baseline engine and TBC engine under different speed conditions (Sivakumar & Senthil Kumar, 2014)

The integrity and durability of the TBC was tested and based on the investigation of a coated 50 μm base coat NiCrAl, and a TBC of 250 μm with 100% of 8YPSZ on a Al-Si casting alloy. The capability of the TBC to guard the substrate material against degradation during both thermal shock and oxidation processes during the diesel engine service with a temperature of 300°C, was ascertained. The TBC was tested for the thermal shock melting point of the Al-Si alloy at 570°C using both the oxy-acetylene flame and with muffle furnaces. Furthermore, the TBC was tested for a continuous long-duration heating with a temperature of 300°C for 1000 hours, to measure the oxidation stability (Reghu et al., 2018).

TBC with various thicknesses ranging from 0.2 mm to 1.6 mm, excluding the bond coat layer, were tested using Magnesia Stabilized Zirconia ceramic materials to evaluate normal and shear stresses. The coated material temperature was reported higher than uncoated parts, and the outcomes showed that the coating surface temperature increased with a decrement in the coating thickness, with a maximum temperature of 64.3% for a 1 mm thickness on the

coated piston. The higher the temperature in the combustion chamber, the better the engine's thermal efficiency. The maximum normal stress and maximum shear stress occurred on the bond coat surface nearly two times the substrate surface area (Ekrem & Cerit, 2007).

A 4-stroke direct, turbocharged engine with four (4) cylinders was coated with 100 μm base coat Ni-Al, and TBC with 400 μm and 8% YSZ, using a plasma spray deposition method. The target coating area was the piston crown. The main test fuel used for this experimental work was conventional diesel, port fueled methane (100% CH_4), synthetic biogas (80% CH_4 + 20% CO_2), and hydrogen traces (80% CH_4 + 10% CO_2 + 10% H_2). The BSFC reported a higher value for the mixture with hydrogen surges than the synthetic biogas, which was 10.3% for the uncoated, and 3% for the coated piston. Based on the outcomes, the reduction in the operating temperature was recommended rather than increasing the wall temperature, to achieve better fuel consumption. In general, the emissions such as CO_2 by 5.16 - 10%, and HC by 4.97% - 30.92%, were reduced for the hydrogen introduction fuel, with that of the TBC, compared to synthetic biogas. However, the NO_x emissions increased by 24.9% at high loads on the uncoated engine, and by 74.9 % at medium load on the coated engine, when the engine was tested with hydrogen base fuel. Hydrogen in fuel is attributed to higher NO_x formation compared to biogas operations (Ali et al., 2021).

A 4-stroke direct, twin-cylinder engine was coated with a 300 μm platinum. The target coating area was the piston crown. The primary test fuel used for this experimental work was a 50 % Apricot oil mixed 50 % with ethanol, 50% Pongamia oil mixed 50% with ethanol, 50% Apricot oil mixed 50% with methanol, and 50% Pongamia oil mixed 50% with methanol. The results showed that the greatest value was obtained for 50 % Apricot oil mixed

50 % with ethanol in the coated piston for higher BTE, with fewer emissions for all the fuel mixes of 50% biofuel with 50% ethanol or methanol used in the investigations (Manjunatha et al., 2021).

The 4-stroke direct compression injection engine with single cylinders were coated with a TBC coat of Zirconium. The target coating area was the piston crown, valves, and cylinder head. The experiment was conducted using ethanol at a retarded timing compared with conventional diesel. The BTE for uncoated diesel engines, ethanol retarded injection timing, and ethanol retarded timing with ceramic coatings were 23.85, 25.8 and 30.18%. The findings showed a slight increase in the thermal efficiency of the engine tuned with the retarded injection timing, and further increased with conversion into low heat rejection diesel engines. The low heat rejection diesel engine known as a coated engine reduced the CO and HC emissions, whereas the NO_x emissions increased because of more significant combustion temperatures (Balu et al., 2021).

The natural gas was tested on the natural gas engine coated with a 100 μm base coat NiCoCrAlY, and a TBC with 400 μm of a Nano 8-PYSZ (8PYSZ) using a plasma spray deposition method. The target coating area was the piston crown, and the output was compared with results from an uncoated piston using the finite element method (simulation). The temperature of the coated piston substrate was lower by 12% (43°C), compared to the uncoated piston, hence, producing better thermal fatigue protection for the piston material. Furthermore, the maximum temperature of the TBC piston was larger than the uncoated piston, with a difference of 153°C (44% incremental) at the piston crown. Hence, the thermal strength and load-carrying capacity were improved. As the outcomes of the studies showed,

reducing the in-cylinder heat dissipation and enhancing the thermal efficiency of the natural gas engine could be achieved by TBC applications (Zhimin et al., 2019).

A 4-stroke direct injection engine with a single-cylinder was coated with a partially stabilized zirconia with a thickness of 125 μm , followed with the second layer of alumina (Al_2O_3) with a bonding material of Ni-Al, to achieve an overall thickness of 250 μm . The target coating area was the piston crown. The primary test fuel used for this experimental work was commercial diesel. The findings indicated an increase in the peak pressure from 68 bar to 72 bar using coated TBC, compared to the uncoated piston. The heat release rate increased as the BTE was increased by 4.6% in the coated engine compared to an uncoated piston. The gas temperature taken at the engine's exhaust increased by 12.6% in the coated engine compared to an uncoated piston. However, the NO_x emissions were increased by 15.67% when the engine was coated with TBC compared to the uncoated piston (Abbas et al., 2021).

A 4-stroke direct compression injection engine with single cylinders was coated with a TBC coat of Zirconia ceramic powder. The target coating area was a piston crown using the plasma spray deposition method. The experiment was conducted using Karanja biodiesel oil compared with conventional diesel. The test was performed under the condition of varying the compression ratio and injection operating pressure of the conventional diesel, and for the Karanja Biodiesel, with and without piston crown coatings. All the tests were maintained at a constant speed of 1500 rpm. In general, for the Karanja Biodiesel with TBC, the brake power, BTE, and BSFC improved by 2.55%, 9.23% and 20.75%, with an increase in the compression ratio, ranging from 13.99 to 17.5. Furthermore, with the increase in the injection pressure from 160 bar to 190 bar, the brake power, BTE, and BSFC improved by 1%, 3.26%

and 9% for the Karanja Biodiesel with TBC. The overall emission was reduced for the HC, NO_x, and CO for the Karanja Biodiesel with TBC for both the compression ratio and injection pressure (Dananjayakumar et al., 2021).

A 4-stroke direct, spark ignition, twin-cylinder engine which was water-cooled, was coated with 78 μm Micro Arc Oxidation (MAO). The target coating area was the piston crown using the MAO method, which had better metallurgical bonds than the plasma spray technology. The primary test fuel used for this experimental work was P10 (Pine oil mixed 10 % with Gasoline, 90%), P20 (Pine oil mixed 20 % with Gasoline, 80%), and P30 (Pine oil mixed 30 % with Gasoline, 70%) (Viswanathan et al., 2019).

In general, the emissions such as a CO of 8% and HC of 14% were reduced for the coated test fuel with P20. The BTE for the coated P20 was 1.8 % higher than uncoated pistons with gasoline fuel. However, NO_x emissions were increased by 19% when the engine was coated with TBC P20, compared to the uncoated piston with gasoline fuel. Lastly, the results indicated that coatings with test fuels of P20 provided promising positive results on the diesel engine's engine performance, and emission characteristics (Manoj et al., 2021).

A 4-stroke direct injection engine with a single-cylinder was coated with a 125 μm base coat of Al₂O₃ and TBC with a 125 μm 100% of TiO₂ using a plasma spray deposition method on the piston crown. The second piston was coated with a 250 μm base coat Al₂O₃ and TBC with 250 μm 100% TiO₂ on the piston crown. The primary test fuel used for this experimental work was conventional diesel (D100), and biofuels (B100) obtained from agriculture waste. The studies investigated the diesel engine's performance and emission characteristics against

the different thicknesses of coatings using biofuels with varying compression ratios (16, 17, and 18). In general, with the increase of thicknesses and higher compression ratios, the emissions such as CO by 24 - 40 %, and HC by 17 – 42 %, were reduced compared to the uncoated piston with diesel. The BTE for the coated P20 was 1.8 % higher than the uncoated piston with diesel. However, the NO_x emissions increased by 11 – 35 % when the engine was coated with an increased thickness and a higher compression ratio than the uncoated piston with the diesel fuel. The heat release rate increased as the BTE was increased by 6 % for the 250 μm, and 8 % for the 500 μm, as the coating thickness increased compared to the uncoated piston. The BSFC was reduced by 18 % for the 250 μm, and 20 % for the 500 μm, as the coating thickness increased compared to the uncoated piston. Lastly, the results proved that coating with TiO₂ + Al₂O₃ provided promising positive results on the diesel engine's performance and emission characteristics. Overall, the coating thickness of 500 μm with a compression ratio of 18 seemed effective for the biofuel application (Akshay & Mahesh, 2020).

An investigation was conducted using ANSYS for a coated piston of TBC with 350 μm 100% MgZrO₃ with a bond coat of 150 μm NiCrAl. From the ANSYS studies, the maximum surface temperature of the AlSi alloy and steel pistons were increased by 48% and 35%, with a temperature difference of 14% for the coated TBC of MgZrO₃ (Buyukkaya & Cerit, 2007).

An investigation was conducted using ANSYS for the coated piston of TBC 500 μm 100% ZrO₂ - 8%Y₂O₃ with a bond coat of NiCoCrAlY 100 μm, grown on a BH136 aluminium alloy piston. The ANSYS results was tested for accuracy by comparing the bench test using natural gas engines (six-cylinder, water cooled and four-stroke). The error analysis computed

was 4.12% and within an acceptable range. The temperature of the coated piston substrate was lower by 16% (55°C) than the uncoated piston, hence producing better thermal fatigue protection for the piston material. Furthermore, the maximum temperature of the TBC piston was larger than the uncoated piston, with a difference of 179°C (52% incremental) at the piston crown. Hence, the thermal strength and load-carrying capacity were improved. As the outcomes of the studies showed, reduction of the in-cylinder heat dissipation and enhancement of the thermal efficiency of the natural gas engines by TBC applications were promising (Zhimin et al., 2019).

An investigation was conducted using 1-dimensional Computational Fluid Dynamics (1D.CFD) for a coated piston of TBC with 100 µm 100% anodized aluminium, grown on an aluminium alloy piston. The anodized aluminium had low thermal conductivity and low heat capacity characteristics. The 1D.CFD results were tested for accuracy by comparing the bench test using the diesel engine (four-cylinder, water cooling and four-stroke). The results of the 1D.CFD analysis revealed that 1% of the Indicated Specific Fuel Consumption and 6% in heat transfer decreased. However, the experimental results showed a cutback of 2% for the engine efficiency at lower loads and speeds due to a roughness in the coating of Ra 8 µm, compared to an uncoated aluminium alloy of Ra 3.2 µm. It is recommended to use 3-dimensional Computational Fluid Dynamics (3D.CFD) to ensure a much more detailed analysis is captured as much as possible with the experimental work. With the EGR, the NO_x emissions decreased a little (Sabino et al., 2019).

A diesel 4-stroke, single-cylinder, water-cooled and direct injection engine was coated with four (4) types of ceramic powder; uncoated piston (BSLN), a PEO coated with a smooth

surface finish in the bowl (PEO1), PEO coating (PEO4), and an anodized piston (ANO1). The thickness of the TBC coats using the plasma spray method for the PEO1, PEO4 and ANO1 were measured as 70 μm , 70 μm and 50 μm . The experiment was conducted using conventional diesel fuels. In general, the emissions such as CO by 16.1%, and HC by 22.5%, were reduced for the diesel fuel with TBC, compared to the uncoated piston. However, the NO_x emissions were increased by 33% when the engine was coated with TBC compared to the uncoated piston. Retarding the combustion steps from the optimum setting would decrease NO_x without losing fuel consumption savings. This indicates that there will be a penalty in terms of the BSFC benefits, to having lower NO_x . The findings showed a reduction in the heat losses for the TBC applications in the CI engine. Lastly, the results proved that the coating with PEO1 provided promising positive results on the diesel engine's performance and emission characteristics (Dahuwa et al., 2021).

Table 2.2: Summary of TBC performance and emission characteristic

No	Fuel	TBC	Performance		Emission			References
			BTE	BSFC	CO	HC	NO_x	
1	Peanut seed oil methyl ester	Fe_2B coating	High	Low	Low	Low	High	Ozturk et al., 2019.
2	Kapok oil methyl ester	Yttria stabilized zirconia coating	High	Low	Low	Low	High	Karthickeyan, 2018.
3	Neem oil methyl ester	Paritally stabilized zirconia coating	High	Low	Low	Low	High	Karthickeyan, 2018.
4	Cymbopogon flexuosus biofuel	Yttria stabilized zirconia), FM: 20 ppm of cerium oxide	High	Low	Low	Low	High	Dhinesh et al., 2018.
5	Moringa oleferia biodiesel	Yttria stabilized zirconia) FM: Cetane improver (Pyrogallol)	High	Low	Low	Low	High	Karthickeyan, 2019.

Table 2.2: Continued

6	Pine oil biofuel	Partially stabilized zirconia) FM: Anti-oxidants (Butylated hydroxyanisole, Butylated Tertiary-hydroxytoluene, butyl hydroquinone)	High	Low	Low	Low	High	Viswanathan et al., 2019.
7	Diesel	Partially Stabilized Zirconia	High	Low	Low	Low	Low	Mohamed Abbas & Elayaperumal, 2019.
8	Lemongrass oil	Partially Stabilized Zirconia	High	Low	Low	Low	Low	Elumalai et al., 2019.
9	Palm oil biodiesel	Partially Stabilized Zirconia	High	Low	Low	Low	Low	Mohamed Musthafa, 2019.
10	Pomegranate Oil	Yttria Stabilized Zirconia	High	Low	Low	Low	High	Karthickeyana et al., 2020.
11	Cottonseed, Frying Oil	PSZ, Aluminium	High	Low	Low	Low	High	Aydin et al., 2015.
12	Cottonseed Methyl ester	PSZ, Aluminium	High	Low	Low	Low	High	Suresh et al., 2014.
13	Pongamia Methyl ester	Titanium Oxide	High	Low	Low	Low	High	Prabhakar & Rajan, 2013.
14	Pongamia and Neem Methyl ester	Aluminium Titanate	High	Low	Low	Low	High	Srithar et al., 2013.
15	Pure cottonseed oil and sunflower oil	Zirconium oxide	High	Low	Low	Low	High	Aydin, 2013.
16	Jatropha oil	PSZ	High	Low	Low	Low	High	Janardhan et al., 2013.
17	Nerium oleander biofuel	Cerium Oxide/30 ppm	High	Low	Low	Low	Low	Dhinesh & Annamalai, 2017.
18	Diesel & Biodiesel	Cerium Oxide/50 ppm	High	Low	Low	Low	Low	Kumaravel et al., 2019.
19	Garcinia gummi-gutta biodiesel	Cerium Oxide, Zirconium Oxide, and Titanium Oxide 25 ppm	High	Low	Low	Low	Low	Janakiraman et al., 2020.
20	Tyre oil diesel blends	Cerium Oxide/50, 100 ppm	High	Low	Low	Low	Low	Mangesh et al., 2020.
21	Biodiesel	Cerium Oxide/80 ppm	High	Low	Low	Low	Low	Ayat & Hossein., 2019.

Table 2.2: Continued

22	Oenothera lamarckiana biodiesel	Graphene Oxide/30, 70, 90 ppm	High	Low	Low	Low	Low	Hoseinia et al., 2020.
23	Mahua methyl ester	Al ₂ O ₃ and Fe ³ O ₄ /40, 120 ppm	High	Low	Low	Low	Low	Syed Aalam, 2020.
24	Pongamia biodiesel	Copper oxide/50 ppm	High	Low	Low	Low	High	VaratharajuPerumala, 2018.

2.7 Blend and Mix TBC

A 4-stroke CI direct injection engine was coated with a TBC of 500 μm , and a blend composition of PSZ. The top of the piston, outlet, and inlet valves were the target coating areas. The target coating area was the piston crown. The main test fuel used for this experimental work was a series of 20% blended waste linseed oil which was converted into an alternative fuel by preheating it with conventional diesel fuel. The additive of TiO₂ nanoparticles was incorporated into the blended fuel, ranging from 0 ppm (LS20), 50 ppm (PLSNP 50), 100 ppm (PLSNP 100), 150 ppm (PLSNP 150) and 200 ppm (PLSNP 200), to enhance the combustion efficiency. The blended PLSNP 200 showed a 8.11% higher BTE than the LS20, due to the preheating process and complete combustion. The TBC retained the temperature of the combustion, which allowed for complete combustion, such as the reduction in the CO (21.05%) and HC (33.82%), compared to the LS20. The presence of oxygen in the waste linseed oil provided excess oxygen supply, promoted CO reduction and ensured that the fuel burnt rapidly to reduce the HC. The drawback, though, was the increase in the NO_x emissions by 6.53%, compared to the LS20, due to the rise in the combustion temperature. The addition of nanoparticles reduced the smoke opacity of the blended PLSNP 200 to 25%, using the availability of oxygen content in the TiO₂ nanoparticles (Elumalai et al., 2021).

The diesel 4-stroke, single-cylinder, water-cooled engine was coated with a 150 μm base coat CoNiCrAlY, and a TBC of 300 μm of a blend coat 20% Al_2O_3 + 80% 8YSZ ($\text{Al}_2\text{O}_3/8\text{YSZ}$) for the first TBC coating candidate for this experiment. For the second coating, the engine was coated with a 150 μm base coat CoNiCrAlY, and a TBC with 300 μm of blend coat 20% CeO_2 +80% 8YSZ ($\text{CeO}_2/8\text{YSZ}$). The target coating area was the piston crown. The experiment was conducted using conventional diesel fuels. The outcomes of this investigation showed that $\text{CeO}_2/8\text{YSZ}$ had a high thermal cyclic characteristic compared to $\text{Al}_2\text{O}_3/8\text{YSZ}$. For both $\text{CeO}_2/8\text{YSZ}$ and $\text{Al}_2\text{O}_3/8\text{YSZ}$ TBC, the BTE reported an increase, and the BSFC reported a decrease compared to the uncoated sample. Further reductions of the HC, CO, smoke opacity, and penalty resulted in an increase of the NO_x emissions, as was reported as well for the $\text{CeO}_2/8\text{YSZ}$ and $\text{Al}_2\text{O}_3/8\text{YSZ}$ TBC, compared to the uncoated sample (Gnanamoorthi & Jayaraman, 2019).

A 4-stroke direct injection engine with a single-cylinder was coated with a 300 μm TBC of YSZ with Ceria (Zirconia 85%, Ytria 10%, and Ceria 5%) using a air plasma spray method on the cylinder liner. The piston head was also coated with a 150 μm TBC YSZ with Ceria. The main test fuel used for this experimental work was a series of blended Citrus Medica Peel Oil (CMPO) biodiesel, dosed with nanoparticle additive of Cerium Oxide (CeO_2) with the conventional diesel fuel, ranging from B15 (15 % CMPO Biodiesel and 15 ppm of CeO_2), B20 (20 % CMPO Biodiesel and 15 ppm of CeO_2) and B25 (25 % CMPO Biodiesel and 15 ppm of CeO_2). The SFC of the TBC B20 was 10.59% lower, and the BTE was better than other fuels and diesels in this experiment. Furthermore, the emissions for the B20 such as CO, HC and NO_x were reduced for the biodiesels, compared to the conventional diesel. The addition of cerium oxide nanoparticles was expected to react as an oxidizing agent in the combustion chamber. The overall mechanical efficiency for the B20 was reported to be

higher than the diesel at lower loads. At higher loads, the mechanical efficiency was sustained close to the conventional diesel (Mohanraj et al., 2021).

A diesel 4-stroke, three-cylinder, direct injection and water-cooled engine was coated with three (3) sets of TBC, with the first set being 500 μm of zirconia, a second set of zirconia & aluminium oxide, and finally the third set used fused zirconia (40FZA). The target coating area was the piston crown using a plasma spray deposition method. The experiment was conducted using conventional diesel fuels. In general, the emissions such as CO by 2.7%, NO_x by 25%, and HC by 30%, were reduced for the diesel fuels with 40FZA. The smoke opacity was decreased by 12% when coated with 40FZA. The BSFC of the TBC was 13% lower, and the BTE was 5 % higher than the uncoated engine. Lastly, the upshots indicated that the coating with 40FZA provided promising positive results on the diesel engine's performance and emission characteristics (Abbas et al., 2021).

A diesel 4-stroke, single-cylinder and direct injection engine was coated with four (4) types of different lanthanum zirconate ($\text{La}_2\text{Zr}_2\text{O}_7$) based ceramic powders; $\text{La}_2\text{Zr}_2\text{O}_7$ (LZ), $\text{La}_{1.4}\text{Dy}_{0.6}\text{Zr}_2\text{O}_7$ (LDZ), $\text{La}_{1.4}\text{Yb}_{0.6}\text{Zr}_2\text{O}_7$ (LYZ) and $\text{La}_{1.4}\text{Nd}_{0.6}\text{Zr}_2\text{O}_7$ (LNZ). The ceramic interlayer was coated with CYSZ (ceria yttria-stabilized zirconia). The thickness of the TBC coats used a plasma spray method for the LZ, LYZ, LDZ and LNZ, and were measured as 384 μm , 395 μm , 480 μm and 375 μm . The variance in the thickness between the TBCs was due to the different deposition effectiveness of the rare additives added into the $\text{La}_2\text{Zr}_2\text{O}_7$, such as Yb, Dy and Nd. The target coating areas were piston crown, valves, and cylinder head. The experiment was conducted using conventional diesel fuels. The results showed that the BSFC achieved a 1.26% lower value in the LZ, 2.6% lower in the LYZ, 1.86% lower

in the LNZ, and 1.71% lower in the LDZ, compared to the uncoated engine, across all speeds. The lowest BSFC reported in the LYZ coating was due to the Yb material. LYZ recorded an increase in the engine torque of about 3% compared to the uncoated engine. LYZ provided better results than other series at the maximum torque value and cylinder pressure (Ömer et al., 2020).

Using the plasma spray deposition method, a 4-stroke direct injection engine with a single-cylinder was coated with a base coat of NiCr and TBC of $\text{Al}_2\text{O}_3 + 13\%$ of TiO_2 . Thickness was not mentioned. The target coating areas were the pistons and valves. The main test fuel used for this experimental work was a conventional diesel fuel blend of 75% diesel and 25% fuel oil-doped fuel (D75F25). The results showed that the use of the TBC with the addition of fuel oil was more effective in reducing the NO_x , CO, HC, and smoke opacity, compared to the uncoated diesel engines (Salih et al., 2021).

A diesel 4-stroke, single-cylinder, water-cooled and direct injection engine was coated with four (4) types of ceramic powders, and these were the 7% YSZ (LHR-1), 2% Nd + YSZ (LHR-2), 2% Gd + YSZ (LHR-3) and 2% Nd + 2% Gd + YSZ (LHR-4). The ceramic interlayer was coated with CYSZ (ceria yttria-stabilized zirconia). The thickness of the TBC coats using the plasma spray method for LHR-1, LHR-2, LHR-3 and LHR-4, were measured as being 250 μm . The piston crown was coated with a 50 μm base coat Ni-Cr-Al-Y. The experiment was conducted using conventional diesel fuels. In general, the emissions such as CO by 16.1%, and HC by 22.5%, were reduced for the diesel fuels with TBC, compared to the uncoated piston. However, the NO_x emissions were increased by 17.7% when the engine

was coated with TBC, compared to the uncoated piston. The findings showed a reduction in the heat losses for the TBC applications in the CI engine (Reddy et al., 2021).

A 4-stroke CI engine was coated with a base coat NiCoCrAlY and TBC of 250 μm , with a blend of ZrO_2 8% Y_2O_3 at 1000°C. The target coating area was the piston crown. Additionally, silicon carbide was attached to the coated piston, as illustrated in Figure 2.7. The main test fuel used for this experimental work was conventional diesel. In general, the thermal efficiency reported an increment of 6% compared to the uncoated piston. Furthermore, the emissions such as CO by 14%, and HC by 38%, were reduced for the diesel fuel with TBC compared to the uncoated piston. However, the NO_x emissions were increased by 3% when the engine was coated with TBC, compared to the uncoated piston. On the contrary, the NO_x decreased by 63% due to the heat recuperation ability of the porous medium of silicon carbide which regenerated the heat from the current cycle to the subsequent cycle (Saravanan et al., 2020).

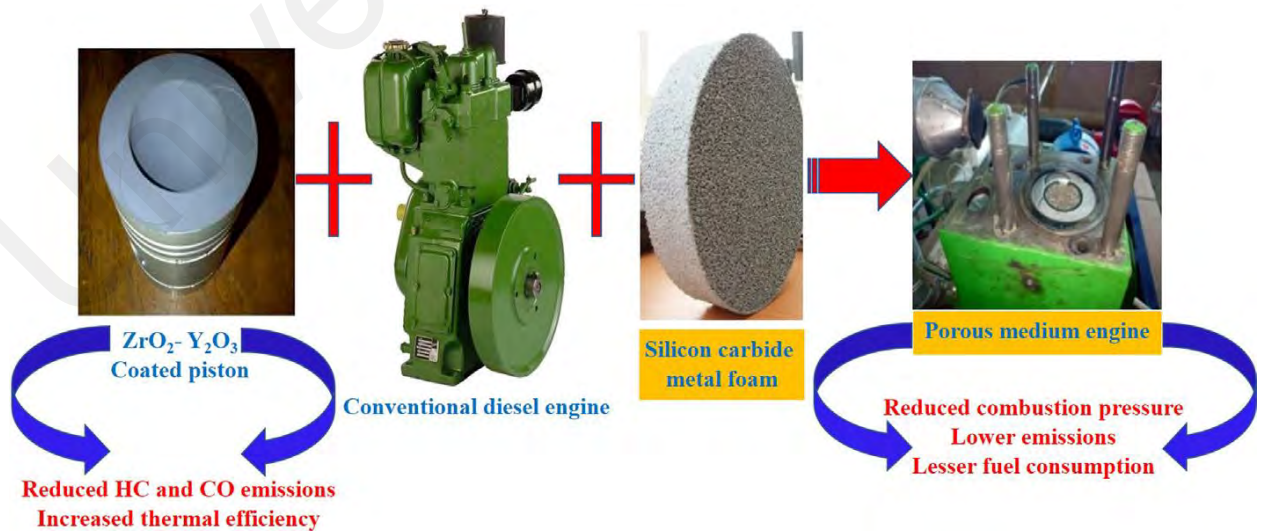


Figure 2.7: Silicon carbide metal foam (Saravanan, et al., 2020)

A 4-stroke direct injection engine with single cylinders was coated with a 200 μm to base coat of Partially Stabilized ZrO_2 and top TBC coat with 100 μm and Cr_3C_2 . The target coating area was the piston crown. The experiment was conducted using 20% Jatropha biodiesel which produced a heat release rate of $62.53 \text{ kJ/m}^3\text{C}$, which was lower than conventional diesel fuels at a compression ratio of 17.5:1. Hence, the authors concluded that the wear resistance of the coated piston improved by 47% to the overall decrease wear rate of 35%, hereby, enhancing tribological characteristics of the piston (Balaji et al., 2020).

A single-cylinder light-duty research engine was tested with a multi-layer TBC. In this study, four (4) layers of the different blends were applied from the start, i.e., a pure Ni_5Al (5% of total thickness) as a bond coat applied to the surface of the standard piston engine. This bond coat represented about 5% of the Ni_5Al coat, a 50% YSZ.50% Ni_5Al by volume layer was coated, creating 10% of the total thickness of the coating. Next, a 70% YSZ.30% Ni_5Al by volume layer was added, creating 20% of the total thickness. Finally, a 95% YSZ.5% Ni_5Al by volume layer was added, creating 65% of the total thickness. For the top seal coat, an additional 97% YSZ (fine coarse) 3% Ni_5Al (fine coarse) was added. The coating layer tested for this experiment work is shown in Table 2.3 as follows:

Table 2.3: Coating layer properties (Ziming et al., 2021)

Layer	L1	L2	L3	L4	L5
1 mm Layer Δx [μm]	50	100	200	650	40
2 mm Layer Δx [μm]	120	240	480	1560	40
2 mm Unsealed Layer Δx [μm]	120	240	480	1560	–
k [W/m-K] [$\text{Wm}^{-1}\text{K}^{-1}$]	14.2	7.57	4.48	0.93	1.74
ρ [kg/m^3]	7511	5893	5577	4490	5706
c [J/kg-K]	410	309	319	363	442
α [mm^2/s]	4.62	4.15	2.52	0.52	0.69
Composition [Main% - Bond%]	100–0	50–50	30–70	95–5	97–3

The target coating area was the piston crown. The experiment was conducted using an 80% ethanol (WE80) gasoline. The thickest TBC extended the low load limit by 14.8% with gasoline, and 15.4% with WE80 with no scuffing at the high load limit. There was no noticeable impact by the TBC application on the burn duration process. The combustion efficiency rose with a TBC thickness increase of up to 1.5% with both fuels. The optimum gasoline performance was low during the load with IMEP_g, at a value of 2-3 bar. The optimum performance of the WE80 was between a mid to high load with the IMEP_g of 3-4.5 bar. The high fuel conversion efficiency increased by 4.3% with a WE of 80 and 3.8% with gasoline. The addition of a dense sealing layer reduced the surface porosity and enhanced the reduction of the HC emissions. No scuffing was noticed after a long run of up to 10-20 hours of operations (Ziming et al., 2021).

Using the plasma spray deposition method, the 4-stroke direct injection engine with a single-cylinder was coated with a TBC of 300 μm thickness consisting of YSZ (ZrO_2 and 6-8 wt % Y_2O_3). Using the plasma spray deposition method, the second piston was coated with a TBC of 300 μm consisting of YSZ + CeO_2 . The addition of CeO_2 is expected to prolong the thermal life cycle of the coated parts. The main test dual-fuel used for this experimental work

was conventional diesel (D100) as a pilot for the Oxy-hydrogen gas (HHO) as an induction fuel, and a blend of JME20 (20% Jatropha oil and 80% conventional diesel) as a pilot, with HHO as an induction fuel. HHO has high octane number, high flame speed, and better blend characteristics, and is suitable for dual fuel modes. In general, the emissions such as CO by 44.1%, smoke opacity 21.5%, and HC by 46.7%, were reduced for the JME20 + HHO + YSZ + CeO₂. The BTE for JME20 + HHO + YSZ + CeO₂ was 5.9 % higher than the uncoated piston running with diesel. However, the NO_x emissions were increased by 33.92% when the engine was running with JME20 + HHO + YSZ + CeO₂ compared to the uncoated piston running with diesel. Lastly, the results indicated that coating with JME20 + HHO + YSZ + CeO₂ provided promising positive results on the diesel engine's performance and emission characteristics (Jami et al., 2021).

A simulation analysis was performed on uncoated and coated piston Aluminium-based alloys (Al-7Si). The whole piston was coated with a thin layer of TiSiCN (90.0% Ti, 9.98% Si, 0.01% C and 0.01% N). The piston needs to sustain all its properties at a higher temperature of 500°C, and a pressure of 120 bar in a typical engine environment. The coating reduces the thermal effects and stresses associated with the piston. This investigation tested two (2) types of piston heads; flat crown and bowl on the crown. From the FEM analysis, a reduction of 1/9 times and noticeable Von Misses stress reductions of 33.97% with the coated TiSiCN piston with bowl head was compared to the flat head uncoated piston, thus improving the lifespan of the piston (Arka et al., 2021).

An investigation was conducted using ANSYS for the coated piston of 400 µm with a Functionally Graded Material (FGM) having a bond coat of NiCrAl 100 µm. The TBC had been developed in five (5) layers of NiCrAl, 30% MgZrO₃ + 70% NiCrAl, 50% MgZrO₃ +

50% NiCrAl, 70% MgZrO₃ + 30% NiCrAl, and the topcoat of 100% MgZrO₃. The FGM coating increased the temperature in the combustion chamber, and the thermal strength of the piston. The FGM coated piston surface temperature was lower than the conventional TBC at a similar coating thickness. The increase in the number of layers cuts the thickness of the topcoat. Thus, it increases the thermal diffusivity and decreases the insulation capability of the coating. From the ANSYS studies, the maximum surface temperature of the FGM AlSi alloy and steel pistons were increased by 28% and 17%, with a temperature difference of 13 - 14% with the coated FGM (Buyukkaya, 2007).

2.8 Palm Oil Methyl Ester as Biodiesel

The present study focused on the research gaps found in the literature on alternative fuels in the automotive field, to improve, enhance, or eliminate these gaps using an engineered mechanical solution, specifically through the adoption of enhanced coating technologies in the diesel engine. There are several disadvantages of biodiesel, such as higher viscosity and low calorific values in this case, and more fuel for burning is required to achieve the same performance as the other conventional fuels. Furthermore, the oxygen content in vegetable oils increases the exhaust NO_x levels. Unlike the 100% palm oil biodiesel, diesel, petrol, Pongamia oil, cottonseed oil, blend of crude Jatropha oil and carbureted oil, and frying oil in the context of coatings, which have been explored and analysed. Malaysia is one of the main palm oil producers. Hence, palm oil in the context of coating technology should be studied. The 100% palm oil biodiesel, also known as B100 palm biodiesel, is a type of biodiesel blend, which contains 100% biodiesel without any diesel blend. Generally, the application of biodiesel as a fuel offers several advantages besides it being a renewable resource, such as a high cetane number, lower content of sulphur and aromatic compounds,

and emits a lower content of CO unburnt HC and particulate matters (Özçelik et al., 2015). Engineers have always driven the exploration of energy-efficient engines as the total consumption of the petroleum-based fuels such as diesel, which was increased proportionally with the demands from power generation, industrial, and transportation areas (Karthickeyan and Balamurugan, 2017). Therefore, introducing TBC into the engine design is necessary to overcome efficiency problems, as this coating technology is proven to significantly increase the power/thrust, and decrease the specific fuel consumption (Ahmaniemi et al., 2004). Besides that, other positive advantages from TBC applications were the reduced heat losses and thermal efficiency, lower pollution, and increased durability of engine components (Azadi et al., 2013).

The depletion of the world's petroleum-based fuel reserves, uncertainty in fuel prices, and increasing greenhouse gas emissions, have raised the interest in researching alternative and sustainable energy resources. Biodiesel, a non-toxic and renewable energy resource, was introduced as an alternative solution for diesel (Johari et al., 2015). This environmentally friendly energy resource led to less emissions of greenhouse gases, unburnt HC, and polycyclic aromatic compounds (Demirbas, 2007). However, the application of biodiesel in unmodified internal combustion diesel engines significantly declines the performance of the engine and combustion characteristics, which might be caused by the physicochemical properties of the biodiesel itself (Hossain and Davies, 2010)(Sakthivel, Selvakumar and Gopalakrishnan, 2014).

Thus, various aspects of engine modification have been explored to overcome this drawback, and the TBC seems to be a positive solution (Masera and Hossain, 2019) (Ganapathy, Gakkhar and Murugesan, 2011).

Diesel fuel (conventional) has a sufficient supply trend which increases compared to demand, due to a surplus and plenty of new extraction methods, such as shallow gas, etc. However, the scenario might change in the future, as crude is a natural resource. Hence, research in alternative fuels will enlighten the spirit of sustaining and innovating available resources for the next generation. Palm Oil Biodiesel B100 would be one of the best alternative resources for crude supplies. Malaysia is known for being one of the major palm oil producers which is able to generate higher production for palm oil, to support the domestic and international market. With the B5 & B7 policy, Malaysia currently covers more than 5% of its gross domestic product (GDP). The key steps taken by the Malaysian government for the successful implementation of the B10 program are discussed in this review study. Today, Malaysia has implemented the B5 (blend of 5% palm oil and 95% petroleum diesel), and B7 (blend of 7% palm oil and 93% petroleum diesel) biodiesel. This initiative by the government will increase the Crude Palm Oil (CPO) prices. If the CPO prices rise, the farmers and the country's revenue will also increase. Hence, the direction towards biodiesel would be wise, and more research efforts towards biodiesel will create a proven successful track record, which might bring governments or authorities to emphasise the B100 policy. If the B100 policy is in place, then conventional diesel will be chemically modified in the refinery to be used as an ultra-low sulphur diesel, or base oil for oil-based mud drilling, feedstock for chemical industries, and so on. Biodiesel B100 will be used for this experiment, and it is believed that it will create a track record for another success story.

2.9 Summary

Generally, the most used in research for TBC is the $Y_2O_3.ZrO_2$ coated piston, and alternately, the $Al_2O_3.SiO_2$ coated piston. TBC was found to be significant in reducing HC and CO_2 . Furthermore, it also reported a slight increase in the BTE and a reduction in the BSFC. Further studies are required for the B100 for the coated $Al_2O_3.SiO_2$. $Al_2O_3.SiO_2$ would be one of the commercial candidates for TBC, as the coating is half of the cost of the $Y_2O_3.ZrO_2$. However, in terms of performance, the $Y_2O_3.ZrO_2$ might perform better than the $Al_2O_3.SiO_2$. A direct comparison between these two coatings has not been reported so far. Hence this study will focus on the effects of TBCs for $Al_2O_3.SiO_2$ and $Y_2O_3.ZrO_2$ toward the engine performance and emission analysis.

Furthermore, the experimental work seeks to identify the best match of blended coatings between $Y_2O_3.ZrO_2$ and $Al_2O_3.SiO_2$ to lower the cost of coatings for the TBC. The market is much more niched, and competitive prices will ultimately match the performance and delivery of the products. In the spirit of “innovate to commercialize”, the blend between these coatings might improve the savings compared to 100% Ytria $Y_2O_3.ZrO_2$ coatings. There has been a gap in the research for TBC, whereby the NO emissions were higher than an uncoated piston. Theoretically, NO values will increase with the increase in the heat. Hence, for this experiment, the coating shall be done on the piston crown only, and it is believed that the NO emission will be reduced, since the heat is capsuled partially.

CHAPTER 3

RESEARCH METHODOLOGY

3.1 Introduction

This chapter presents the research methodology and experimental setup for achieving the primary objective of this research investigation. The diesel engine experiment setup is explained in this chapter. The detailed schematic of the research methodology is shown in Figure 3.1, and the test details including test conditions are tabulated in Table 3.5. The TBC and blend between $Y_2O_3.ZrO_2$ and $Al_2O_3.SiO_2$ were developed and coated on the top surface of the piston crown using a plasma spray method, which is described in detail in this chapter, and was established to accomplish the objectives of the research study. The raw powder of TBC $Y_2O_3.ZrO_2$ and $Al_2O_3.SiO_2$ was purchased through a local supplier. The B100 palm biodiesels and baseline petroleum diesel fuel was used as a direct injected fuel in the Kubota diesel engine. The tested fuel of the B100 palm biodiesel and conventional petroleum diesel was also purchased through local supplier. The engine-out-responses parameter analysis included the aspects of the engine's performance, emissions, and durability.

3.2 Research Flow Chart

The detailed schematic of the research methodology is shown in Figure 3.1

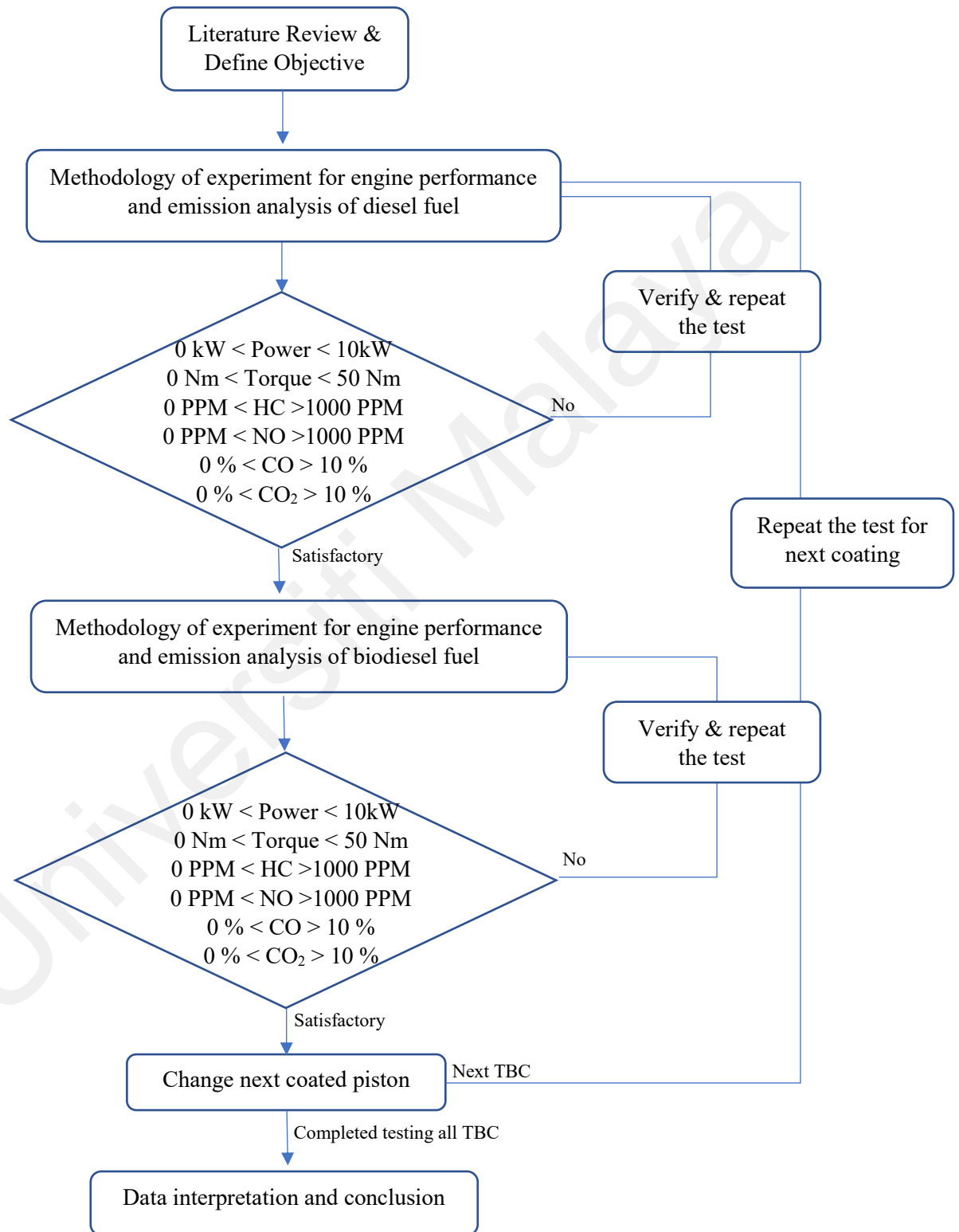


Figure 3.1: Schematic representation of the research methodology

3.3 Morphological Characteristic of TBC

Both the $Y_2O_3.ZrO_2$ and $Al_2O_3.SiO_2$ were in powder form, and originated from Oerlikon Metco in Shanghai, China. The raw material was purchased through a local supplier, and was coated on a piston crown top surface by a local service provider, Metatech Sdn Bhd. By applying plasma spray, the abrasive powder was melted into ionized gas on the piston's surface, resulting in the formation of a coating layer on the piston crown. The plasma spray was equipped with a powder feeder, gas supply, spray gun, power unit, controller, cooling unit, and holder. The ceramic coating materials were $Y_2O_3.ZrO_2$ (purity 99.9 %) and $Al_2O_3.SiO_2$ (purity 99.9 %), which was used in this experimental test. Before the application of the coating, acetone was used to clean the surface of the piston, and the process proceeded with a grit blasting to increase its surface roughness to enhance the grip of the coating toward the surface of the piston.

$Al_2O_3.SiO_2$ is a fused and crushed material developed specifically for applying plasma spray as part of a TBC. The SEM of the $Al_2O_3.SiO_2$ powder morphology is shown in Figure 3.2. The typical material characteristics of $Al_2O_3.SiO_2$ are presented in Table 3.1. $Al_2O_3.SiO_2$ has a lower thermal expansion compared to $Y_2O_3.ZrO_2$. Furthermore, $Al_2O_3.SiO_2$ also delivers lower thermal conductivity, superior abrasion resistance, and higher phase stabilization through the life span of the coating, and an allowable operating temperature in the combustion engine's operations.

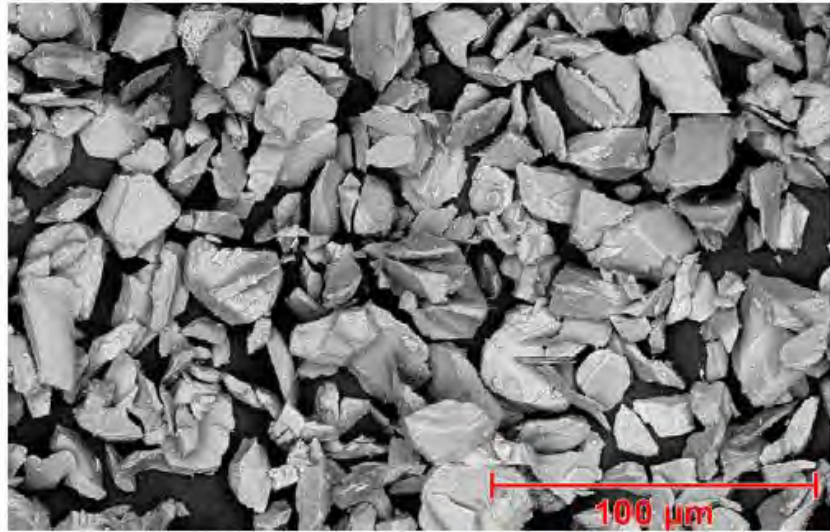


Figure 3.2: SEM photomicrographs (1000X of magnification) of $\text{Al}_2\text{O}_3.\text{SiO}_2$ powder morphology (Oerlikon, 2014)

Table 3.1: $\text{Al}_2\text{O}_3.\text{SiO}_2$ Material Characteristic

Classification	Ceramic, Aluminium Silicate		
Chemistry	$3\text{Al}_2\text{O}_3 \cdot 2\text{SiO}_2$		
Manufacture	Fused & Crushed		
Morphology	Irregular		
Thermal Expansion Coefficient	$5 - 6 \times 10^{-6} / ^\circ\text{C}$		
Thermal Conductivity	2.5 – 3.5 W/mK		
Service Temperature	$\leq 1300 ^\circ\text{C}$		
Chemical Composition	Weight percentage (nominal)	Al_2O_3	Balance
		SiO_2	23 – 28
		Other Oxides	1 max
Powder Characteristics	Nominal range (μm)		- 45 +5
		D90	35 – 40
		D50	20 – 25
		D10	10 – 15

$\text{Y}_2\text{O}_3.\text{ZrO}_2$ was fused with a pre-alloy and crushed into powder form and a consistent size, before dry spraying. As shown in Figure 3.3, the spheroidal shape promotes chemical homogeneity, structural stability, and exceptional flow, which enhances the life span and reliability of the TBC. The typical material characteristics of the $\text{Y}_2\text{O}_3.\text{ZrO}_2$ is presented in Table 3.2, and the TBC working parameter is shown in Table 3.3.

Powders formed with fine particle distributions such as $Y_2O_3.ZrO_2$ are shown in figure 3.3, and compared to $Al_2O_3.SiO_2$ in figure 3.2. They archetypally produce denser coating microstructures that show better material deposition characteristics for the TBC, and have slightly better bonding characteristics.

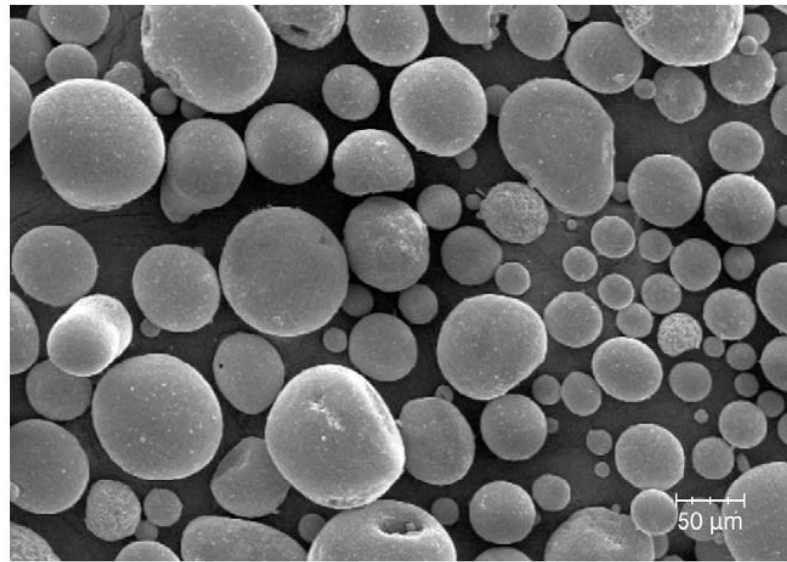


Figure 3.3: SEM photomicrographs (1000X of magnification) of $Y_2O_3.ZrO_2$ powder morphology (Oerlikon, 2014)

Table 3.2. $Y_2O_3.ZrO_2$ Material Characteristic.

Classification	Ceramic, Zirconia Based	
Chemistry	ZrO_2 8 Y_2O_3	
Manufacture	Agglomerated & HOSP™	
Morphology	Spheroidal	
Thermal Expansion Coefficient	$10 \times 10^{-6} / ^\circ C$	
Thermal Conductivity	0.8 – 1.3 W/mK	
Service Temperature	≤ 1250 °C	
Chemical Composition	ZrO_2	Balance
	Y_2O_3	7.0 – 9.0
	SiO_2	0.7
	TiO_2	0.2
	Al_2O_3	0.2
	Fe_2O_3	0.2
	Monoclinic Phase	~6
Powder Characteristics	Nominal range (μm)	-125 +11
	D90	93 – 103
	D50	50 – 57
	D10	21 – 25

Table 3.3: TBC Working Parameters.

Parameter	Y ₂ O ₃ .ZrO ₂	Al ₂ O ₃ .SiO ₂
Voltage	20 kV	20 kV
Working distance	15 mm	15 mm
Rotating Speed	25 rpm	25 rpm
Temperature	800 ± 50 °C	800 ± 50 °C

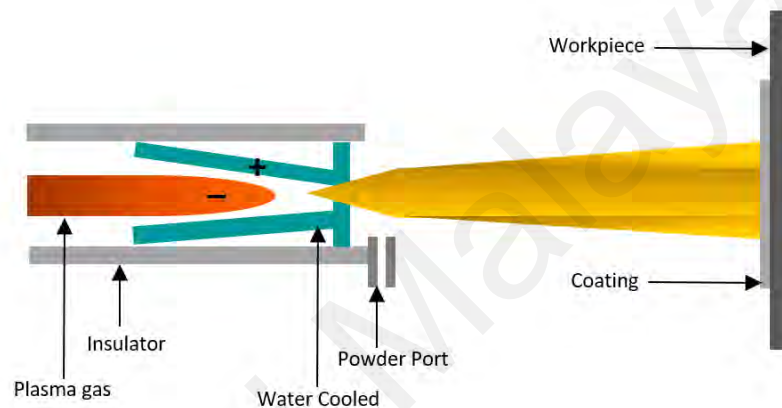


Figure 3.4: Plasma Spray Coating

As shown in Figure 3.4, the Plasma Spray Method is a methodology performed under atmospheric pressure. The high-frequency electric arc is ignited between a tungsten cathode and an anode. Gas penetrates through the interelectrode space, and becomes ionised, and creates a plasma plume (temperature ranging from 6000-13000 °C) towards the substrate's surface. TBC in the form of a powder is directed in front of the gas nozzle to the ionized plasma plume, whereby a molten TBC layer is created on the surface top crown of the piston as a randomly stacked lamellae.

This experimental test involved three-piston types; an uncoated piston, a Y₂O₃.ZrO₂-coated piston crown, and an alumina-coated piston crown. The TBC was built on the piston crown using the plasma spray technique.

A small amount of SiO_2 was introduced and blended into the Al_2O_3 coating. NiCrAl was used to bond the TBC with the surface of the piston crown. Figure 3.5 presents a schematic diagram for the TBC of $\text{Y}_2\text{O}_3\cdot\text{ZrO}_2$ and alumina on the piston crown.

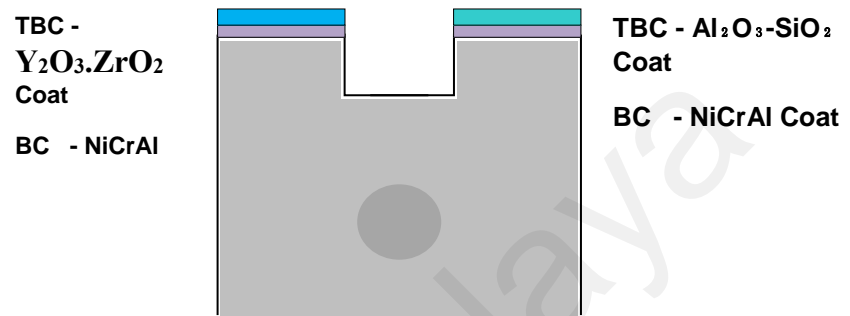


Figure 3.5: TBC layer on piston

For the second phase of the experiment, five (5) piston types were prepared, including an uncoated piston. The piston crowns were coated with a blend between the coating powder of $\text{Y}_2\text{O}_3\cdot\text{ZrO}_2$ and the $\text{Al}_2\text{O}_3\text{-SiO}_2$ coating. The TBC were built on the piston crown using the plasma spray technique. NiCrAl was used to bond the TBC with the surface of crown piston. The configuration of the blended TBC between the $\text{Y}_2\text{O}_3\cdot\text{ZrO}_2$ and $\text{Al}_2\text{O}_3\text{-SiO}_2$ coating built on the piston crown is presented in Figure 3.6.

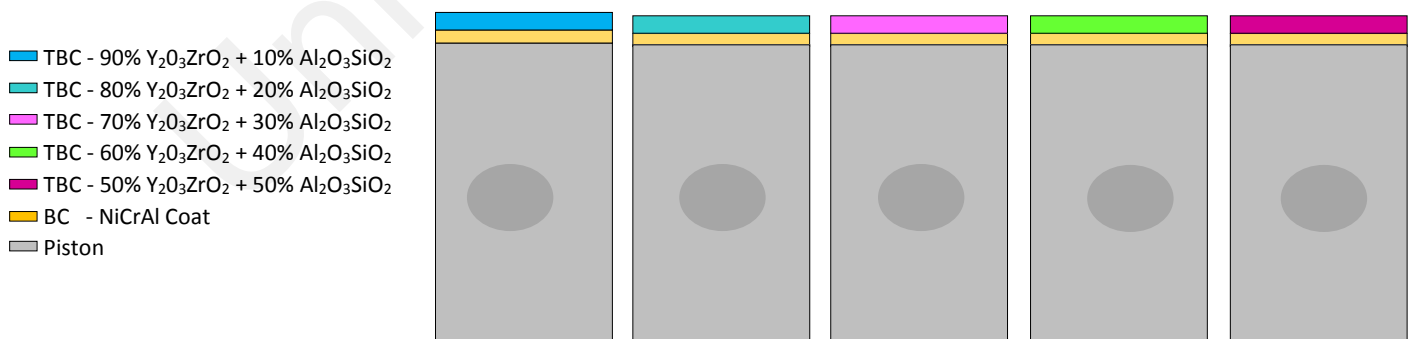


Figure 3.6 Piston crown configuration with specific coating mixture

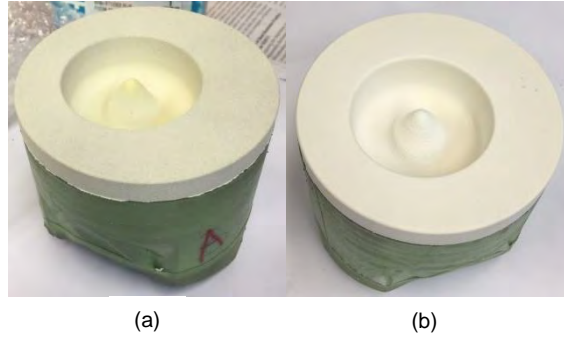


Figure 3.7: Piston coated with (a) $Y_2O_3.ZrO_2$ and (b) $Al_2O_3.SiO_2$

Both $Y_2O_3.ZrO_2$ and alumina were in powder form. By applying plasma spray, the abrasive powder is melted in the ionized gas on the piston's surface, resulting in the formation of a coating layer on the piston's crown. The plasma spray was equipped with a powder feeder, gas supply, spray gun, power unit, controller, cooling unit, and holder. The ceramic coating materials of the $Y_2O_3.ZrO_2$ (purity 99.9%) and alumina (purity 99.9%) used in this experimental test was readily available. Prior to applying the coating, acetone was used to clean the surface of the piston, and the process proceeded with grit blasting to increase the surface roughness to enhance the grip of the coating toward the surface of the piston. In addition, the tested fuels were commercial diesel and B100 palm biodiesel. Table 3.4 lists the TBC used in this study, while Table 3.6, Table 3.7, and Table 3.8 list the biodiesel and diesel fuel's physical and chemical properties.

Table 3.4: List of the TBC

Piston	Fuel	Type
First Phase : Conventional TBC		
Uncoated	Diesel	P1D
	B100 Palm	P1B
Coated Pure 100% $Y_2O_3.ZrO_2$	Diesel	P2D
	B100 Palm	P2B
Coated Pure 100% $Al_2O_3.SiO_2$	Diesel	P3D
	B100 Palm	P3B
Second Phase : Blend TBC		
Coated Pure 90% $Y_2O_3.ZrO_2$ + 10% $Al_2O_3.SiO_2$	Diesel	90/10D
	B100 Palm	90/10B
Coated Pure 80% $Y_2O_3.ZrO_2$ + 20% $Al_2O_3.SiO_2$	Diesel	80/20D
	B100 Palm	80/20B
Coated Pure 70% $Y_2O_3.ZrO_2$ + 30% $Al_2O_3.SiO_2$	Diesel	70/30D
	B100 Palm	70/30B
Coated Pure 60% $Y_2O_3.ZrO_2$ + 40% $Al_2O_3.SiO_2$	Diesel	60/40D
	B100 Palm	60/40B
Coated Pure 50% $Y_2O_3.ZrO_2$ + 50% $Al_2O_3.SiO_2$	Diesel	50/50D
	B100 Palm	50/50B

3.4 Equipment Setup

The experiment was conducted in the Heat Engine Laboratory, at the Department of Mechanical Engineering, University of Malaya. The working area and complete setup of the experiment for this research study is shown in Figure 3.8.

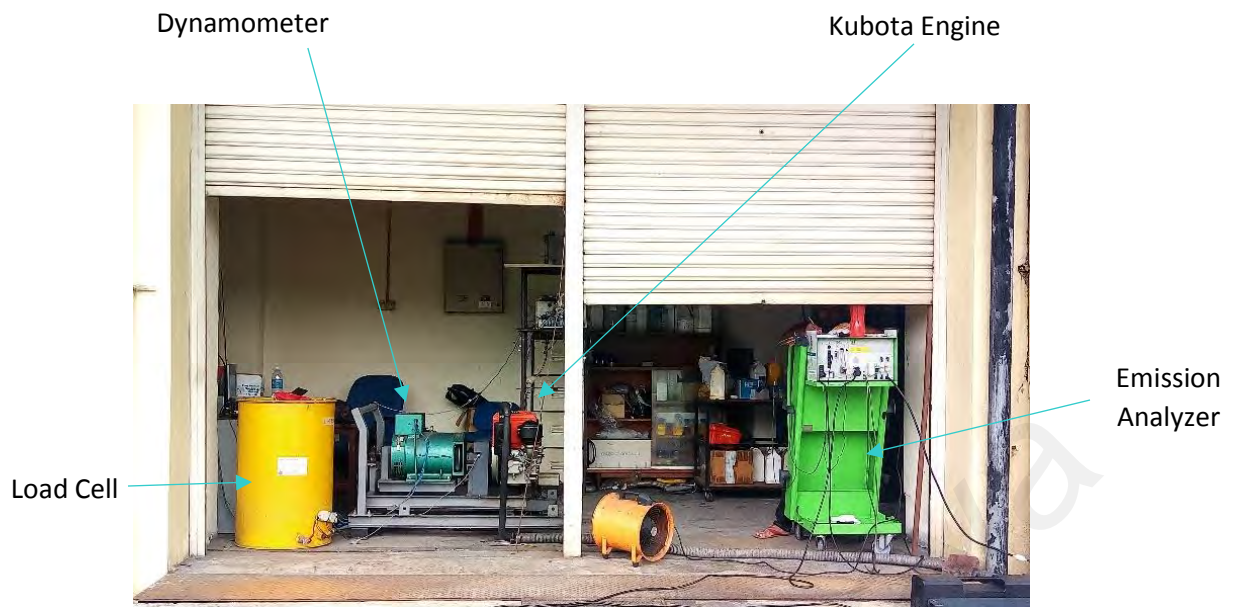
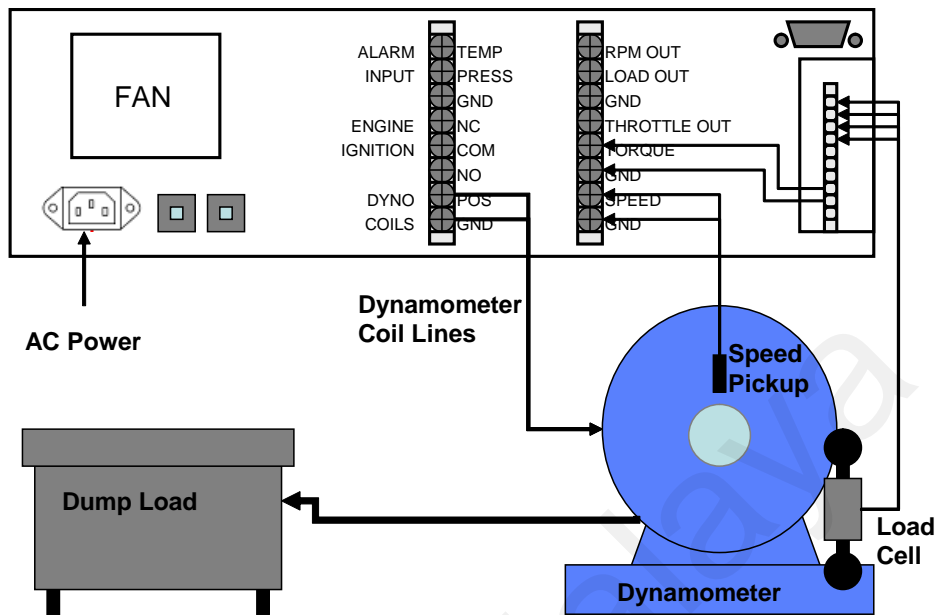


Figure 3.8: Complete setup of experiment

A single-cylinder, four-stroke, water-cooled, naturally aspirated direct injection diesel engine was employed for this research. The specifications of the engine are listed in Table 3.5. As shown in Figure 3.9, an eddy current dynamometer was connected to the engine to measure and adjust the engine's speed.



! NOTE: Wiring shown for use with internal load cell amplifier.
 When using external amplifier take the analog output directly into the 0-10V Torque Input and leave the internal amplifier unconnected.
 Dyno Coil lines may carry >100V and >10A. Dump Load lines may carry >300VAC and >30A. Use appropriate wiring and precautions.

Figure 3.9: Dynamometer setup of experiment (Focus Applied Technologies, 2017)

A positive-displacement type flow meter was used to measure the fuel flow. The engine fuel system was adjusted by including two individual tanks with two-way valves for diesel and biodiesel blends, which empowered a fast fuel exchange. The performance data was collected from a data-acquisition system, which was monitored with the help of software.

Table 3.5: Specification of a single cylinder Kubota RT125 diesel engine in heat engine laboratory, department of mechanical engineering, University of Malaya

Model	RT125DI-ES
Type	Water cooled 4 stroke horizontal diesel engine
Cylinder No	1
Bore x Stroke	94 mm x 96 mm
Displacement	666 cc
Max Output	9.2 kW / 2400 rpm
Compression Ratio	18:1
Max. Torque	4.7 kg-m / 1600 rpm
Combustion System	Direct injection
Piston Material	High Strength Aluminium Alloy JIS AC8A

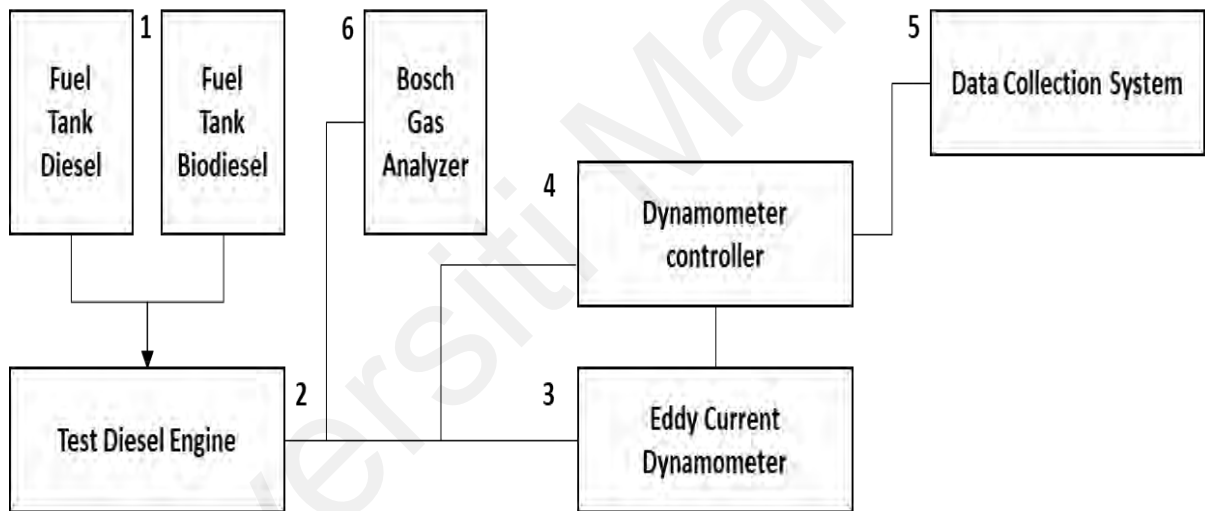


Figure 3.10: Engine setup for the experiment

Figure 3.10 shows the schematic view of the experimental test setup which includes a single-cylinder, four stroke, direct injection diesel engine. The details of the test engine (Kubota RT 125) are presented in Table 3.5 and Figure 3.11. A generator type dynamometer was included for this experimental test setup to hold the engine load and speed. The function of an eddy current dynamometer is to provide brake power (Karthickeyan and Balamurugan, 2017).

Besides that, this experimental test setup was also equipped with a data acquisition system to collect data and analyse the performance of the tested fuels according to various types of piston coatings. The injection system used for this experiment was a direct injection combustion system (KUBOTA RT125DI-ES), and the details are shown in Table 3.5.



Figure 3.11: Kubota RT-125 diesel engine

The thickness of the coating on the piston was $400\mu\text{m}$ with a $100\mu\text{m}$ lining layer of NiCrAl. For the engine loading, an electric dynamometer which could operate at 7.5 kW and a max 5000 rpm (± 50) was used. The data obtained during the engine tests were recorded in the computer, as shown in Figure 3.11, using the interface of the engine test device, depending on the time. Simultaneously with these measurements, the emission values were measured from the emission device, and recorded by print out.



Figure 3.12: Controller setup & data collection

The experimental test was conducted at a temperature of 32°C and humidity of 61%, according to different speed settings at full loaded engine operation conditions. According to the manufacturer, the full load engine speed can be achieved at the lowest engine speed of 1000 rpm. However, for safety reasons, this experimental test's lowest engine test speed was reduced to 1200 rpm since the engine's vibration was excessively high during the full load condition. Besides that, the engine's throttle was set at the maximum requirement. Following that, the engine's speed was gradually reduced at the interval of 200 rpm, from 2400 rpm to 1200 rpm. Expectedly, the dynamometer increased the load applied to the engine to achieve the desired speed as the speed decreased. A similar step was repeated for each coated piston and fuel type. Furthermore, each experimental test was repeated three times to obtain an average value. The consistency of the recorded values was ensured with minimal measurement errors. The recorded data was transformed into a graph format to facilitate the analysis and observations.

Prior to taking each reading, the engine was operated at a steady condition for 5 to 7 minutes for all tested pistons and fuel types. The data for the fuel consumption, torque, power, HC, CO, CO₂, NO, and HC were all recorded. All testing and data collection were performed using a controller, and recorded on the computer. An exhaust emission test was conducted using a BOSCH model emission analyser. This device was equipped with a NO sensor and can measure the smoke opacity using an additional probe linked to the opacimeter unit. A positive-displacement type flow meter was used to measure the fuel flow rate.

The physicochemical properties of tested fuels and the local suppliers of the commercial diesel and B100 palm oil methyl ester is shown in Table 3.6 and Table 3.7. The fatty acid composition of palm oil methyl ester is listed in Table 3.8. The palm oil methyl ester was purchased from Future Prelude Sdn. Bhd.

Table 3.6: Physicochemical properties of the tested fuels, diesel

Properties	Guaranteed Level		Test Method
	Minimum	Maximum	
Colour (ASTM)	-	2.5	MS 2010/ ASTM D1500/ D6045
Ash, mass %	-	0.01	MS 2013/ ASTM D482
Pour point, °C	-	15	MS 2009/ ASTM D97/ D5950/ D5985/ D5949
Flash point, °C	60	-	MS 686/ ASTM D93
Calorific value, MJ/kg	45.27		
Kinematic viscosity at 40°C, mm ² / s	1.5	5.8	MS 1831/ ASTM D445
Copper corrosion (3 h at 100°C)	-	1	MS 787/ ASTM D130
Water by distillation, vol %	-	0.05	MS 1800/ ASTM D95/ D6304
Sediment by extraction, mass %	-	0.01	MS 790/ ASTM D473
Carbon residue, mass %	-	0.20	MS 962/ ASTM D189/ D4530
Density at 15°C, kg/l	0.810	0.870	MS 1893/ ASTM D1298/ D4052
Acid number, mg KOH/g	-	0.25	MS 2011/ ASTM D664/ D974/D2624
Electrical conductivity, pS/m	50	-	MS 1889/ ASTM D2624
Cetane index or Cetane number	49 49	- -	MS 1890/ ASTM D976/ D4737 MS 1895/ D613/ D6890/ IP498
Distillation at 95 %, °C	-	370	MS 563/ ASTM D86
Total sulphur, mg/kg	-	500	MS 1891/ ASTM D4294/ D2622/ D5453
Lubricity, µm	-	460	MS 1892/ ASTM D6079

Table 3.7: Physicochemical properties of the tested fuels, palm oil methyl ester

Test Parameter	Analysis Method	Unit	Specification	Result
Ester Content	EN 14103	%	96.50 min	98.12
Density at 15°C	EN ISO 3675	Kg/m ³	860.00 - 900.00	875.3
	EN ISO 12185	Kg/l	0.86 - 0.90	0.8753
Kinematic Viscosity at 40 °C	EN ISO 3104	mm ² /sec	3.50 - 5.00	4.35
Flash point	EN ISO 2719	Deg C	101 min	175
Calorific value	D240	MJ/kg	-	39.9
Cold filter plugging point	EN 116	Deg C	12-13	12
Sulfated ash content	EN ISO 3987	% (m/m)	0.02 max	<0.02
Water content	EN ISO 12937	mg/kg	500 max	356
		%	0.050 max	0.036
Acid value	EN 14104	mg KOH/g	0.50 max	0.32
Iodine value	EN 14111	g l/100g	120.00 max	51.70
Linoleic acid methylester content	EN 14103	% (m/m)	12.00 max	0.22
Methanol content	EN 14110	% (m/m)	0.20 max	0.01
Monoglycerides content	EN 14105	% (m/m)	0.70 max	0.62
Diglycerides content	EN 14110	% (m/m)	0.20 max	0.16
Triglycerides content	EN 14105	% (m/m)	0.20 max	0.03
Content of free glycerol	EN 14105	% (m/m)	0.02 max	0.011
Content of total glycerol	EN 14105	% (m/m)	0.25 max	0.19
Oxidation stability	EN 14112	Hrs	8.00 min	28.05

Table 3.8: Fatty acid composition of palm oil methyl ester

Property	Formula	PME
C4:0 (Butyric acid)	C ₄ H ₈ O ₂	0.15
C6:0 (Caproic acid)	C ₆ H ₁₂ O ₂	0.08
C8:0 (Caprylic acid)	C ₈ H ₁₆ O ₂	0.21
C10:0 (Capric acid)	C ₁₀ H ₂₀ O ₂	0.18
C12:0 (Lauric acid)	C ₁₂ H ₂₄ O ₂	1.56
C14:0 (Myristic acid)	C ₁₄ H ₂₈ O ₂	1.4
C15: 0 (Pentadecanoic acid)	C ₁₅ H ₃₀ O ₂	0.05
C16:0 (Palmitic acid)	C ₁₆ H ₃₂ O ₂	36.74
C17:0 (Heptadecanoic acid)	C ₁₇ H ₃₄ O ₂	0.10
C18:0 (Stearic acid)	C ₁₈ H ₃₆ O ₂	4.23
C20:0 (Arachidic acid)	C ₂₀ H ₄₀ O ₂	0.00
C21:0 (Heneicosanoic acid)	C ₂₁ H ₄₂ O ₂	0.07
C24:0 (Lignoceric acid)	C ₂₄ H ₄₈ O ₂	0.10
C16:1n7 (Palmitoleic acid)	C ₁₆ H ₃₀ O ₂	0.19
C18:1n9t (Elaidic acid)	C ₁₈ H ₃₄ O ₂	0.7
C18:1n9c (Oleic acid)	C ₁₈ H ₃₄ O ₂	41.9
C18:2n6c (Linoleic acid)	C ₁₈ H ₃₂ O ₂	10.03
C18:2n6t (Linolelaidic acid)	C ₁₈ H ₃₂ O ₂	0.31
C18:3n6 (γ -Linoleic acid)	C ₁₈ H ₃₀ O ₂	0.42
C18:3n3 (Linolenic acid)	C ₁₈ H ₃₀ O ₂	0.19
C20:1 (<i>cis</i> -11-Eicosenoic acid)	C ₂₀ H ₃₈ O ₂	0.19
C20:2 (<i>cis</i> -11,14-Eicosadienoic acid)	C ₂₀ H ₃₆ O ₂	1.13
C20:3n6 (<i>cis</i> -8,11,14-Eicosatrienoic acid)	C ₂₀ H ₃₄ O ₂	0.08
Fatty acid saturation /unsaturation ratio (wt.%/wt.%)	-	44.87 / 55.14

3.5 Engine performance analysis

3.5.1 BSFC and BTE

The Brake Specific Energy Consumption (BSEC) is the ratio of the energy obtained by burning fuels for an hour, to the actual energy obtained at the wheels. The BSEC of diesel engines depends on the relationship between the BSFC and the calorific value of any fuel (Mishra & Nayak, 2018). The BSFC is the ratio between the mass fuel consumption and brake's effective power, and for a given fuel, it is inversely proportional to the thermal efficiency (Enweremadu & Rutto, 2010). If the latter is unchanged for a fixed engine operation mode, the specific fuel consumption when using a biodiesel fuel is expected to increase by around 13% in relation to the consumption of the diesel fuel, corresponding to the increase in the heating value on a mass basis (N. Kumar, Varun, & Chauhan, 2013). Hence, the loss in the heating value of the biodiesel must be compensated by a higher fuel consumption.

The BSFC and BTE were calculated using the following equations:

$$BSFC(g/kWh) = \frac{m_f}{BP} \quad [3.1]$$

Where,

m_f = Fuel consumption, g/h,

BP = Brake power, kW

3.5.2 Brake power

The Brake Power (BP) is the ultimate output power provided by the engine, and is defined as the outcomes of the engine torque and angular speed. The brake power of an engine is directly proportional to the torque and engine speed.

The brake power was calculated using the following equation:

$$BP (kW) = \frac{2\pi NT}{60} \quad [3.2]$$

Where, N is the engine speed in rpm, and T represents the engine torque.

3.5.3 BTE

BTE is the ratio between the power output and the energy introduced through fuel injection. The latter is the product of the injected fuel mass flow rate, and the lower heating value (Basha, Gopal, & Jebaraj, 2009). Thus, the inverse of thermal efficiency is often called brake-specific energy consumption. Since it is usual to use the brake power for determining thermal efficiency in experimental engine studies, the efficiency obtained was a brake-specific efficiency. This parameter was more appropriate than fuel consumption, to compare the performance of different fuels, besides their heating values.

The BTE was calculated using the following equation:

$$BTE (\%) = \frac{BP \times 100}{C.V \times m_f} \quad [3.3]$$

Where, m_f = Fuel consumption, and $C.V$ = Calorific value.

3.5.4 Exhaust emission analysis

Biodiesel seems to be much more environmentally friendly compared to ordinary fossil diesel. In this study, the emission of test blended fuels were measured and compared to pure diesel fuel in a diesel engine. The emissions were measured using an exhaust gas analyser to show the data for the CO, CO₂, HC, and NO. The readings of the gas analyser was changed every five seconds, so that three readings were taken at three different times. The mean value was recorded from these three readings, and the average values were taken. The smoke opacity was measured using the smoke tester device, mentioned previously in section 3.6 of the user equipment for the experiment. The first fuel which had been used as the baseline diesel, and the average time for the fuel run in the engine, was 15 minutes. The reading data on the emission was taken after the exhaust temperatures and the engine's cooling water was stable. The gas analyser took measurements every 5 seconds for 15 minutes, and then the file of the emission reading data was then saved to calculate the mean values. The same procedure was repeated for the other blended fuels.

3.5.5 Exhaust gas analyser

The exhaust emissions were measured from the engine by utilizing an exhaust gas analyser, BOSCH BEA-350. For measuring the smoke intensity, BOSCH RTM-430 was used. To read the emission data, a digital camera was placed, and the data was taken three times for retaining the measuring accuracy. The mean value of the three readings was recorded, and the average values were taken. Furthermore, the data was taken after 10 to 15 minutes when the engine achieved a stable condition during, and while running experiments for every fuel sample. Figure 3.13 show the picture of the BOSCH gas analyser and smoke meter.



Figure 3.13: BOSCH BEA-350 exhaust gas analyser

3.6 Statistically significance value

Experimental errors and uncertainties can arise from instrument selection, conditions, calibration, environment, observations, readings, and test procedures. The measurement range, accuracy, and percentage of uncertainties are associated with the instruments used in this experiment, and are listed in Table 3.9. Uncertainty analysis is necessary to verify the accuracy of the experiments. The percentage of uncertainties of various parameters, such as BSFC and BTE were determined using the percentage uncertainties of the different instruments employed in the experiment. To compute the overall percentage uncertainty due to the combined effects of the uncertainties of various variables, the principle of the propagation of errors were considered and can be estimated as $\pm 3.5\%$.

The overall experimental uncertainty was computed as follows:

$$\begin{aligned}
 \text{Overall experimental uncertainty (\%)} &= \text{Square root of [(uncertainty of Fuel Flow Rate)}^2 + \\
 &\quad \text{(uncertainty of BSFC)}^2 + \text{(uncertainty of BTE)}^2 + \\
 &\quad \text{(uncertainty of exhaust gas temperature, EGT)}^2 + \\
 &\quad \text{(uncertainty of Smoke)}^2 + \text{(uncertainty of Pressure} \\
 &\quad \text{sensor)}^2] \\
 &= \text{Square root of [(2)}^2 + (1.9)^2 + (1.7)^2 + (0.15)^2 + (1)^2 \\
 &\quad + (1)^2] \\
 &= \sqrt{(4 + 3.61 + 2.89 + 0.0225 + 1 + 1)} \\
 &= \sqrt{12.5225} \\
 &= \pm 3.54
 \end{aligned}$$

Table 3.9: List of measurement accuracy and percentage uncertainties

Measurement	Measurement range	Accuracy	Measurement techniques	% Uncertainty
Load (Nm)	±120	±0.1	Strain gauge type load cell	±1.0
Speed (rpm)	60-10,000	±1	Magnetic pick up type	±0.1
Time (s)	-	±0.1	-	±0.2
Fuel flow measurement (L/hr)	0.5-36	±0.01	Positive displacement gear wheel flow meter	±2.0
Air flow measurement (L/s)	2-70	±0.04	Turbine flow meter	±0.5
CO (%)	0-10.	±0.001	Non-dispersive infrared	±1.0
NO _x (ppm)	0-5,000	±1	Electrochemical	±1.3
Smoke (%)	0-100	±0.1	Photodiode detector	±1.0
EGT sensor (°C)	0-1200	±0.3	Type K thermocouple	±0.15
Pressure sensor (kPa)	0-25,000	±12.5	Piezoelectric crystal type	±1.0
BSFC (g/kWh)	-	±7.8	-	±1.9
BTE (%)	-	±0.5	-	±1.7

CHAPTER 4

RESULT AND DISCUSSION

4.1 Introduction

This chapter presents the experimental results and effects of the TBC base coat and blend coats between $Y_2O_3.ZrO_2$ and $Al_2O_3.SiO_2$ for the emission characteristics, and engine performance of the diesel engine using conventional diesel fuel as baseline fuel, and its pure biodiesel palm oil. Firstly, the effect of an uncoated piston, coated piston with a TBC of $Y_2O_3.ZrO_2$ and a coated piston with $Al_2O_3.SiO_2$ on the engine performance and emissions characteristics of the diesel engine are discussed. Secondly, the impact of conventional diesel and pure palm biodiesel and their respective TBC blends between $Y_2O_3.ZrO_2$ and $Al_2O_3.SiO_2$ in a diesel engine is analysed and discussed. Thirdly, the effect of engine durability running continuously for 6 hours on the piston head surface is discussed. Lastly, commercial studies dealing with the identified optimum TBC blends between $Y_2O_3.ZrO_2$ and $Al_2O_3.SiO_2$ are compared with the baseline TBC of $Y_2O_3.ZrO_2$.

4.2 First Phase: Conventional TBC

This section discusses the effect of the coated piston with the TBC of $Y_2O_3.ZrO_2$ and the coated piston with $Al_2O_3.SiO_2$ on the engine-out responses. Upon completion of the engine setup, three series of tests were conducted to evaluate the performance of the TBC of $Y_2O_3.ZrO_2$ and $Al_2O_3.SiO_2$. The effect of on the engine's performance and emission characteristics of the diesel engine are discussed in the following sub-sections.

4.2.1 Exhaust emission analysis

Figure 4.1 presents the trend of the HC formation at the variable engine speed for the coated piston with the TBC of $Y_2O_3.ZrO_2$, coated piston with $Al_2O_3.SiO_2$ and an uncoated piston. The reason for the HC formation in the combustion products is that the air-fuel remains below the ignition temperatures, due to oxygen shortage in the surrounding environment, whereby partial oxidization is induced.

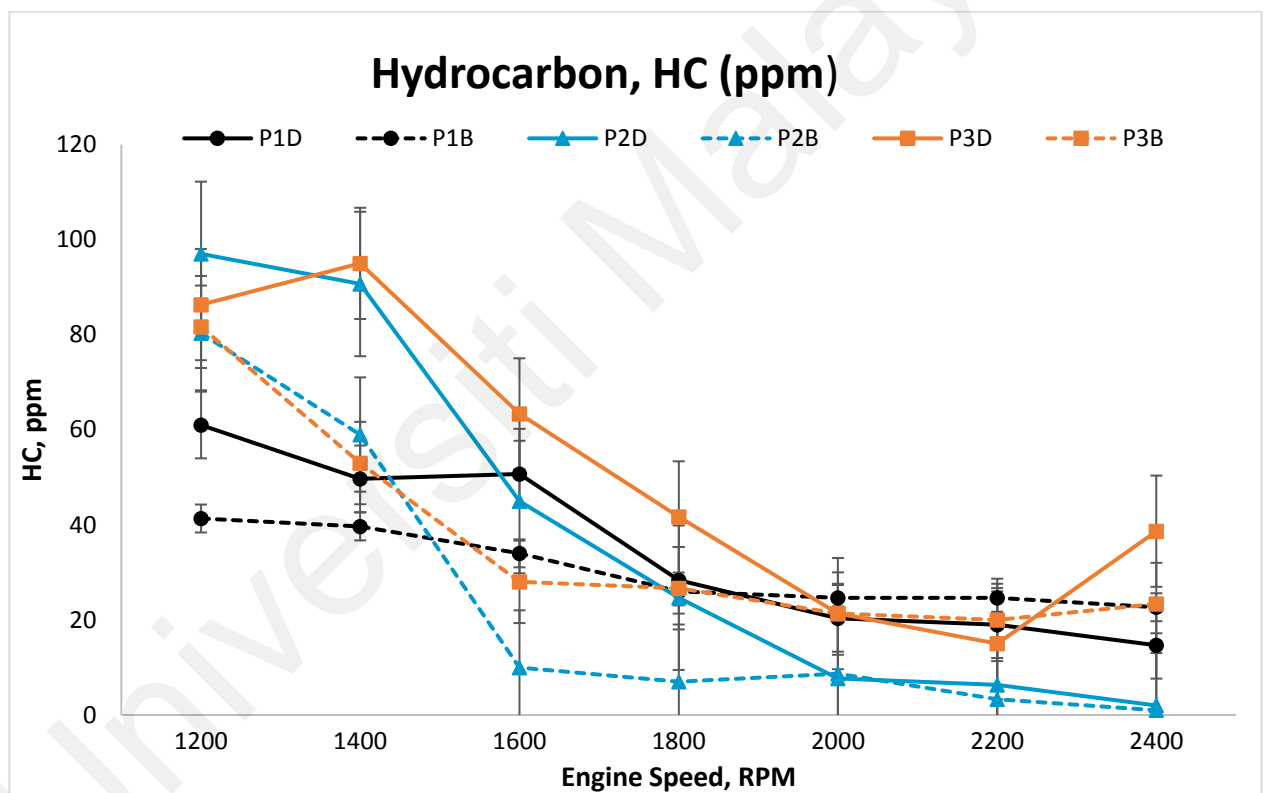


Figure 4.1: HC emission at the variable engine speed

At the maximum load of 1200 rpm, P1D recorded the lowest HC emission (61 ppm), followed by P3D (86 ppm) and P2D (97 ppm). As for the engine operation with biodiesel, P1B recorded the lowest HC emission (41 ppm), followed by P2B (80 ppm) and P3B (82 ppm). The obtained results at the maximum load of 1200 rpm revealed that P1B and P1D yielded a lower HC content.

At the maximum torque of 1600 rpm, P2D recorded the lowest HC emission (45 ppm), followed by P1D (51 ppm) and P3D (63 ppm). As for the engine operation with biodiesel, P2B recorded the lowest HC emission (10 ppm), followed by P3B (28 ppm) and P1B (34 ppm). The obtained results at the maximum torque of 1600 rpm revealed that P2B and P2D yielded a lower HC content.

At the maximum speed of 2400 rpm, P2D recorded the lowest HC emission (2 ppm), followed by P1D (15 ppm) and P3D (39 ppm). As for the engine operation with biodiesel, P2B recorded the lowest HC emission (1 ppm), followed by P3B (23 ppm) and P1B (23 ppm). The obtained results at the maximum speed of 2400 rpm revealed that P2B and P2D yielded a lower HC content.

The results indicated that $Y_2O_3.ZrO_2$ (P2D and P2B) yielded the lowest HC emission, followed by $Al_2O_3.SiO_2$ (P3D and P3B). The uncoated pistons (P1D and P1B) exhibited higher HC emissions. Referring to the decreasing trend of HC emissions with increasing speed in Figure 4.1, the study proved that speed increases the effect of HC emissions. Although HC emissions at low speeds for the coated piston with TBC of $Y_2O_3.ZrO_2$, coated piston with $Al_2O_3.SiO_2$ and uncoated piston were high, with the increase in the engine speed, it was observed that there have been reductions in the HC emissions. In direct injection systems, the fuel pump injects fuel with less fragmentation at lower speeds, as the atomization in the fuel is poor. Hence, this causes formation of higher HC emissions at lower engine speed conditions (Selman et al., 2015).

The average HC emission of the coatings decreased compared to coated $Y_2O_3.ZrO_2$ and $Al_2O_3.SiO_2$ as the fuel reached ignition temperatures, with the high temperatures in the cylinder restricting the TBC (Selman et al., 2015). The combustion chamber and piston head in a standard engine generates less heat than the coated piston; thus, it affects the evaporation capability of the tested fuels. The $Y_2O_3.ZrO_2$ recorded a better fuel evaporation rate due to the increased temperatures in the combustion chamber, and the coated piston's crown. The higher combustion temperatures due to the TBC makes the fuel burn easier and much more effectively (Thiruselvam and Ganesh, 2019). Besides that, TBC initiated a quicker rate of breaking HC into hydrogen and oxygen, when mixed with excess oxygen available in the combustion chamber. Therefore, the lower emissions of HC were recorded for the coated piston (Karthickeyan and Balamurugan, 2017).

In addition, the B100 palm biodiesel was found to yield lower HC emissions compared to conventional diesel. Biodiesel enhances the oxygen molecules, resulting in better and a much more complete combustion, which subsequently decreases the HC emissions (Senthikumar et al., 2015; Behçet et al., 2015). The oxidation chemistry was found to be suppressed due to the limited availability of oxygen in the air-fuel mixture at lower speeds. At higher speeds, the coated engine, particularly the $Y_2O_3.ZrO_2$, was found to perform well for both tested fuels due to the lower thermal conductivity, compared to $Al_2O_3.SiO_2$. Overall, the experimental results revealed that biodiesel yielded lower HC emissions than the use of diesel. Besides that, $Y_2O_3.ZrO_2$ (P2D and P2B) were found to maintain good stability and released the lowest HC emissions for both tested fuels at high speeds and high torque engine settings.

Figure 4.1 shows the trend of NO formation at variable engine speeds for the coated pistons with the TBC of $Y_2O_3.ZrO_2$, coated pistons with $Al_2O_3.SiO_2$ and the uncoated piston. Both $Y_2O_3.ZrO_2$ -coated and alumina-coated pistons substantially reduced the NO emission, compared to the uncoated piston. With or without the coating layer, all pistons yielded lower NO emissions, as the engine speed increased.

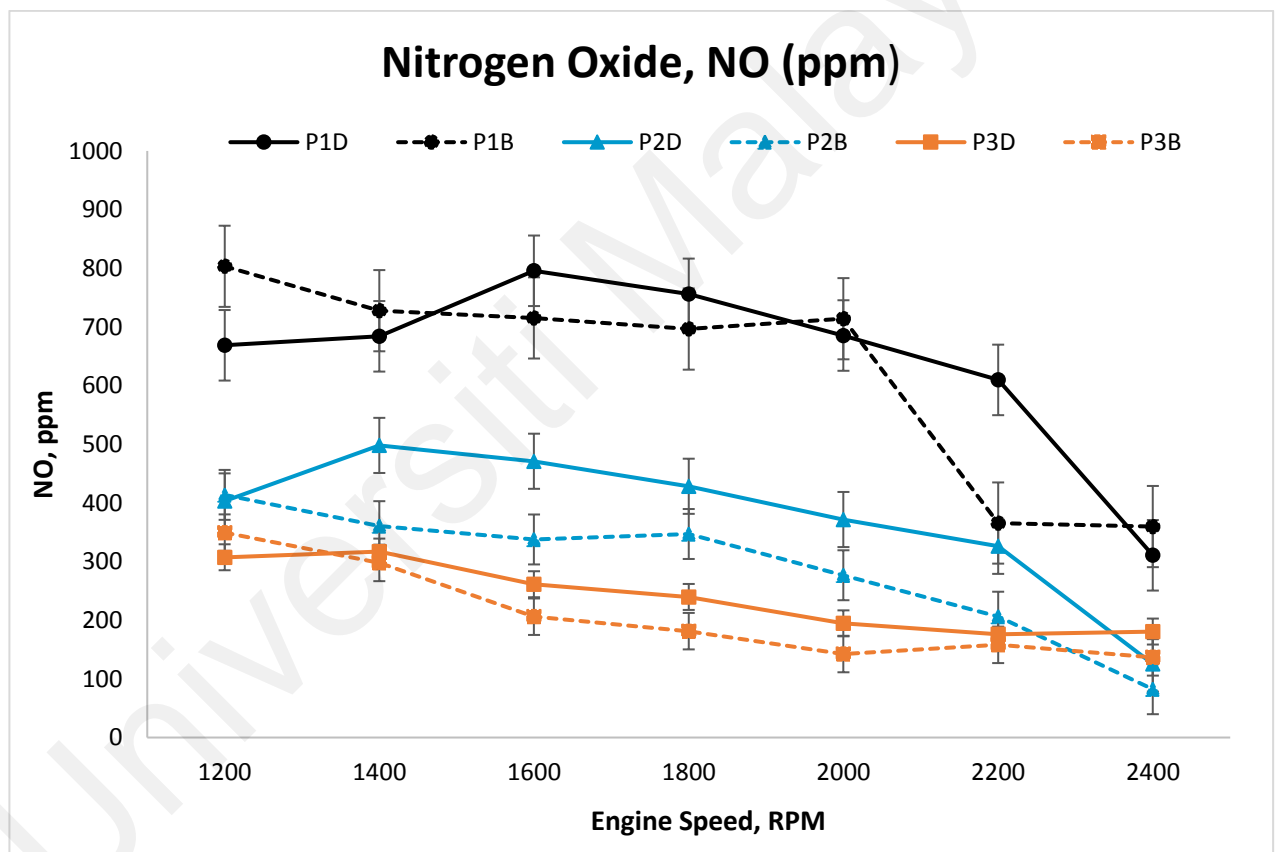


Figure 4.2: NO emission at the variable speed

Based on the reading recorded for the NO emission, at the higher load of 1200 rpm, P3D showed the lowest NO emission (307 ppm), followed by P2D (403 ppm) and P1D (669 ppm). As for the engine operation with biodiesel, the reading recorded for the NO emission at a higher load, P3B showed the lowest NO emission (349 ppm), followed by P2B (414 ppm)

and P1B (803 ppm). In summary, the obtained results at the higher load of 1200 rpm showed that $\text{Al}_2\text{O}_3\cdot\text{SiO}_2$ (P3B and P3D) yielded lower NO emissions.

Secondly, based on the reading recorded for the NO emission, at the higher torque rate of 1600 rpm, P3D recorded the lowest NO emission (261 ppm), followed by P2D (471 ppm) and P1D (796 ppm). As for the engine operation with biodiesel, the readings recorded for NO emissions at higher torque showed that P3B recorded the lowest NO emission (206 ppm), followed by P2B (338 ppm) and P1B (715 ppm). In summary, the obtained results at the higher torque of 1600 rpm showed that $\text{Al}_2\text{O}_3\cdot\text{SiO}_2$ (P3B and P3D) yielded the lowest NO content.

Lastly, based on the readings recorded for the NO emission, at the highest speed of 2400 rpm, P2D recorded the lowest NO emission (125 ppm), followed by P3D (181 ppm) and P1D (311 ppm). As for the engine operation with biodiesel, the readings recorded for NO emission at higher speed, showed that P2B recorded the lowest NO emission (82 ppm), followed by P3B (137 ppm) and P1B (360 ppm). It can be concluded that, from the obtained results at the higher speeds of 2400 rpm, $\text{Y}_2\text{O}_3\cdot\text{ZrO}_2$ (P2B and P2D) yielded the lowest NO content.

Overall, the use of biodiesel was found to perform better in terms of reducing the NO emissions compared to diesel. Additionally, $\text{Al}_2\text{O}_3\cdot\text{SiO}_2$ (P3D and P3B) was found to maintain good stability, and release the lowest NO emission for both tested fuels across the higher loads and higher torque engine settings. These findings proved the impact of the TBC in terms of reducing the NO_x emissions, one of the sources of environmental pollution that

should be controlled (Karthickeyan and Arulraj, 2014). The increase in the combustion duration increases the fraction of the fuel, which burns later in the cycle, and consequently decreases the NO_x emissions (Dananjayakumar et al., 2021).

NO production involves the reaction between the formed hydroxide (OH) ions, and a nitrogen atom. In this study, alumina-coated piston recorded an excellent NO reduction compared to the Y₂O₃.ZrO₂ coated piston. The present study also found that the use of alumina coatings contributed to lower NO emissions, as compared to Y₂O₃.ZrO₂ coatings. On the other hand, for the engine tested under the maximum load at the lowest speed, the NO emission was higher for the biodiesel, which may be attributed to the increased amount of fuel (for burning) in the combustion chamber.

Three mechanisms contribute to the production of NO_x. The initiation process of the thermal NO_x is produced through the reaction between nitrogen and oxygen at high temperatures. The higher temperature in the combustion chamber increases the formation of NO_x. Secondly, the rapid HC, nitrogen, and oxygen reaction prompts NO_x. Prompt NO_x is potentially a primary contributor toward the combustion at low temperatures. Thirdly, fuel NO_x is formed along with excess oxygen combustion of a nitrogen-containing organic compound. The earlier adoption of the sub-stoichiometric combustion process can reduce the formation of NO_x (Buyukkaya, 2010).

The trapezoidal-shaped piston provides a swirl effect and acts as a staged combustion. A portion of the combustion product from the previous combustion cycle is temporarily stored

in the mixing compartment of the trapezoidal-shaped piston. The combustion products remain in the heated zone, as illustrated in Figure 4.3.

The staged combustion acts as a preheat agent that introduces the subsequent fuel and air into the combustion chamber. The product of the combustion which mainly contains NO_x , CO_2 , and HC, enhances the fuel-rich condition. The combination of preheating from the staged combustion, improved mixing of combustion products, the swirl effect from the trapezoidal-shaped piston, and the fuel-rich condition, helps in the formation of combustion intermediates, resulting in the destruction of the previously formed NO_x . NO acts as an oxidiser in the reducing environment, which reacts with the combustion intermediates and produce N_2 . This pre-heat results from the TBC and the mixture in the product (from staged combustion), which may contribute toward the reduction of the NO, as shown in Figure 4.3.

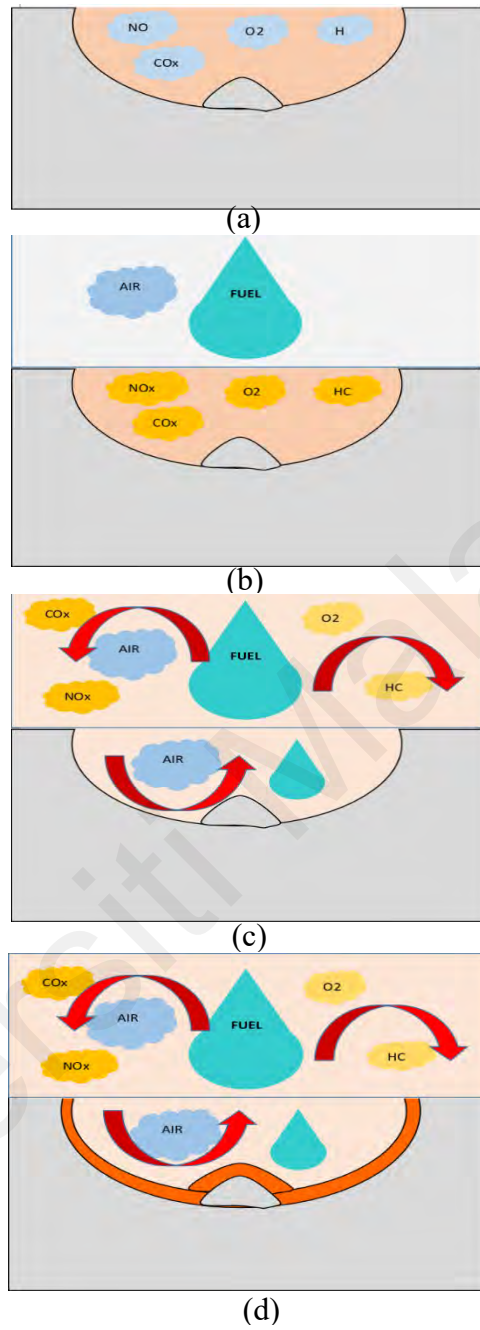


Figure 4.3: Staged combustion concept: (a) primary combustion, (b) introduction of subsequent fuel, (c) heated subsequent fuel and blend with previous traces product of combustion, (d) staged combustion of (c)

Overall, for coated and uncoated pistons, the CO₂ level decreased with increasing speeds, due to the conversion of more CO into CO₂ (Sivakumar and Senthil Kumar, 2014). The pre-heat and mixture of the combustion products from the staged combustion contributed toward higher CO₂ compared to CO. Figure 4.4 depicts the trend of CO formation at the variable engine speeds for the coated pistons with the TBC of Y₂O₃.ZrO₂, coated piston with Al₂O₃.SiO₂ and an uncoated piston. The product of the incomplete combustion is CO, which is commonly found in trace quantities (Öztürk et al., 2019). A low amount of oxygen in the combustion chamber leads to incomplete combustion, which increases the CO formation. Both in the coated and uncoated engine, at low speeds, the CO emissions were measured as high. With the increase in engine speed, decreases in CO emissions were observed.

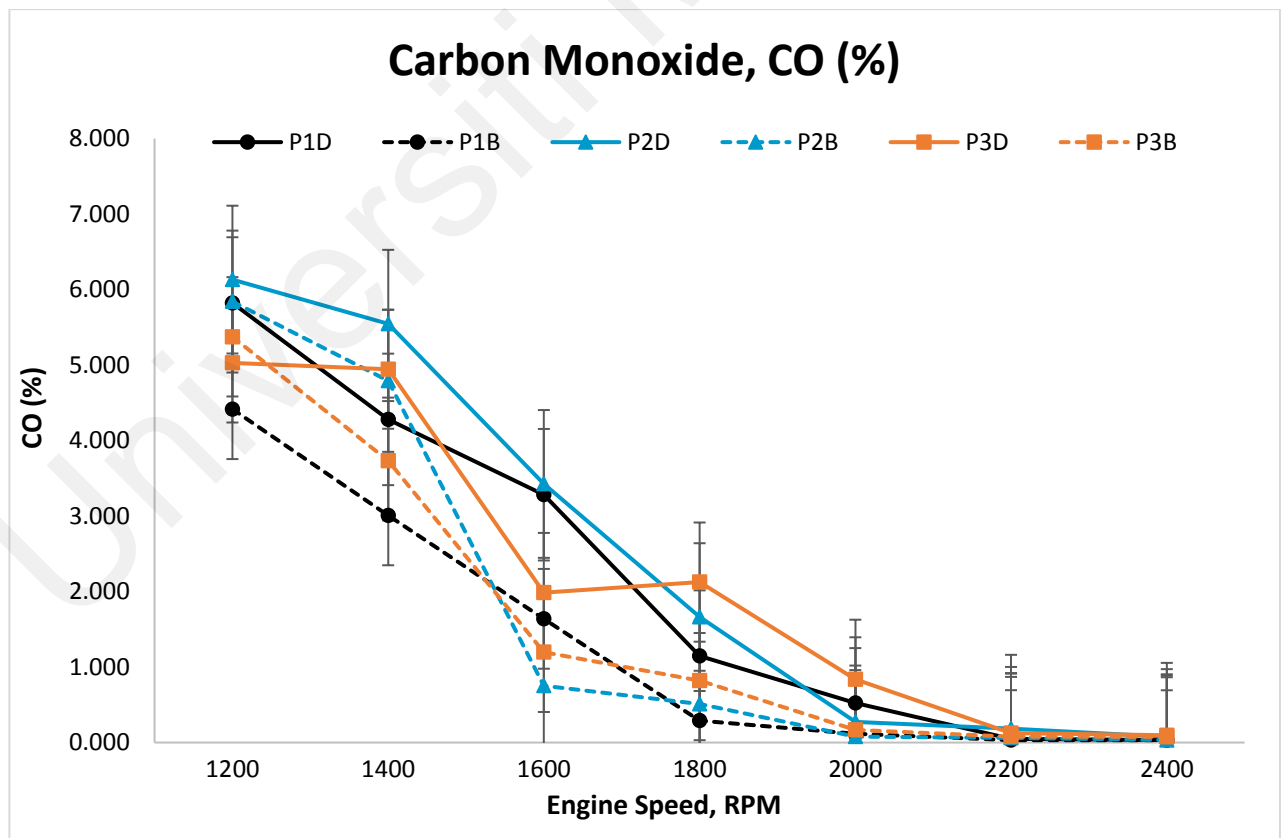


Figure 4.4: CO emission at variable speed

P3D registered the lowermost CO emission (5.029 %), followed by P1D (5.823 %), and P2D (6.133 %), at the maximum load of 1200 rpm. Secondly, P1B recorded the lowermost CO emission (4.416 %), followed by P3B (5.375 %), and P2B (5.842 %), for the engine operation with biodiesel. The obtained results at the maximum load of 1200 rpm indicated that P3D and P1B yielded the lowest CO content.

P3D registered the lowermost CO emission (1.987 %), followed by P1D (3.283 %), and P2D (3.426 %), at the maximum torque of 1600 rpm. Whereas, as for the engine operation with biodiesel, P2B recorded the lowermost CO emission (0.753 %), followed by P3B (1.195 %), and P1B (1.639 %). The obtained results at the maximum torque of 1600 rpm indicated that P3D and P2B yielded the lowest CO content.

P1D registered the lowermost CO emission (0.033 %), followed by P2D (0.077 %), and P3D (0.097 %), at the maximum speed of 2400 rpm. As for the engine operation with biodiesel, P1B recorded the lowermost CO emission (0.032 %), followed by P2B (0.033 %), and P3B (0.075 %). The obtained results at the maximum speed of 2400 rpm indicated that P1D and P1B yielded the lowest CO content.

When compared with biodiesel fuel conditions, the CO emissions were measured lower than the diesel fuels in the engine, and a probable reason for this is the presence of oxygen in the chemical structure of the biodiesel fuels, and the cetane index, which is higher than diesel fuels. With the increase in the air fuel ratio, or O_2 in the combustion chamber, the CO amount will be lowered. In fact, it consistently decreased with an increase in the biodiesel blending ratio. Moreover, biodiesel was the primary oxygen supplier to the combustion, resulting in

lower CO emissions (Behçet et al., 2019). This is mainly due to the oxygen content in the biodiesel, which promotes a much more complete combustion in the engine (Buyukkaya, 2013). Besides that, the air-fuel ratio, compression, combustion cylinder temperature, and oxygen, are vital factors for CO formation (Aydin and Sayin 2014 and Hazar, 2011). Overall, the use of biodiesel was found to perform better in terms of reducing the CO emissions, compared to diesel. Additionally, P3D and P1B were found to maintain good stability, and released the lowest CO emissions for both tested fuels across the high loads, high speeds, and high torque engine settings.

Despite the CO having slightly higher values for the coated piston compared to uncoated samples, it will be fit enough if the comparisons were made simultaneously with CO₂. By combining both the trend of CO in figure 4.4 and the CO₂ in figure 4.5, the coated piston delivered a lower combined value of CO and CO₂ compared to the uncoated version. The observation also showed the effect of a TBC on the CO and CO₂ emissions, due to the reduction of CO and CO₂ emission in the coated engine, compared to the uncoated engine. Öztürk et al. (2019) explained that the thermal insulation of the TBC increased post-compression temperature, and initiated a late phase combustion and oxidation of the CO and CO₂. Figure 4.5 depicts the trend of CO₂ emission at the variable speed for coated and uncoated pistons.

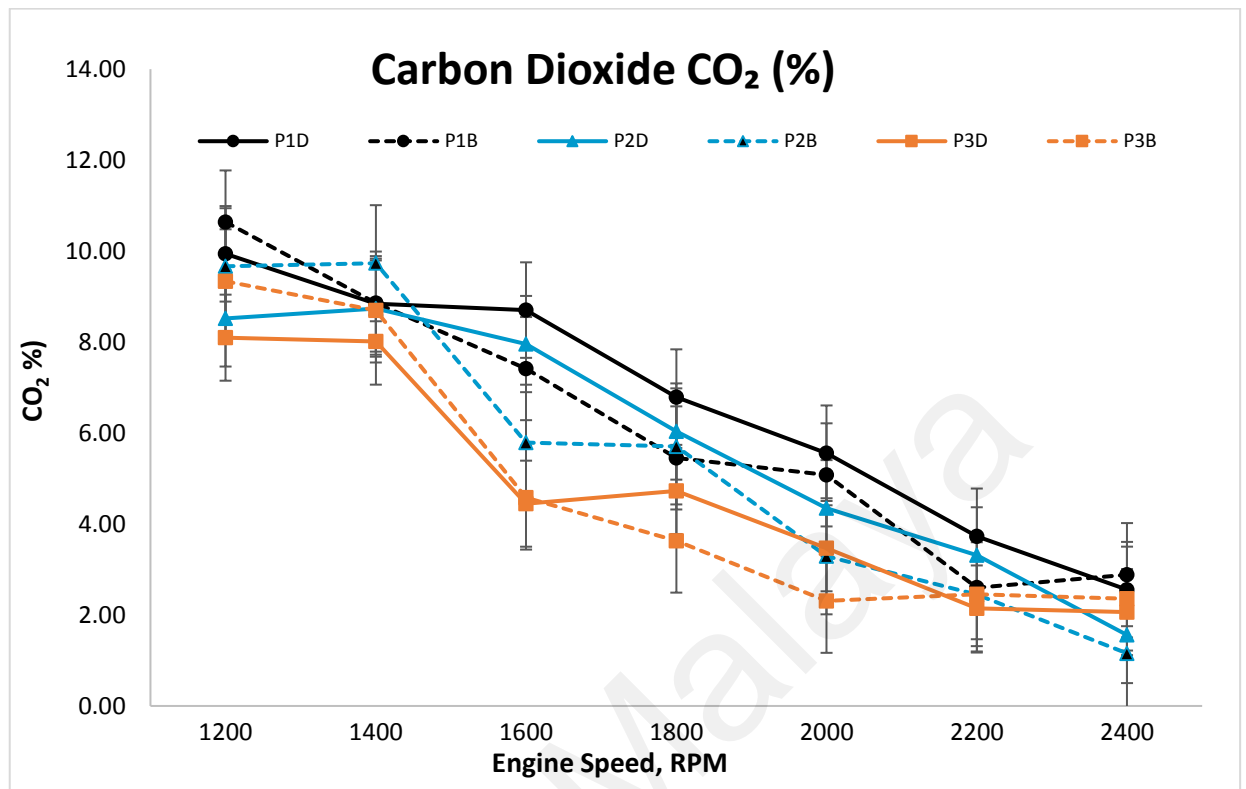


Figure 4.5: CO₂ emission at variable speed

For results at the highest load of 1200 rpm, P3D was listed as the lowest CO₂ emission (8.1 %), followed by P2D (8.52 %), and P1D (9.94 %). For the result of the engine operating with biodiesel, P3B had the lowest CO₂ emission (9.34 %), followed by P2B (9.67 %) and P1B (10.64 %). In summary, at the maximum load of 1200 rpm, coated Al₂O₃.SiO₂ (P3D and P3B) yielded the lowest CO₂ content.

For results at the highest torque of 1600 rpm, P3D had the lowest CO₂ emission (4.45 %), followed by P2D (7.96 %), and P1D (8.7 %). For the result of the engine operation with biodiesel, P3B recorded the lowest CO₂ emission (4.58 %), followed by P2B (5.79 %), and P1B (7.42 %). In summary, at the maximum torque of 1600 rpm, coated Al₂O₃.SiO₂ (P3D and P3B) yielded the lowest CO₂ content.

Finally, for the result at the highest speed of 2400 rpm, P3D recorded the lowest CO₂ emission (8.10 %), followed by P2D (8.52 %), and P1D (9.94 %). As for the engine operation with biodiesel, P3B recorded the lowest CO₂ emission (9.34 %), followed by P2B (9.67 %), and P1B (10.64 %). In summary, at the maximum speed of 2400 rpm, coated Al₂O₃.SiO₂ (P3D and P3B) yielded the lowest CO₂ content.

Overall, the use of biodiesel was found to perform better in terms of reducing the CO₂ emissions compared to diesel. Additionally, coated Al₂O₃.SiO₂ (P3D and P3B) was found to maintain good stability and released the lowest CO₂ emission for both tested fuels across high loads, high speeds and high torque engine settings. Additionally, the results also illustrated the engine's effectiveness in achieving almost complete combustion for both tested fuels. With the presence of TBC, it was found to lower the CO₂ emission compared to uncoated pistons. For this investigation, a higher CO₂ emission was recorded than the CO emission, as complete combustion of a fuel produces more CO₂ than CO. Overall, by combining both the trends of CO and CO₂, the coated piston delivered a lower total sum value of CO and CO₂ compared to the uncoated version.

4.2.2 Engine performance analysis

The effects of a TBC on the engine performance were examined in power generation, engine torque, BSFC and BTE, under various speeds using conventional diesel and biodiesel. BSFC is defined as the ratio of the fuel consumption rate over the brake power output. Whereas BTE is a combination of two important efficiencies, that is, the mechanical efficiency, and the net indicated thermal efficiency. BTE can be calculated by dividing the brake power output over the delivered total energy. Due to the effect of countless loss mechanisms, such

as combustion inefficiency, exhaust, flow, heat transfer and friction, the BTE of an original and field operating diesel cycle is typically below 50% (Heywood, 1988). Based on the obtained results in Figure 4.6, the power and torque developed in the TBC engine were reduced for both $Y_2O_3.ZrO_2$ coated and alumina-coated pistons across all engine speed settings, compared to the uncoated piston as the baseline.

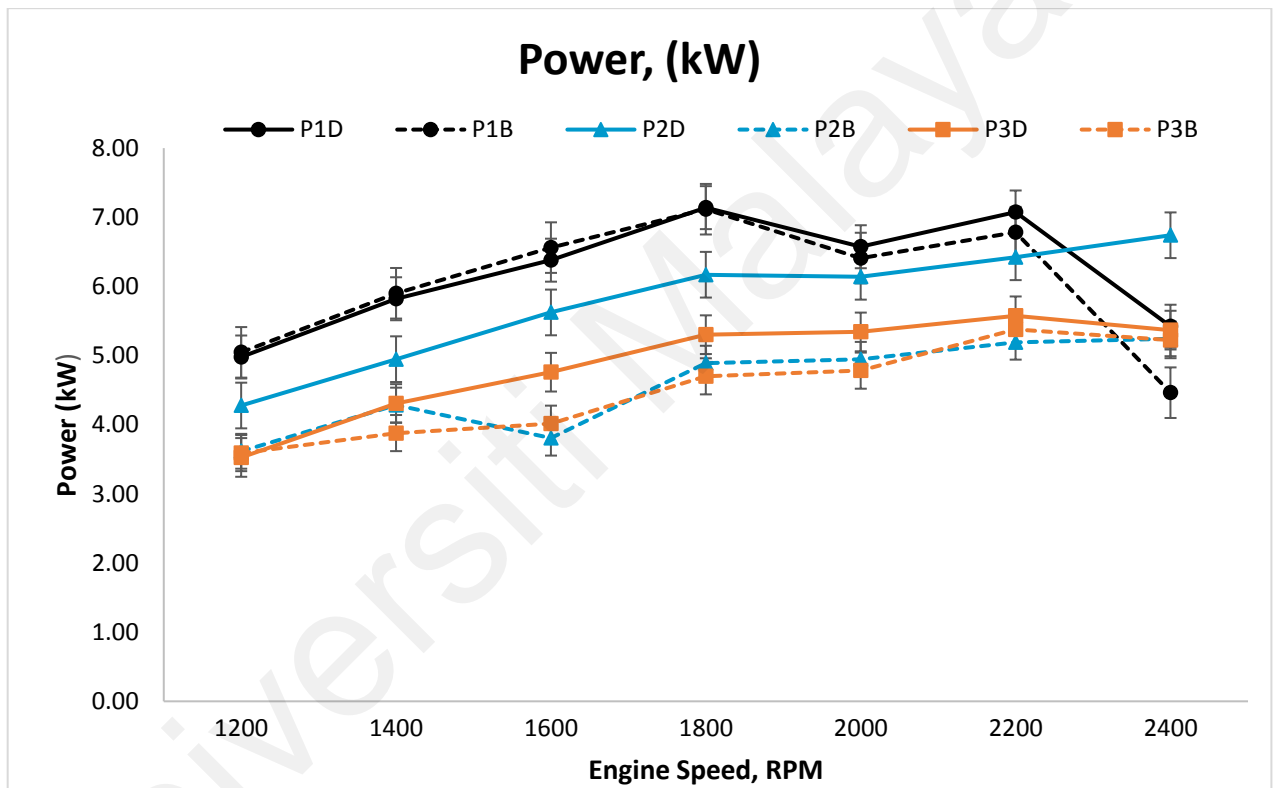


Figure 4.6: Power (kW) produced at variable speed

For the power generated for diesel fuel at the maximum load of 1200 rpm, P1D recorded the uppermost power (4.98 kW), followed by P2D (4.28 kW), and P3D (3.53 kW). As for the power generated for the biodiesel fuel at the maximum load, P1B recorded the uppermost power (5.05 kW), followed by P2B (3.62 kW), and P3B (3.59 kW). Decisively, from the results at the maximum load of 1200 rpm, it was revealed that the uncoated piston (P1D and P1B) yielded the highest power.

When the diesel fuel fired diesel engine was at the maximum torque of 1600 rpm, P1D recorded the uppermost power (6.38 kW), followed by P2D (5.62 kW), and P3D (4.76 kW). As for the engine operation fired up with the biodiesel fuel, P1B recorded the uppermost power (6.56 kW), followed by P3B (4.01 kW), and P2B (3.81 kW). The obtained results at the maximum torque of 1600 rpm revealed that the uncoated piston (P1D and P1B) yielded the highest power.

Finally, for the engine operated with diesel fuel, at the maximum speed of 2400 rpm, the P2D recorded the most power (6.74 kW), followed by P1D (5.42 kW) and P3D (5.37 kW). As for the engine operated with the biodiesel fuel, P2B recorded the most power (5.24 kW), followed by P3B (5.22 kW) and P1B (4.46 kW). The obtained results at the maximum speed of 2400 rpm revealed that $Y_2O_3.ZrO_2$ (P2D and P2B) yielded the most power.

Overall, the uncoated piston (P1D and P1B) was found to maintain a high power running engine for both tested fuels across the high load and high torque engine settings. Additionally, the use of biodiesel was found to produce lower power than the use of diesel (as a baseline). Similar results were reported in prior studies, where biodiesel generated lower power than diesel due to its lower heating values and higher kinematic viscosity (Hasimuglu et al., 2008; Murali Krishna et al., 2016; Aydin et al., 2016).

As presented in Figure 4.7, the use of biodiesel recorded lower torque as compared to the use of diesel (as a baseline) for both coated and uncoated pistons. Similar results were also reported in several prior studies (Hasimuglu et al., 2008). This observation can be explained

by the combined effect of relatively higher viscosity and lower caloric values in palm oil biodiesel than conventional diesel (Mahamalingam et al., 2018).

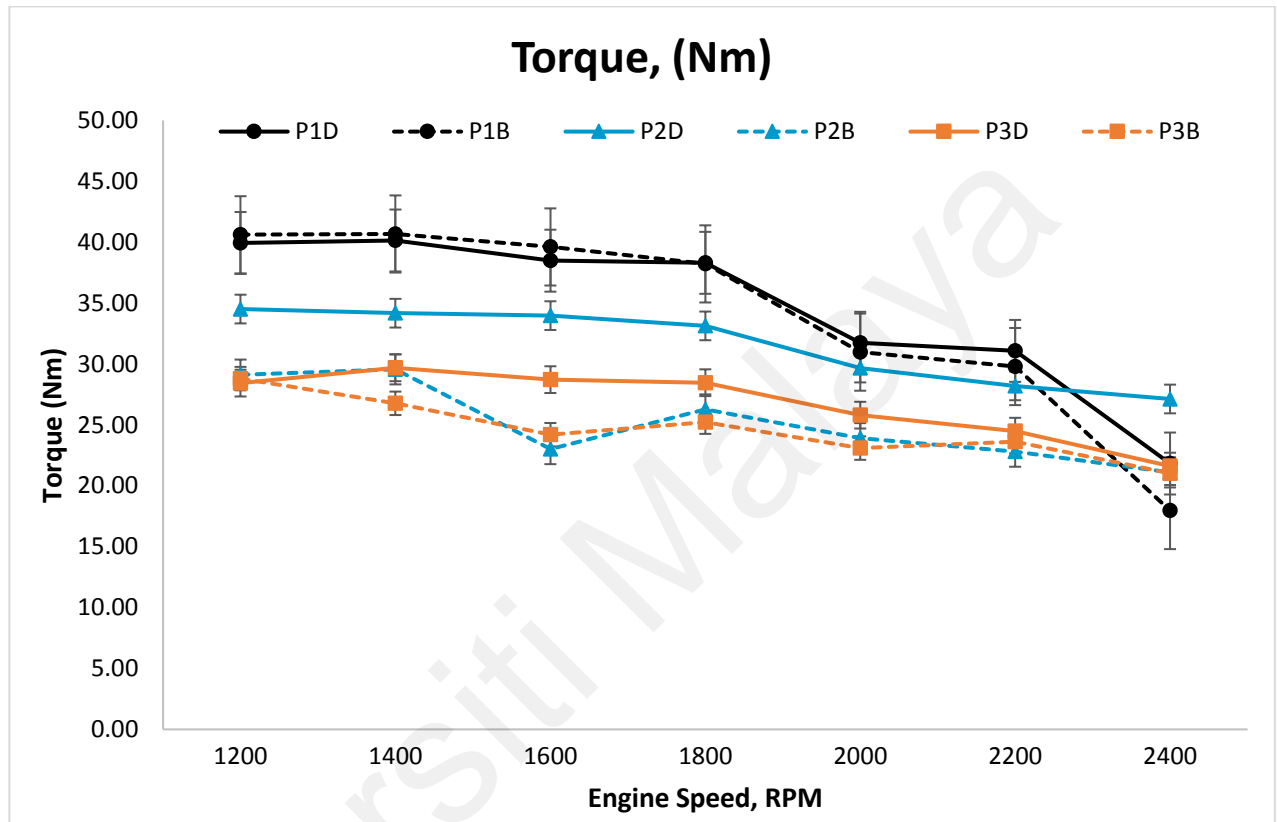


Figure 4.7: Torque (Nm) produced at variable speed

To evaluate the effect of the diesel fuel at the maximum load of 1200 rpm, P1D logged the peak torque (39.94 Nm), followed by P2D (34.51 Nm), and P3D (28.43 Nm). As for the effect of the engine operated with biodiesel, P1B logged the peak torque (40.61 Nm), followed by P2B (29.13 Nm), and P3B (28.80 Nm). As can be observed, the maximum load of 1200 rpm revealed that the uncoated piston (P1D and P1B) yielded the highest torque.

Additionally, for the effect of the diesel fuel at the maximum torque of 1600 rpm, P1D logged the peak torque effect (38.48 Nm), followed by P2D (33.97 Nm) and P3D (28.72 Nm). As

for the effect of the engine operated with biodiesel, P1B logged the peak torque effect (39.61 Nm), followed by P3B (24.20 Nm), and P2B (23.02 Nm). In the case of the results at the maximum torque of 1600 rpm, this showed that the uncoated piston (P1D and P1B) yielded the highest torque effect.

In relation to the effect of diesel fuel at the maximum speed of 2400 rpm, P2D logged the peak torque (27.13 Nm), followed by P1D (21.83 Nm), and P3D (21.62 Nm). As for the engine effect of the engine operated with biodiesel at the maximum speed, P2B logged the peak torque (21.10 Nm), followed by P3B (21.03 Nm), and P1B (17.97 Nm). It is observed that, at the maximum speed of 2400 rpm, $Y_2O_3.ZrO_2$ (P2D and P2B) yielded the highest torque.

Overall, the uncoated piston was found to maintain highest torque engine running for both the tested fuels across the high load and high torque engine settings. However, for the case of the coated pistons, the $Y_2O_3.ZrO_2$ coated piston with the biodiesel yielded a lower torque effect than the $Y_2O_3.ZrO_2$ coated piston with diesel. In contrast, both tested fuels produced a similar torque effect for the alumina-coated piston. Although the TBC is expected to reduce the heat loss transferred to the cooling medium, it affects the engine's compression ratio, decreasing the power and torque in the diesel engine. (Sivakumar & Senthil Kumar, 2014).

BTE and BSFC are other significant factors that determine an engine's performance. In this study, BSFC was measured within the speed range of 1200 rpm to 2400 rpm for all coated and uncoated pistons under both diesel and biodiesel operational conditions. Figure 4.8 presents the results of the BSFC at variable speeds.

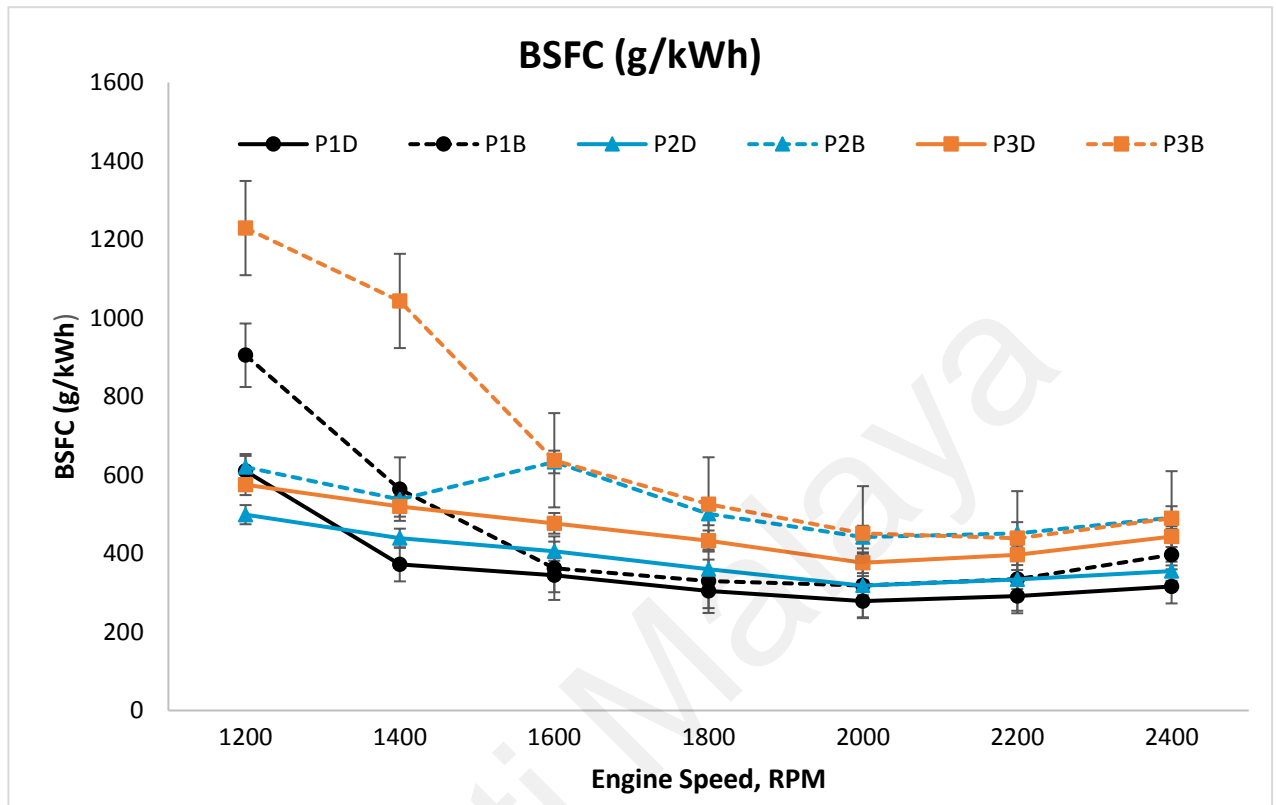


Figure 4.8: BSFC at variable speed

The results showed that for the engine fuelled with diesel, at the maximum load of 1200 rpm, P2D recorded the lowest BSFC (498.96 g/kWh), followed by P3D (575.16 g/kWh), and P1D (609.98 g/kWh). As for the engine fuelled with biodiesel, P2B recorded the lowest BSFC (619.81 g/kWh), followed by P1B (905.07 g/kWh), and P3B (1229.06 g/kWh). This finding indicates that at the maximum load of 1200 rpm, $Y_2O_3.ZrO_2$ (P2D and P2B) yielded the lowest BSFC. This finding is further reinforced by the similar trend of the coated engine up to the full load condition, but the SFC at the full load is slightly lower than that of the baseline engine (A. J. Modi & D. C. Gosai, 2010).

The results also show that for engine fuelled with diesel at the maximum torque of 1600 rpm, P1D recorded the lowest BSFC (344.79 g/kWh), followed by P2D (405.88 g/kWh), and P3D

(476.85 g/kWh). As for the engine fuelled with biodiesel at the maximum torque of 1600 rpm, P1B recorded the lowest BSFC (362.63 g/kWh), followed by P2B (633.18 g/kWh), and P3B (637.57 g/kWh). This finding indicates that at the maximum torque of 1600 rpm, the uncoated piston (P1D and P1B) yielded the lowest BSFC. Literature studies indicated that for the trend of coated engines up to the full load condition, the SFC at the maximum torque was slightly higher than that of the uncoated engine (A. J. Modi & D. C. Gosai, 2010).

Finally, for engine fuelled with diesel at the maximum speed of 2400 rpm, P1D recorded the lowest BSFC (316.22 g/kWh), followed by P2D (354.82 g/kWh), and P3D (443.02 g/kWh). As for the engine fuelled with biodiesel at the maximum speed of 2400 rpm, P1B recorded the lowest BSFC (396.61 g/kWh), followed by P3B (489.69 g/kWh), and P2B (491.59 g/kWh). As can be observed, the obtained results at the maximum speed of 2400 rpm indicates that the uncoated piston (P1D and P1B) yielded the lowest BSFC. This result is supported by the trend of the coated engine up to a full load condition, whereby the SFC at the maximum speed is much higher than that of the uncoated engine. This is due to the higher temperatures at to which the combustion characteristics are improved (A. J. Modi & D. C. Gosai, 2010).

Overall, the uncoated piston (P1D and P1B) maintained the lowest BSFC running engine for both the tested fuels across the high load and high torque engine settings. Similar results were reported in several prior studies, which supported the results of the present study (Rahiman M.K et al., 2013). The load on the engine increases with the decrease in speed. Thus, at the lowest speed of 1200 rpm, where the load was at its highest, $Y_2O_3.ZrO_2$ coated pistons reported lower BSFC than the BSFC of the uncoated piston. Specifically, in the case

of diesel, the results in Figure 4.8 revealed a slightly higher value of BSFC with the increase of speed for both the $Y_2O_3.ZrO_2$ and alumina-coated pistons, compared to those of the uncoated piston (as baseline). Furthermore, the BSFC for the biodiesel was higher than the BSFC for the diesel, due to the palm oil biodiesel's lower caloric values than the conventional diesel (Aydin et al., 2016; Krishnamoorthi and Vinayagasundram, 2019).

Figure 4.9 shows the trend of the BTE at the variable speed for coated and uncoated pistons. Overall, it showed an increasing trend for the BTE with the increase in the speed for both the $Y_2O_3.ZrO_2$, $Al_2O_3.SiO_2$ pistons, and the uncoated piston (as baseline). Overall, the biodiesel recorded lower BTE than the use of the diesel, which may be attributed to the poor fuel atomisation characteristics, higher flash point, and lower volatility (Pandian et al., 2017; Devarajan et al., 2018).

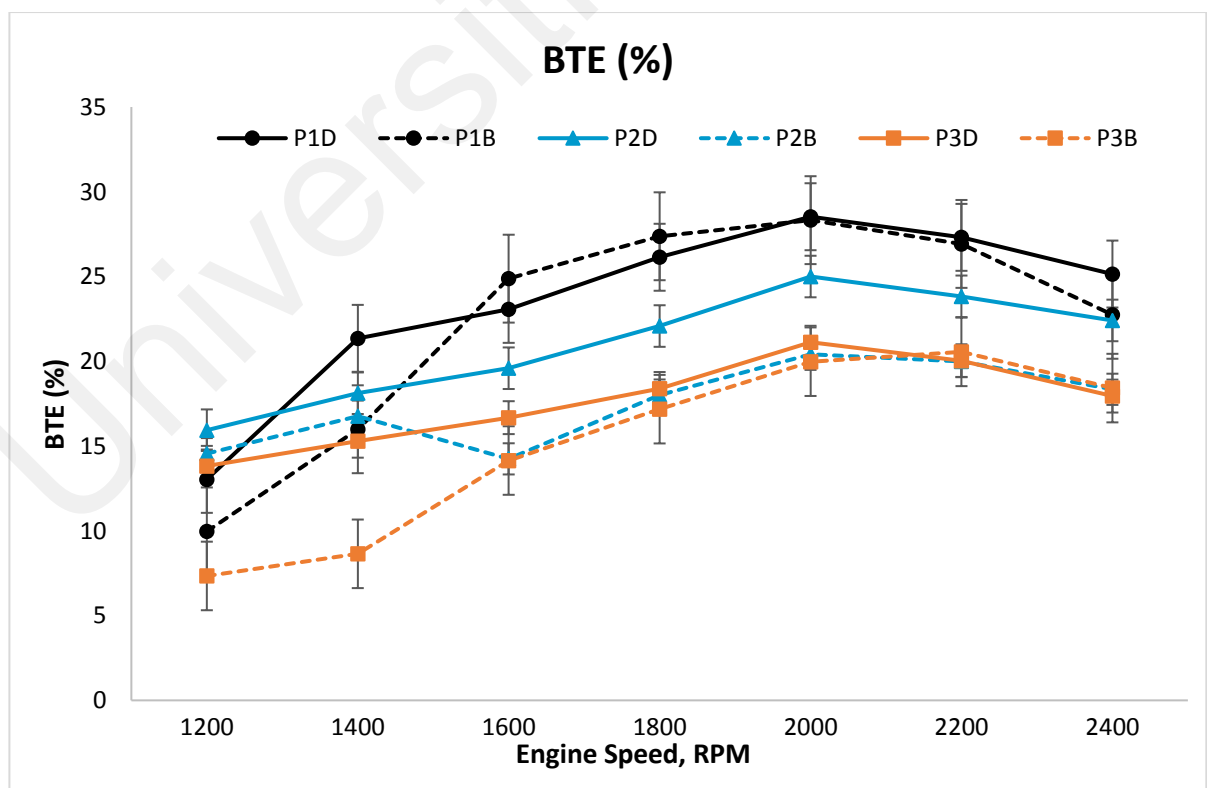


Figure 4.9: BTE at variable speed

During the maximum load of 1200 rpm for the diesel fuel, P2D recorded the highest BTE (15.94 %), followed by P3D (13.83 %), and P1D (13.04 %). As for the engine operation with biodiesel, P2B recorded the highest BTE (14.55 %), followed by P1B (9.97 %), and P3B (7.34 %). Thus, the gained results at the maximum load of 1200 rpm revealed that the coated $Y_2O_3.ZrO_2$ (P2D and P2B) yielded the highest BTE. This finding was further reinforced by the similar trend of the coated engine up to the full load condition, whereby, the BTE at the full load was slightly higher than that of the uncoated piston (A. J. Modi & D. C. Gosai, 2010).

The maximum torque of at 1600 rpm for the diesel fuelled engine, P1D, recorded the highest BTE (23.06 %), followed by P2D (19.59 %), and P3D (16.68 %). As for the engine operation with the biodiesel fuel, P1B recorded the highest BTE (24.87 %), followed by P2B (14.25 %), and P3B (14.15 %). Thus, the gained results at the maximum torque of 1600 rpm revealed that the uncoated piston (P1D and P1B) yielded the highest BTE. Literature studies indicated that for the trend of the coated engine up to the full load condition, the BTE at the maximum torque was slightly lower than that of the coated engine (A. J. Modi & D. C. Gosai, 2010).

As can be seen, at the maximum speed of 2400 rpm for the diesel fuelled engine, P1D recorded the highest BTE (25.15 %), followed by P2D (22.41 %), and P3D (17.95 %). As for the engine operating with biodiesel fuelled engine, P1B recorded the highest BTE (22.74 %), followed by P3B (18.42 %), and P2B (18.35 %). The obtained results at the maximum speed of 2400 rpm revealed that the P1D and P1B yielded the highest BTE. This result was supported by the trend of the coated engine up to the full load condition, where the BTE at



the maximum speed was lower than that of the uncoated engine (A. J. Modi & D. C. Gosai, 2010).


During testing, the engine speed was lowered by adding more load to the system. Compared to the $Y_2O_3.ZrO_2$ coated and $Al_2O_3.SiO_2$ coated pistons, the uncoated pistons recorded higher BTE. The uncoated pistons in this study recorded a higher BTE due to the increased heat from the gas expansion. TBCs can achieve higher BTEs than uncoated pistons with full application of the TBC at the piston's surface, valves, and combustion liner, to increase its thermal efficiency. However, the coating was limited to the piston crown only for this experiment. Overall, the value of the BTE is promising for the $Y_2O_3.ZrO_2$ coating compared to the $Al_2O_3.SiO_2$ coating. $Y_2O_3.ZrO_2$ showed a significant performance during the maximum load at speeds of 1200 rpm, hereby, recording the highest BTE.

4.2.3 Condition of the piston crown after 6 hours of engine operation

Table 4.1 exemplifies the comparison between the conditions of the piston crown after running continuously for 6 hours, to test the durability of the coated pistons. The surface of the piston crown was observed to identify any abnormalities such as cracks or damages on the TBC which was coated on the piston crown.

Table 4.1: Comparison between conditions of piston crown after running 6 hours

Piston crown	Observation
<p data-bbox="318 317 821 352">a) Non coated piston crown (baseline)</p> 	<p data-bbox="854 317 1455 936">The carbon gets accumulated (fouling) over the piston crown surface after 6 h engine operation on the surface of the uncoated piston. Besides, the surface of the piston crown was seen to have minor cracks on the top surface. There was no abnormality at the remaining uncoated parts of the combustion chamber. Overall, no failure was detected after 6 h of engine running condition.</p>
<p data-bbox="318 1346 691 1381">b) Coated 100% $Y_2O_3.ZrO_2$</p> 	<p data-bbox="854 1346 1455 1881">The surface of piston coated with TBC 100% $Y_2O_3.ZrO_2$, and there was no abnormalities other than a few traces of carbon deposits on the surface, observed based on visual inspection on the coated layer on piston crown part after 6 h of engine running condition. There was no abnormality at the remaining uncoated parts of the combustion chamber. Overall, no failure</p>

	<p>was detected after 6 h of engine running condition. This shows that the TBC can effectively protect by reducing the temperature of the piston alloy substrate.</p>
<p>c) Coated 100% $\text{Al}_2\text{O}_3\cdot\text{SiO}_2$</p> 	<p>The surface of piston coated with TBC 100% $\text{Al}_2\text{O}_3\cdot\text{SiO}_2$, and there were no abnormalities other than a few traces of carbon deposits on the surface, observed based on visual inspection on the coated layer on piston crown part after 6h of engine running condition. Besides, the surface of the piston crown was seen to have minor cracks on the top surface. There was no abnormality at the remaining uncoated parts of the combustion chamber. Overall, no failure was detected after 6h of engine running condition. This shows that the TBC is 100% $\text{Al}_2\text{O}_3\cdot\text{SiO}_2$ can effectively protect by reducing the temperature of the piston alloy substrate. By comparing 100% $\text{Al}_2\text{O}_3\cdot\text{SiO}_2$ coated piston between 100% $\text{Y}_2\text{O}_3\cdot\text{ZrO}_2$ coated piston, 100% $\text{Y}_2\text{O}_3\cdot\text{ZrO}_2$ shows overwhelming coating durability without minor cracks.</p>

Based on the Table 4.1, by comparing 100% $\text{Al}_2\text{O}_3.\text{SiO}_2$ coated pistons with 100% $\text{Y}_2\text{O}_3.\text{ZrO}_2$ coated pistons, the 100% $\text{Y}_2\text{O}_3.\text{ZrO}_2$ showed an overwhelming coating durability without minor cracks. However, the 100% $\text{Al}_2\text{O}_3.\text{SiO}_2$ coated piston showed a positive result in terms of having very minor cracks. Hence with the blend between $\text{Al}_2\text{O}_3.\text{SiO}_2$ and $\text{Y}_2\text{O}_3.\text{ZrO}_2$, $\text{Y}_2\text{O}_3.\text{ZrO}_2$ material characteristics, this might strengthen the blend of the TBC properties. Furthermore, minor cracks noticed on the uncoated piston and with the introduction of the TBC in the piston crown, this will enhance the durability and life span of the piston.

4.2.4 Summary

In this test series, the effect of the TBC on the engine performance, emission, and combustion characteristics of the palm biodiesel and diesel fuels have been experimentally investigated in a DI diesel engine. The following main findings can be drawn from this test series. The engine performance measurement for the coated and uncoated pistons for both the conventional diesel (as a baseline), and the B100 palm biodiesel, can be concluded as shown in Table 4.2.

Table 4.2: Summary of the first phase of the engine performance

TBC	Performance			
	BTE	BSFC	Power	Torque
Diesel Fuel				
Uncoated piston	Good	Good	Good	Good
100% $\text{Y}_2\text{O}_3.\text{ZrO}_2$	Fair	Fair	Fair	Fair
100% $\text{Al}_2\text{O}_3.\text{SiO}_2$	Poor	Poor	Poor	Poor
Biodiesel Fuel				
Uncoated piston	Good	Good	Good	Good
100% $\text{Y}_2\text{O}_3.\text{ZrO}_2$	Fair	Fair	Fair	Fair
100% $\text{Al}_2\text{O}_3.\text{SiO}_2$	Poor	Poor	Poor	Poor

Based on the analysis, the use of the $\text{Al}_2\text{O}_3.\text{SiO}_2$ coating had a less promising result on the engine performance. Unlike the $\text{Al}_2\text{O}_3.\text{SiO}_2$ coated piston, the $\text{Y}_2\text{O}_3.\text{ZrO}_2$ coated piston demonstrated a better engine performance for both the diesel and biodiesel fuels. Hence, the second phase of the research will be extended to identify the optimum blend between the $\text{Y}_2\text{O}_3.\text{ZrO}_2$ and $\text{Al}_2\text{O}_3.\text{SiO}_2$ to balance the gap between both materials. The engine emission analysis for the coated and uncoated pistons for both conventional diesel (as a baseline), and the B100 palm biodiesel can be concluded as shown in Table 4.3.

Table 4.3: Summary of the first phase of the emission analysis

TBC	Emission			
	CO	CO ₂	HC	NO
Diesel Fuel				
Uncoated piston	Fair	Poor	Fair	Poor
100% $\text{Y}_2\text{O}_3.\text{ZrO}_2$	Poor	Fair	Good	Fair
100% $\text{Al}_2\text{O}_3.\text{SiO}_2$	Good	Good	Poor	Good
Biodiesel Fuel				
Uncoated piston	Good	Poor	Fair	Poor
100% $\text{Y}_2\text{O}_3.\text{ZrO}_2$	Fair	Fair	Good	Fair
100% $\text{Al}_2\text{O}_3.\text{SiO}_2$	Poor	Good	Poor	Good

It is observed that the use of the $\text{Al}_2\text{O}_3.\text{SiO}_2$ coating had an excellent result on the engine emission. Unlike the $\text{Y}_2\text{O}_3.\text{ZrO}_2$ coated piston, the $\text{Al}_2\text{O}_3.\text{SiO}_2$ coated piston demonstrated a better engine emission release for both the diesel and biodiesel fuels. This study produced an overwhelming result on reducing the NO emission using the $\text{Al}_2\text{O}_3.\text{SiO}_2$ coating. The correlation of other effects on the variation of the NO emissions when using the TBC can be evaluated much more comprehensively. Hence, the second phase of the research will be extended to identify the optimum blend between the $\text{Al}_2\text{O}_3.\text{SiO}_2$ and $\text{Y}_2\text{O}_3.\text{ZrO}_2$ and the balance gap between both materials, to enhance further lower emission releases to the

environment. The durability studies for the coated and uncoated pistons can be concluded as shown in Table 4.4.

Table 4.4: Summary of the first phase of the durability studies

TBC	Durability
Diesel Fuel	
Uncoated piston	Poor
100% Y ₂ O ₃ .ZrO ₂	Good
100% Al ₂ O ₃ .SiO ₂	Fair
Biodiesel Fuel	
Uncoated piston	Poor
100% Y ₂ O ₃ .ZrO ₂	Good
100% Al ₂ O ₃ .SiO ₂	Fair

Conversely by comparing 100% Al₂O₃.SiO₂ coated pistons between 100% Y₂O₃.ZrO₂ coated pistons, the 100% Y₂O₃.ZrO₂ showed an overwhelming coating durability without minor cracks. Hence with the blend between Al₂O₃.SiO₂ and Y₂O₃.ZrO₂, Y₂O₃.ZrO₂ material characteristics might strengthen the blend of the TBC properties. The overall criteria of the selection between the uncoated, 100% Y₂O₃.ZrO₂ and 100% Al₂O₃.SiO₂ for the piston crown is evaluated in Table 4.5.

Table 4.5: Piston selection for the first phase of the research work

TBC	Performance	Emission	Durability	Overall
Uncoated piston	Good	Poor	Poor	Poor
100% Y ₂ O ₃ .ZrO ₂	Fair	Fair	Good	Good
100% Al ₂ O ₃ .SiO ₂	Poor	Good	Fair	Fair

Conclusively, the coated piston with 100% Y₂O₃.ZrO₂ showed a promising result in the low emission category, and higher durability (TBC coatings had a longer lifespan) during diesel

engine testing. Despite slightly lower engine performance of the 100% $Y_2O_3.ZrO_2$ coated piston compared to the uncoated piston, the 100% $Y_2O_3.ZrO_2$ coated piston was expected to extend the maintenance downtime intervals (major overhaul, change piston), and had a high toughness capacity versus the high BTE and low BSFC during the high load engine operation at 1200 rpm. RT125 is commonly used in agricultural industries, whereby in general practices, the engine will be used for farming activities for longer durations, and with higher load running for daily usage.

4.3 Second Phase: Blend TBC

The effects of the TBC with a various blend ratios of $Y_2O_3.ZrO_2$ and $Al_2O_3.SiO_2$ on the emission control and engine performance using conventional diesel and biodiesel were further discussed. Upon completion of the engine setup, five series of tests were conducted to evaluate the performance of the TBC; 90% $Y_2O_3.ZrO_2$ + 10% $Al_2O_3.SiO_2$, 80% $Y_2O_3.ZrO_2$ + 20% $Al_2O_3.SiO_2$, 70% $Y_2O_3.ZrO_2$ + 30% $Al_2O_3.SiO_2$, 60% $Y_2O_3.ZrO_2$ + 40% $Al_2O_3.SiO_2$ and 50% $Y_2O_3.ZrO_2$ + 50% $Al_2O_3.SiO_2$. The effect on the engine performance and emissions characteristics of the diesel engine are discussed in the following sub-sections. For the rest of the parameters, 90/10B & 90/10D will not be evaluated, as the overall value of all the parameters are outranged, and the engine was underperforming due to abnormal vibration. Hence, the coated 90% $Y_2O_3.ZrO_2$ + 10% $Al_2O_3.SiO_2$ is not a good coating to be considered for TBC. The reason for the underperforming blend ratio of the coated 90% $Y_2O_3.ZrO_2$ + 10% $Al_2O_3.SiO_2$ was due it having poor final material characteristics.

4.3.1 Exhaust emission analysis

In this section, the engine emissions such as HC, NO, CO, and CO₂ were evaluated using a series of TBC ratios blended between Y₂O₃.ZrO₂ and Al₂O₃.SiO₂. Figure 4.10 presents the trend of the HC formation at the variable engine speeds for the coated piston with a TBC of 80% Y₂O₃.ZrO₂ + 20% Al₂O₃.SiO₂, 70% Y₂O₃.ZrO₂ + 30% Al₂O₃.SiO₂, 60% Y₂O₃.ZrO₂ + 40% Al₂O₃.SiO₂ and 50% Y₂O₃.ZrO₂ + 50% Al₂O₃.SiO₂.

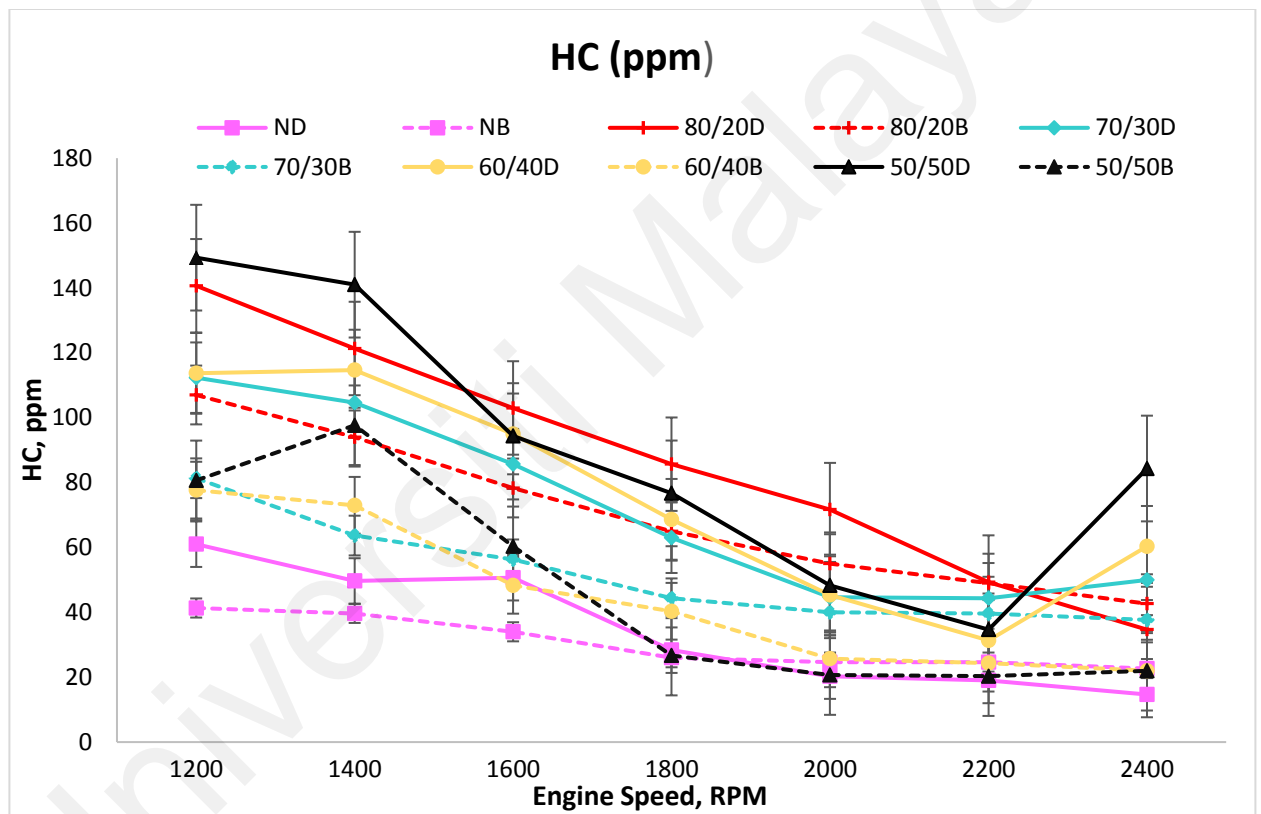


Figure 4.10: HC emission for blended coat

Another interesting observation which can be made from the maximum load at 1200 rpm was for the HC emission against all coated pistons tested under the diesel fuel, where 70/30D recorded the lowest HC emission (112 ppm), followed by 60/40D (114 ppm), 80/20D (141 ppm), and 50/50D (149 ppm). As for the engine operation with biodiesel, the 60/40B recorded the lowest HC emission (78 ppm), followed by 50/50B (81 ppm), 70/30B (81 ppm),

and 80/20B (107 ppm). The obtained results at the maximum load of 1200 rpm revealed that the 70/30D and 60/40B yielded the lowest HC content. However, the 60/40D had a difference of 1.75% compared to the 70/30D. Hence it was concluded that at the speed 1200 rpm, the piston coated with 60% $Y_2O_3.ZrO_2$ + 40% $Al_2O_3.SiO_2$ (60/40D and 60/40B) yielded the lowermost HC emission.

At the maximum torque of 1600 rpm, 70/30D recorded the lowest HC emission (86 ppm), followed by 50/50D (94 ppm), 60/40D (95 ppm), and 80/20D (103 ppm). As for the engine operation with biodiesel, 60/40B recorded the lowest HC emission (48 ppm), followed by 70/30B (56 ppm), 50/50B (60 ppm), and 80/20B (78 ppm). The obtained results at the maximum torque of 1600 rpm revealed that the 70/30D and 60/40B yielded the lowest HC content. Nevertheless, the 60/40D had a difference of 1.1% compared to the 70/30D. Hence it was concluded that at the maximum torque of 1600 rpm, the piston coated with 60% $Y_2O_3.ZrO_2$ + 40% $Al_2O_3.SiO_2$ (60/40D and 60/40B) yielded the lowermost HC emission.

At the maximum speed of 2400 rpm, the 80/20D recorded the lowest HC emission (35 ppm), followed by the 70/30D (50 ppm), 60/40D (60 ppm) and 50/50D (84 ppm). As for the engine operation with biodiesel, the 50/50B recorded the lowest HC emission (22 ppm), followed by the 60/40B (22 ppm), 70/30B (38 ppm) and 80/20B (43 ppm). The obtained results at the maximum speed of 2400 rpm revealed that the 80/20D and 60/40B yielded the lowermost HC content.

The results indicated that the piston coated with 60% $Y_2O_3.ZrO_2$ + 40% $Al_2O_3.SiO_2$ (60/40D and 60/40B) yielded the lowest HC emission. Referring to the decreasing trend of the HC

emission with increasing speeds, the study proved that the speed increased the effect of the HC emission. In direct injection systems, the fuel pump injects fuel with less fragmentation at lower speeds, because the atomization in the fuel is poor. Hence, this causes the formation of higher HC emissions at the lowermost engine speed conditions (Selman et al., 2015).

As summarized, biodiesel releases a lower HC than diesel. Biodiesel fuels contain more oxygen molecules, and achieves better combustion, thus reducing the HC emission (Prabhakar and Rajan, 2013). The piston coated with 60% $Y_2O_3.ZrO_2$ + 40% $Al_2O_3.SiO_2$ registered a better fuel evaporation rate due to the increased temperature in the combustion chamber. The improved material characteristics of the TBC developed from the coating of 60% $Y_2O_3.ZrO_2$ + 40% $Al_2O_3.SiO_2$ performed much better than other blend coatings for the HC reduction. Overall, the experimental results revealed that the biodiesel yielded a lower HC emission than the use of diesel.

Figure 4.11 presents the trend of the HC formation at the variable engine speeds for the coated pistons with a TBC of 80% $Y_2O_3.ZrO_2$ + 20% $Al_2O_3.SiO_2$, 70% $Y_2O_3.ZrO_2$ + 30% $Al_2O_3.SiO_2$, 60% $Y_2O_3.ZrO_2$ + 40% $Al_2O_3.SiO_2$ and 50% $Y_2O_3.ZrO_2$ + 50% $Al_2O_3.SiO_2$.

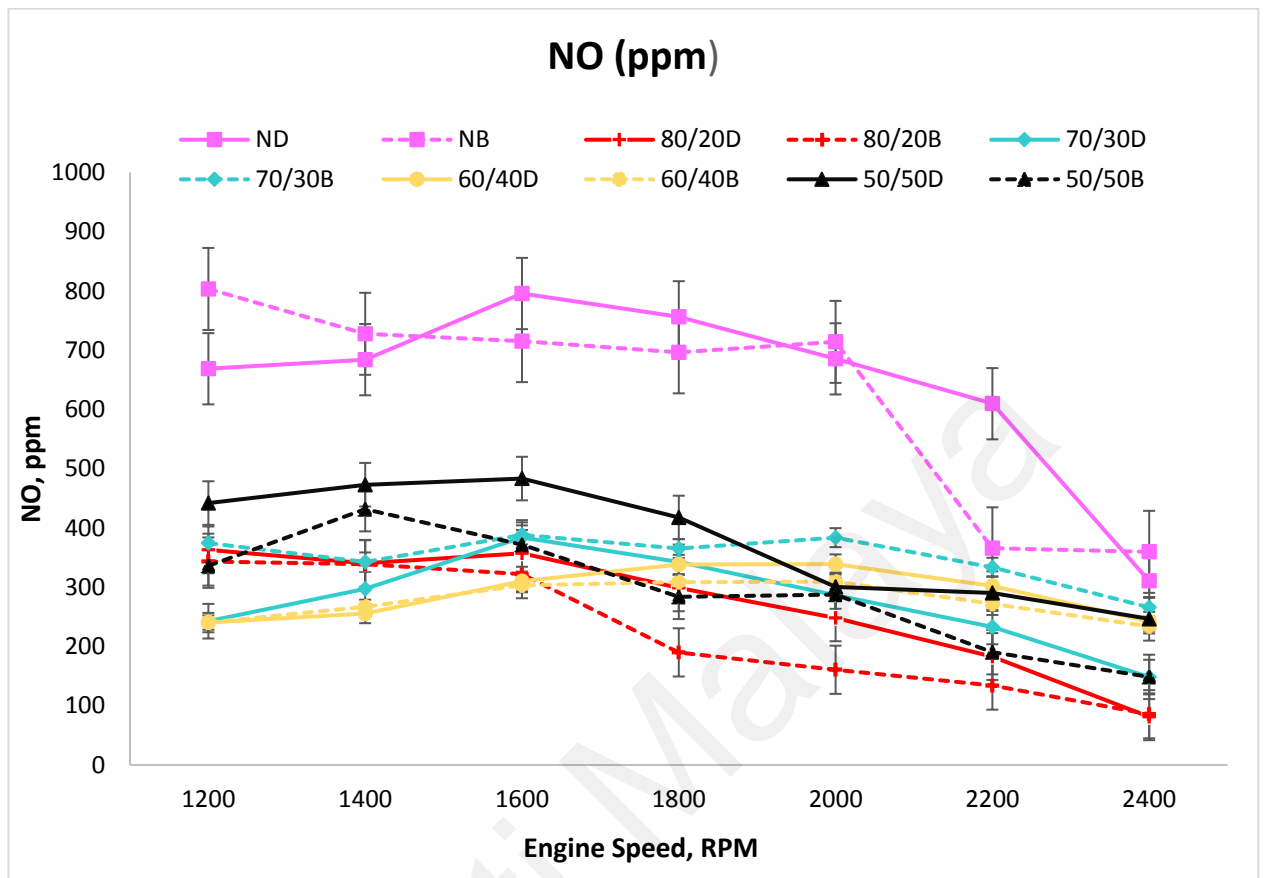


Figure 4.11: NO emission for blended coat at the variable speed

Based on the readings recorded for the NO emission, at the higher load of 1200 rpm, the 60/40D showed the lowest NO emission (240 ppm), followed by 70/30D (243 ppm), 80/20D (363 ppm), and 50/50D (442 ppm). As for the engine operation with biodiesel, the 60/40B showed the lowest NO emission (240 ppm), followed by 50/50B (336 ppm), 80/20B (343 ppm), and 70/30B (374 ppm). In summary, the obtained results at the higher load of the 1200 rpm showed that the 60% $Y_2O_3.ZrO_2$ + 40% $Al_2O_3.SiO_2$ (60/40D and 60/40B) yielded the lowest NO emission.

Secondly, based on the reading recorded for the NO emission, at the higher torque of 1600 rpm, 60/40D showed the lowest NO emission (310 ppm), followed by the 80/20D (357 ppm),

70/30D (384 ppm), and 50/50D (483 ppm). As for the engine operation with biodiesel, the 60/40B showed the lowest NO emission (303 ppm), followed by the 80/20B (322 ppm), 50/50B (372 ppm), and 70/30B (388 ppm). In summary, the obtained results at the higher torque of 1600 rpm showed that the 60% $Y_2O_3.ZrO_2$ + 40% $Al_2O_3.SiO_2$ (60/40D and 60/40B) yielded the lowest NO content.

Lastly, based on the readings recorded for the NO emission, at the higher speeds of 2400 rpm, the 80/20D showed the lowest NO emission (81 ppm), followed by 70/30D (148 ppm), 60/40D (242 ppm), and 50/50D (247 ppm). As for the engine operation with biodiesel, 80/20B - showed the lowest NO emission (86 ppm), followed by 50/50B (149 ppm), 60/40B (234 ppm), and 70/30B (266 ppm). It can be concluded that, from the obtained results at the higher speeds of 2400 rpm, it was revealed that the 80% $Y_2O_3.ZrO_2$ + 20% $Al_2O_3.SiO_2$ (80/20D and 80/20B) yielded the lowest NO content.

Overall, the use of biodiesel was found to perform better in reducing NO emissions compared to diesel. Additionally, the 60% $Y_2O_3.ZrO_2$ + 40% $Al_2O_3.SiO_2$ (60/40D and 60/40B) were found to maintain good stability, and released the lowest NO emission for both tested fuels across the highest loads and highest torque engine settings. The lower percentage content of the $Y_2O_3.ZrO_2$ with low thermal conductivity enhanced the NO reduction at the highest load and highest torques. Coated pistons 80% $Y_2O_3.ZrO_2$ + 20% $Al_2O_3.SiO_2$ (80/20D and 80/20B) emitted the lowermost NO at higher speeds. Additionally, at high speeds with decreasing temperatures, the highest percentage content of $Y_2O_3.ZrO_2$ (80%) emitted the lowermost NO due to the lower combustion temperature at high speeds (2400 rpm).

These findings proved the impact of the TBC in reducing NO_x emissions, one of the environmental pollution sources that should be controlled (Karthickeyan and Arulraj, 2014). Increase in combustion duration increases the fraction of the fuel, which burns later in the cycle, and consequently decreases the emission of NO_x (Dananjayakumar et al., 2021). Thus, the application of biodiesel fuel releases a lower amount of NO compared to Diesel. The release of NO_x emission to the environment should be controlled, as this gas has a negative impact on the environment. Thus, achieving lower NO will ensure the sustainability of the environment.

Figure 4.12 illustrates the trend of CO formation at variable engine speeds for the coated pistons with TBCs of 80% Y₂O₃.ZrO₂ + 20% Al₂O₃.SiO₂, 70% Y₂O₃.ZrO₂ + 30% Al₂O₃.SiO₂, 60% Y₂O₃.ZrO₂ + 40% Al₂O₃.SiO₂ and 50% Y₂O₃.ZrO₂ + 50% Al₂O₃.SiO₂.

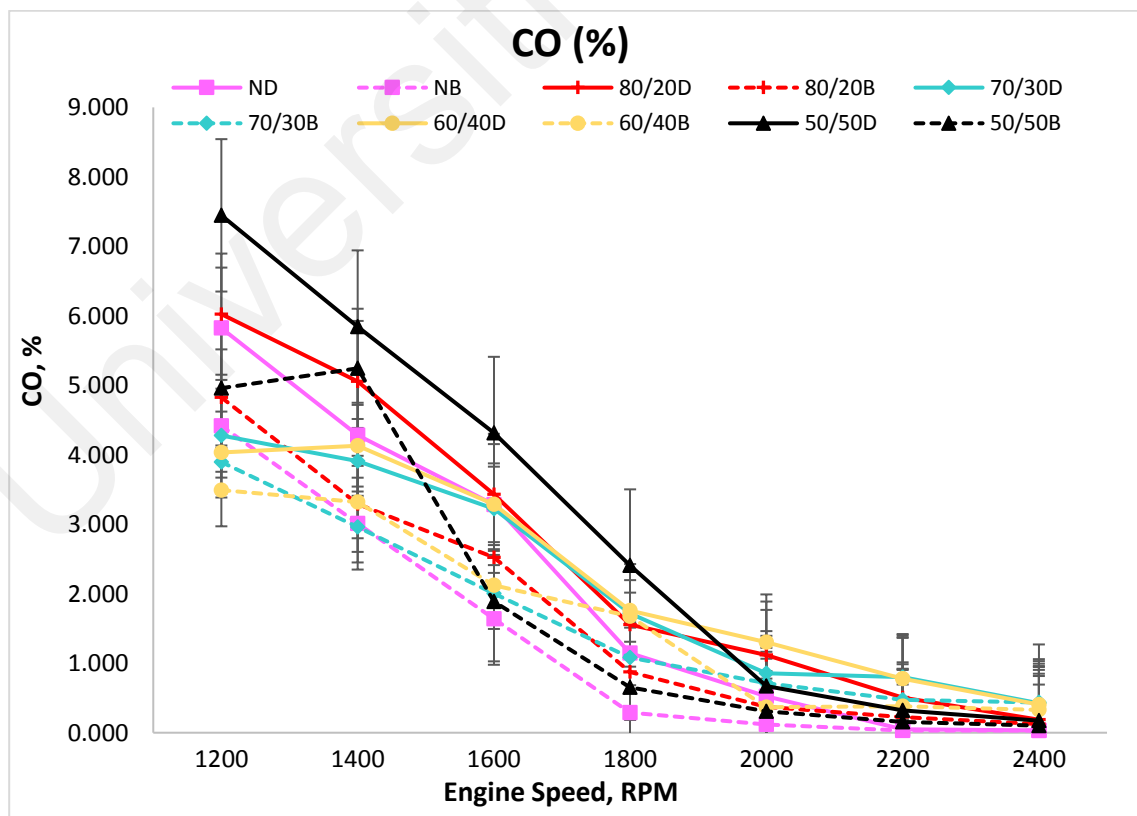


Figure 4.12: CO emission

Pistons coated with 60/40D recorded the lowest CO emission (4.03 %), followed by 70/30D (4.28 %), 80/20D (6.02 %), and 50/50D (7.45%), for the engine operation with diesel fuels at the maximum load of 1200 rpm. Secondly, pistons coated with 60/40B recorded the lowest CO emission (3.49 %), followed by 70/30B (3.90 %), 80/20B (4.83 %) and 50/50B (4.96 %), for the engine operation with biodiesel at the maximum load of 1200 rpm. Hence it was concluded that at speeds of 1200 rpm, the piston coated with 60% $Y_2O_3.ZrO_2$ + 40% $Al_2O_3.SiO_2$ (60/40D and 60/40B) yielded the lowermost CO emission.

Piston coated with 70/30D recorded the lowest CO emission (3.22 % ppm), followed by 60/40D (3.29 %), 80/20D (3.43 %), and 50/50D (4.31 %), for the engine operation with diesel fuel at the maximum torque of 1600 rpm. Likewise, it was observed that for the results of the engine operation with biodiesel fuel, 50/50B recorded the lowest CO emission (1.89 %), followed by 70/30B (2.00 %), 60/40B (2.12 %), and 80/20B (2.52 %). The obtained results at the maximum torque of 1600 rpm revealed that 70/30D and 50/50B yielded the lowest CO content. However, the piston coated with 70/30D did not manage to sustain the TBC for the durability test, due to the poor blend coating material characteristics. Hence, the next inline piston coated 60/40D was chosen to yield a lower CO content for the diesel fuelled engine.

The piston coated with 50/50D recorded the lowest CO emission (0.17 %), followed by 80/20D (0.19 %), 60/40D (0.41 %), and 70/30D (0.42 %), for the engine operation with diesel fuel at the maximum speed of 2400 rpm. Additionally, it was observed that for the engine operation with biodiesel, 50/50B recorded the lowest CO emission (0.10 %), followed by 80/20B (0.12 %), 60/40B (0.33 %), and 70/30B (0.44 %). Hence it was concluded that at

the speed of 2400 rpm, the piston coated with 50% $Y_2O_3.ZrO_2$ + 50% $Al_2O_3.SiO_2$ (50/50D and 50/50B) yielded the lowest CO emission.

Overall, the use of biodiesel was found to perform better in terms of reducing the NO emissions compared to diesel. Additionally, the 60% $Y_2O_3.ZrO_2$ + 40% $Al_2O_3.SiO_2$ (60/40D and 60/40B) was found to maintain good stability and release a lower CO emission for both the tested fuels at the high load engine settings. Whereas, the piston coated with 50% $Y_2O_3.ZrO_2$ + 50% $Al_2O_3.SiO_2$ (50/50D and 50/50B) was found to release the lowest CO emission for both the tested fuels at the high-speed engine settings. Both pistons coated with 60% $Y_2O_3.ZrO_2$ + 40% $Al_2O_3.SiO_2$ and 50% $Y_2O_3.ZrO_2$ + 50% $Al_2O_3.SiO_2$ released a lower CO emission for the high torque engine setting. Referring to the first phase of testing, the 100% coated $Al_2O_3.SiO_2$ released a lower CO. Hence the higher the content of the blend $Al_2O_3.SiO_2$, the more the CO emission was expected to reduce.

The CO emission was suggestively decreased with an increase in the speed. When the engine was running at an optimum speed, the CO emission was suppressed to the minimum, and almost eliminated its presence. This test also proved that regardless of pistons coated with any coating, the emission of CO was well suppressed. CO is a dangerous and toxic gas, and it is a mandatory requirement to ensure a lower emission for the CO release to the environment, as stipulated in the local environmental statutory. The lower emission of CO when biodiesel is applied as fuel was caused by higher oxygen content in the biodiesel, which was part of the combustion, leading to complete combustion at the lowered CO emission (Behçet et al., 2015)

Figure 4.13 shows the trend of CO₂ formation at variable engine speeds for the coated pistons with TBCs of 80% Y₂O₃.ZrO₂ + 20% Al₂O₃.SiO₂, 70% Y₂O₃.ZrO₂ + 30% Al₂O₃.SiO₂, 60% Y₂O₃.ZrO₂ + 40% Al₂O₃.SiO₂ and 50% Y₂O₃.ZrO₂ + 50% Al₂O₃.SiO₂.

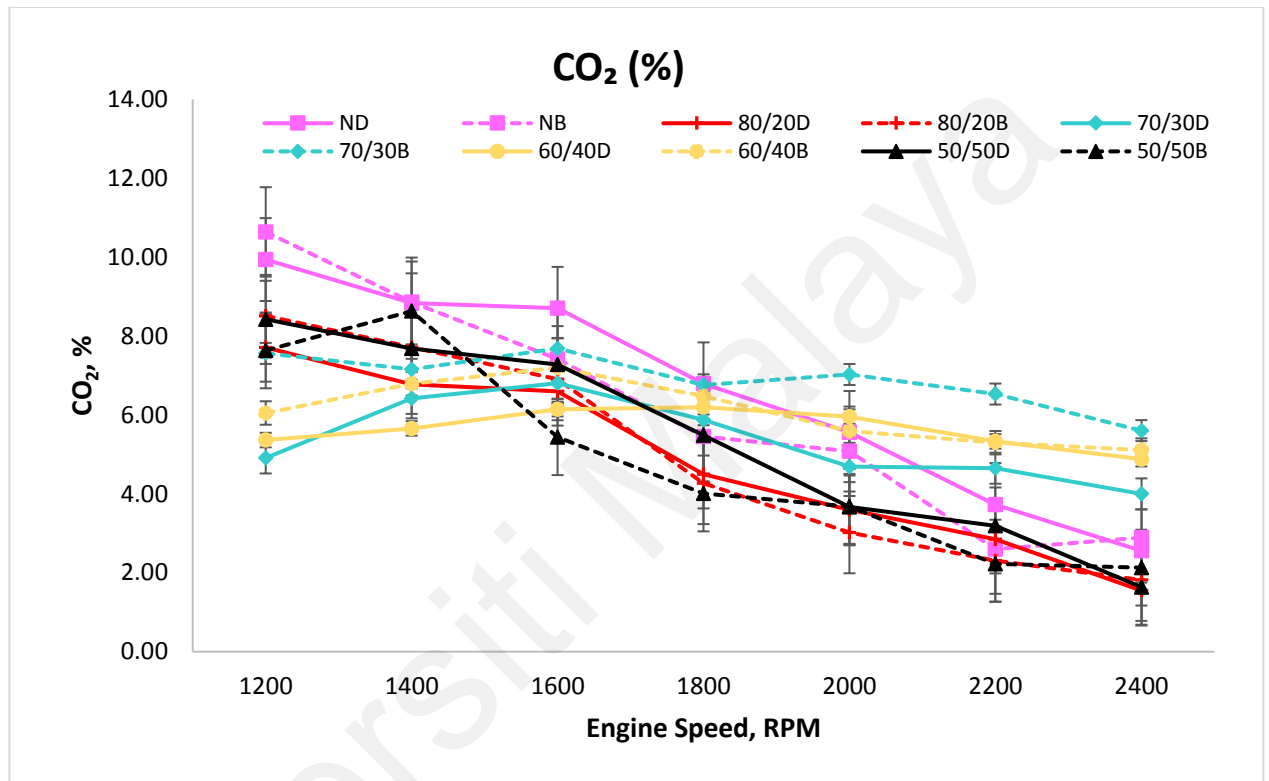


Figure 4.13: CO₂ emission

Results at the highest load of 1200 rpm for the diesel fuelled engine, and pistons coated with 70/30D, recorded the lowest CO₂ emission (4.91 %), followed by 60/40D (5.36 %), 80/20D (7.71 %), and 50/50D (8.43 %). As the result for the engine operating with biodiesel, the 60/40B recorded the lowest CO₂ emission (6.05 %), followed by 70/30B (7.56 %), 50/50B (7.64 %), and 80/20B (8.51 %). In summary, at the maximum load of 1200 rpm, the coated 70/30D and 60/40B yielded the lowest CO₂ content. However, the piston coated with 70/30D did not manage to sustain the TBC for the durability test, due to the poor blend coating

material characteristic. Hence, the next inline piston coated with 60/40D was chosen to yield a lower CO₂ content for the diesel fuelled engine.

Secondly, for result at the highest torque of 1600 rpm, the 60/40D recorded the lowest CO₂ emission (6.15 %), followed by 80/20D (6.60 %), 70/30D (6.81 %), and 50/50D (7.28 %). For the result of the engine operation with biodiesel, the 50/50B recorded the lowest CO₂ emission (5.44 %), followed by 80/20B (6.90 %), 60/40B (7.20 %) and 70/30B (7.69 %). In summary, at the maximum torque of 1600 rpm, samples coated with 60/40D and 50/50B yielded the lowest CO₂ content.

Finally, for the results at the highest speed of 2400 rpm, the 80/20D recorded the lowest CO₂ emission (1.55 %), followed by 50/50D (1.64 %), 70/30D (4.00 %), and 60/40D (4.88 %). As for the engine operation with biodiesel, the 80/20B recorded the lowest CO₂ emission (1.82 %), followed by 50/50B (2.13%), 60/40B (5.11 %), and 70/30B (5.60 %). In summary, at the maximum speed of 2400 rpm, the coated 80/20D and 80/20B samples yielded a lower CO₂ content.

Overall, the use of biodiesel was found to perform better in reducing CO₂ emissions compared to diesel. Additionally, the 60% Y₂O₃.ZrO₂ + 40% Al₂O₃.SiO₂ (60/40D and 60/40B) were found to maintain good stability and release the lowest NO emission for both tested fuels across the high load, and high torque engine settings. The lower percentage content of the Y₂O₃.ZrO₂ with low thermal conductivity enhanced the CO₂ reduction at the highest load and highest torques. The coated piston with 80% Y₂O₃.ZrO₂ + 20% Al₂O₃.SiO₂ (80/20D and 80/20B) emitted the lowest CO₂ at higher speeds. Additionally, at high speeds

with a decrease in temperature, the higher percentage content of $Y_2O_3.ZrO_2$ (80%) emitted the lowest CO_2 due to the combustion temperature being lower at higher speeds (2400 rpm).

4.3.2 Engine performance analysis

The impact of a TBC on the engine performance were examined for power generation, engine torque, BSFC, and BTE under various speeds using conventional diesel and biodiesel. Five series of tests were conducted to evaluate the engine performance of the TBC for the 90% $Y_2O_3.ZrO_2$ + 10% $Al_2O_3.SiO_2$, 80% $Y_2O_3.ZrO_2$ + 20% $Al_2O_3.SiO_2$, 70% $Y_2O_3.ZrO_2$ + 30% $Al_2O_3.SiO_2$, 60% $Y_2O_3.ZrO_2$ + 40% $Al_2O_3.SiO_2$ and 50% $Y_2O_3.ZrO_2$ + 50% $Al_2O_3.SiO_2$. BSFC is defined as the ratio of the fuel consumption rate over the brake power output. Additionally, BTE can be calculated by dividing the brake power output over the total energy input delivered. Because of countless loss mechanisms, such as combustion inefficiency, exhaust, flow, heat transfer and friction, the BTE of an original and field operating diesel cycle is typically far below 50% (Heywood, 1988).

Figure 4.14 shows the power results for the variable speed tested with diesel and biodiesel fuel. Five series of tests were conducted to evaluate the engine performance of the TBC for 90% $Y_2O_3.ZrO_2$ + 10% $Al_2O_3.SiO_2$, 80% $Y_2O_3.ZrO_2$ + 20% $Al_2O_3.SiO_2$, 70% $Y_2O_3.ZrO_2$ + 30% $Al_2O_3.SiO_2$, 60% $Y_2O_3.ZrO_2$ + 40% $Al_2O_3.SiO_2$ and 50% $Y_2O_3.ZrO_2$ + 50% $Al_2O_3.SiO_2$.

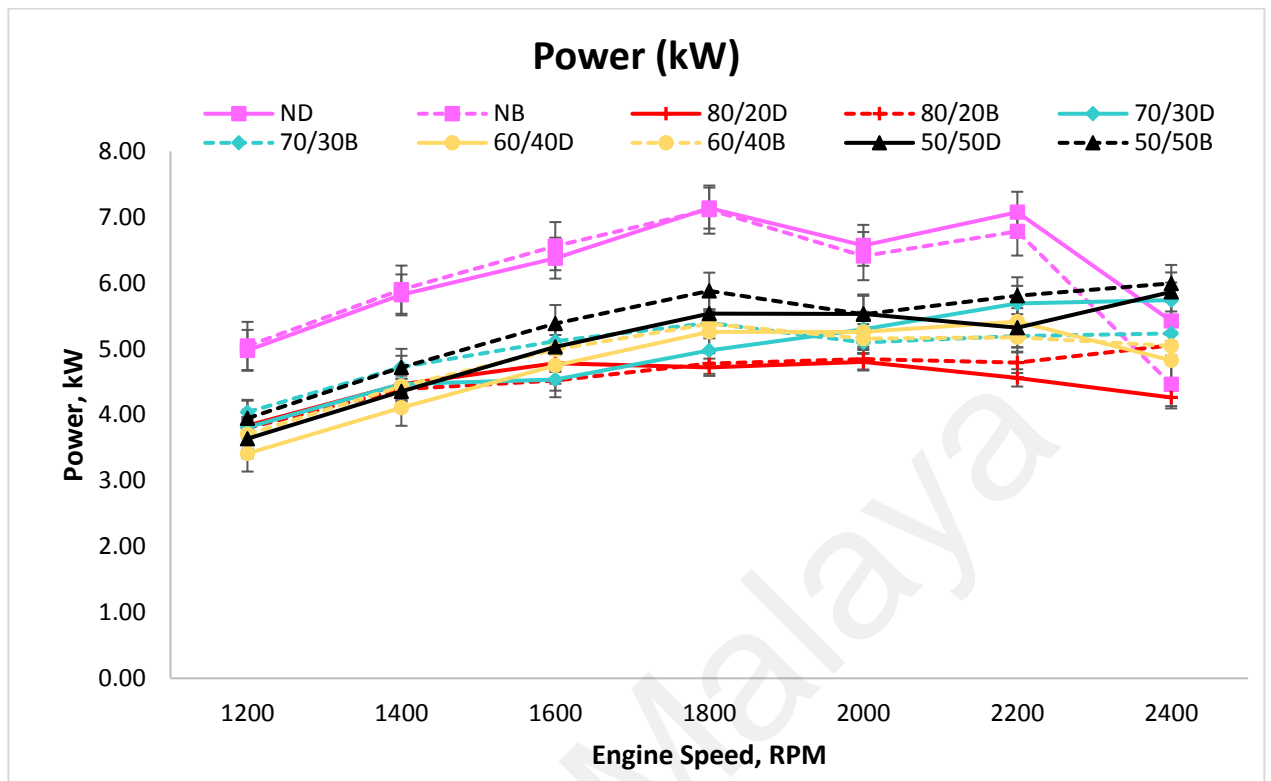


Figure 4.14: Power (kW) produced at various engine speed

When the diesel fuel fired diesel engine was at the maximum torque of 1600 rpm, the 80/20D recorded the most power (3.84 kW), followed by 70/30D (3.81 kW), 50/50D (3.64 kW), and 60/40D (3.41 kW). As for the power generated for the biodiesel fuel at the maximum load, the 70/30B recorded the most power (4.04 kW), followed by 50/50B (3.95 kW), 80/20B (3.80 kW), and 60/40B (3.70 kW). From the results at the maximum load of 1200 rpm, it was revealed that the uncoated piston (80/20D and 70/30B) yielded the highest power. However, the piston coated with 70/30D did not manage to sustain the TBC for the durability test due to poor blend coating material characteristics. Hence, the next inline piston coated 60/40D was chosen to be yield much higher power for the diesel fuelled engine.

Secondly, for the diesel fuel fired diesel engine at the maximum torque of 1600 rpm, the 50/50D recorded the uppermost power (5.03 kW), followed by the 80/20D (4.78 kW),

60/40D (4.75 kW), and 70/30D (4.53 kW). As for the engine operation fired up with biodiesel fuel, the 50/50B recorded the peak power (5.39 kW), followed by the 70/30B (5.12 kW), 60/40B (4.99 kW), and 80/20B (4.52 kW). Conclusively, from the results at the maximum torque of 1600 rpm, it was revealed that the piston coated with 50% $Y_2O_3.ZrO_2$ + 50% $Al_2O_3.SiO_2$ (50/50D and 50/50B) yielded the highest power.

Finally, for the engine operated with diesel fuel, at the maximum speed of 2400 rpm, the 50/50D recorded the peak power (5.87 kW), followed by 70/30D (5.74 kW), 60/40D (4.83 kW), and 80/20D (4.26 kW). As for the engine operation with biodiesel, the 50/50B recorded the highest power (6.00 kW), followed by 70/30B (5.24 kW), 80/20B (5.06 kW), and 60/40B (5.05 kW).

Conclusively, from the results at the maximum speed of 2400 rpm revealed that the piston coated with 50% $Y_2O_3.ZrO_2$ + 50% $Al_2O_3.SiO_2$ (50/50D and 50/50B) yielded the highest power.

As summarized, among all the blends, the piston coated with 60% $Y_2O_3.ZrO_2$ + 40% $Al_2O_3.SiO_2$ (60/40D and 60/40B) was found to maintain a high-power running engine for both tested fuels across the high loads, high torques and high-speed engine settings.

Figure 4.15 shows that the torque results for the variable speed tested with diesel and biodiesel fuel. Five series of tests were conducted to evaluate the engine performance of the TBC of the 90% $Y_2O_3.ZrO_2$ + 10% $Al_2O_3.SiO_2$, 80% $Y_2O_3.ZrO_2$ + 20% $Al_2O_3.SiO_2$, 70%

Y₂O₃.ZrO₂ + 30% Al₂O₃.SiO₂, 60% Y₂O₃.ZrO₂ + 40% Al₂O₃.SiO₂ and 50% Y₂O₃.ZrO₂ + 50% Al₂O₃.SiO₂.

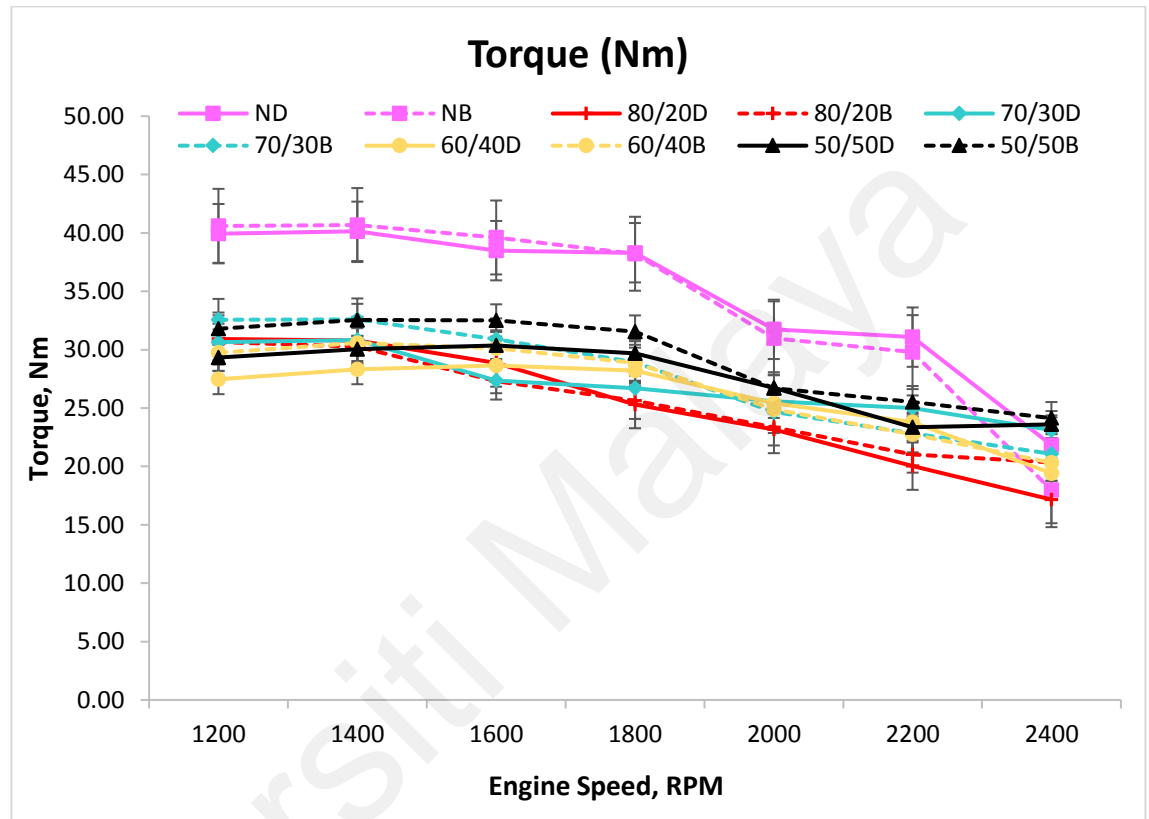


Figure 4.15: Engine torque at various engine speed

At the maximum load, for the Torque (Nm) generated against variable speeds for the Kubota Diesel Engine for all coated pistons tested with Diesel at the maximum load of 1200 rpm, the 80/20D logged the peak torque (30.92 Nm), followed by 70/30D (30.66 Nm), 50/50D (29.32 Nm), and 60/40D (27.46 Nm). As for the effect on the engine operated with biodiesel, the 70/30B recorded a peak torque (32.55 Nm), followed by 50/50B (31.80 Nm), 80/20B (30.65 Nm), and 60/40B (29.74 Nm). As can be observed, at the maximum load of 1200 rpm, it was revealed that the 80/20D and 70/30B yielded the highest torque. From the results of the piston coated 70/30B, it was seen that it did not manage to sustain the TBC for the

durability test due to poor blend coating material characteristics. Henceforth, the next inline piston coated 60/40B was chosen to yield higher power for the biodiesel fuelled engine.

To evaluate the effect of the diesel fuel at the maximum load of 1600 rpm, the 50/50D logged a peak torque (30.36 Nm), followed by 80/20D (28.86 Nm), 60/40D (28.65 Nm), and 70/30D (27.36 Nm). As for the effect of engines operated with biodiesel, the 50/50B logged a peak torque (32.51 Nm), followed by 70/30B (30.88 Nm), 60/40B (30.11 Nm), and 80/20B (27.30 Nm). In the case of the results at the maximum torque of 1600 rpm, the piston coated with 50% $Y_2O_3.ZrO_2 + 50\% Al_2O_3.SiO_2$ (50/50D and 50/50B) yielded the highest torque value.

In relation to the effect of diesel fuel at the maximum speed of 2400 rpm, the 50/50D logged a peak torque (23.59 Nm), followed by 70/30D (23.12 Nm), 60/40D (19.42 Nm), and 80/20D (17.16 Nm). As for the engine effect of the engine operated with biodiesel at the maximum speed of 2400 rpm, the 50/50B logged the peak torque (24.14 Nm), followed by 70/30B (21.08 Nm), 80/20B (20.35 Nm), and 60/40B (20.32 Nm). Hence it was concluded that at speeds of 2400 rpm, the piston coated with 50% $Y_2O_3.ZrO_2 + 50\% Al_2O_3.SiO_2$ (50/50D and 50/50B) yielded the highest torque value.

Another interesting topic which can be further discussed is that at all speeds, the 50% $Y_2O_3.ZrO_2 + 50\% Al_2O_3.SiO_2$ (50/50D and 50/50B) maintained a high torque engine for both tested fuels across the high load, and high torque engine settings.

Figure 4.16 shows the BSFC results for the variable speeds tested with diesel and biodiesel fuels. Five series of tests were conducted to evaluate the engine performance of the TBC for the samples of 90% $Y_2O_3.ZrO_2 + 10\% Al_2O_3.SiO_2$, 80% $Y_2O_3.ZrO_2 + 20\% Al_2O_3.SiO_2$, 70%

Y₂O₃.ZrO₂ + 30% Al₂O₃.SiO₂, 60% Y₂O₃.ZrO₂ + 40% Al₂O₃.SiO₂ and 50% Y₂O₃.ZrO₂ + 50% Al₂O₃.SiO₂.

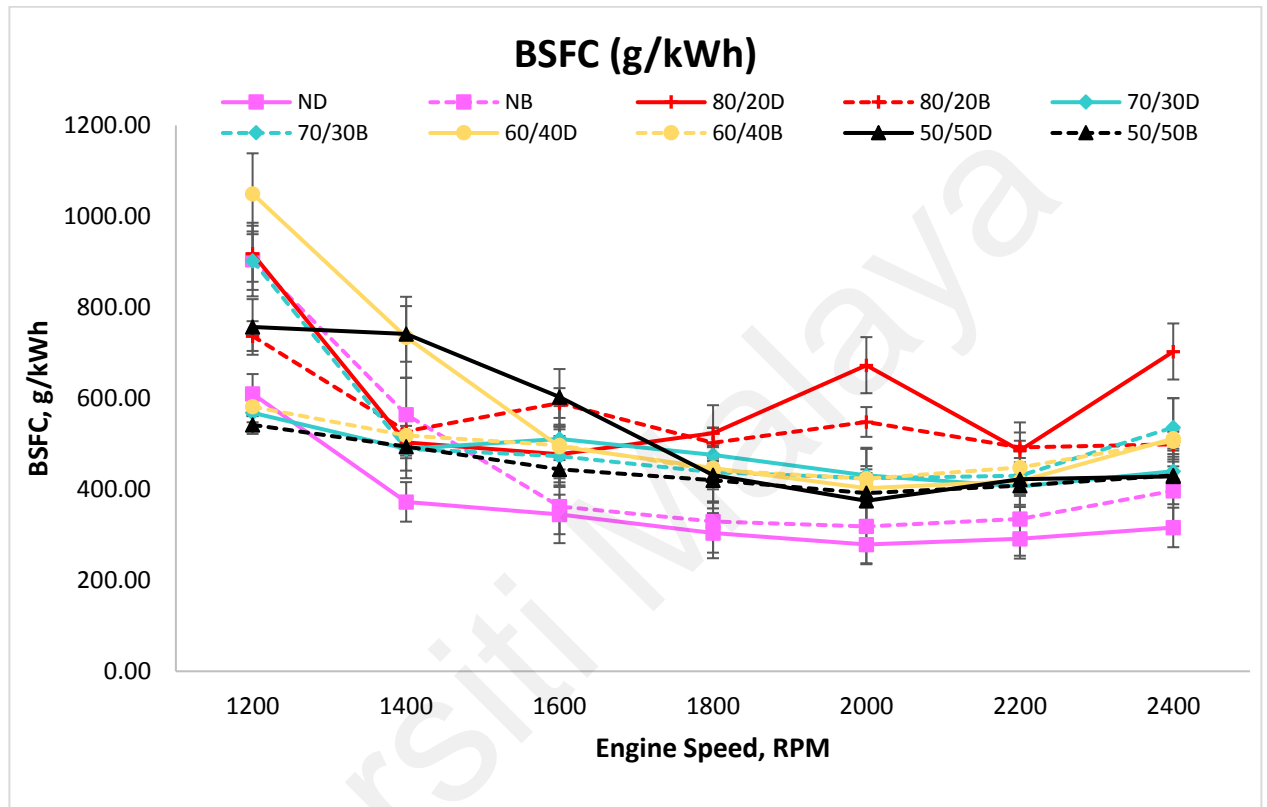


Figure 4.16: BSFC at various engine speed

The BSFC for the biodiesel fuelled engines is generally higher than the diesel-fuelled engines due to the lower caloric values of palm oil biodiesel, compared to the conventional diesel fuel (Behçet et al., 2015). The results showed that for engine fuelled with diesel, at the maximum load of 1200 rpm, the 70/30D registered the lowest BSFC (568.23 g/kWh), followed by the 50/50D (756.94 g/kWh), 80/20D (917.88 g/kWh) and 60/40D (1049.75 g/kWh). As for the engine operation with biodiesel, at the maximum load of 1200 rpm, the 50/50B recorded the lowest BSFC (541.73 g/kWh), followed by 60/40B (581.54 g/kWh), 80/20B (736.94 g/kWh), and 70/30B (902.67 g/kWh). The obtained results at the maximum

load of 1200 rpm revealed that the 70/30D and 50/50B yielded the lowest BSFC. From the results of the piston coated with 70/30D, it did not manage to sustain the TBC for the durability test, due to a poor blended coating material characteristic.

Henceforth, the next inline piston coated 50/50D was chosen to be yield a lower BSFC for the diesel fuelled engine. It was concluded that at speeds of 1200 rpm, the piston coated with 50% $Y_2O_3.ZrO_2$ + 50% $Al_2O_3.SiO_2$ (50/50D and 50/50B) yielded the lowest BSFC.

The results also show that for the engine fuelled with diesel at the maximum torque of 1600 rpm, the 80/20D recorded the lowest BSFC (477.08 g/kWh), followed by 60/40D (494 g/kWh), 70/30D (511.13 g/kWh), and 50/50D (603.27 g/kWh). As for the engine fuelled with biodiesel at the maximum torque of 1600 rpm, the 50/50B recorded the lowest BSFC (444.28 g/kWh), followed by 70/30B (472.97 g/kWh), 60/40B (496.41 g/kWh), and 80/20B (589.72 g/kWh). This finding indicates that at the maximum torque of 1600 rpm, the 80/20D and 50/50B yielded the lowest BSFC.

Finally, for engines fuelled with diesel at the maximum speed of 2400 rpm, the 50/50D recorded the lowest BSFC (428.41 g/kWh), followed by the 70/30D (440.12 g/kWh), 60/40D (511.65 g/kWh), and 80/20D (703.03 g/kWh). As for the engine fuelled with biodiesel at the maximum speed of 2400 rpm, the 50/50B recorded the lowest BSFC (430.52 g/kWh), followed by the 80/20B (498.68 g/kWh), 60/40B (505.77 g/kWh), and 70/30B (535.91 g/kWh). As can be observed, the obtained results at the maximum speed of 2400 rpm indicates that the 50% $Y_2O_3.ZrO_2$ + 50% $Al_2O_3.SiO_2$ (50/50D and 50/50B) yielded the lowest BSFC.

Overall, the biodiesel contributed to the lowest BSFC for the diesel. At all speeds, the 50% $Y_2O_3.ZrO_2$ + 50% $Al_2O_3.SiO_2$ (50/50D and 50/50B) maintained a good stability, and produced a lower BSFC for both the diesel & biodiesel test fuels.

Figure 4.17 shows the BTE results for the variable speeds tested with diesel and biodiesel fuels. Five series of tests were conducted to evaluate the engine performance of the TBC of for the samples of 90% $Y_2O_3.ZrO_2$ + 10% $Al_2O_3.SiO_2$, 80% $Y_2O_3.ZrO_2$ + 20% $Al_2O_3.SiO_2$, 70% $Y_2O_3.ZrO_2$ + 30% $Al_2O_3.SiO_2$, 60% $Y_2O_3.ZrO_2$ + 40% $Al_2O_3.SiO_2$ and 50% $Y_2O_3.ZrO_2$ + 50% $Al_2O_3.SiO_2$.

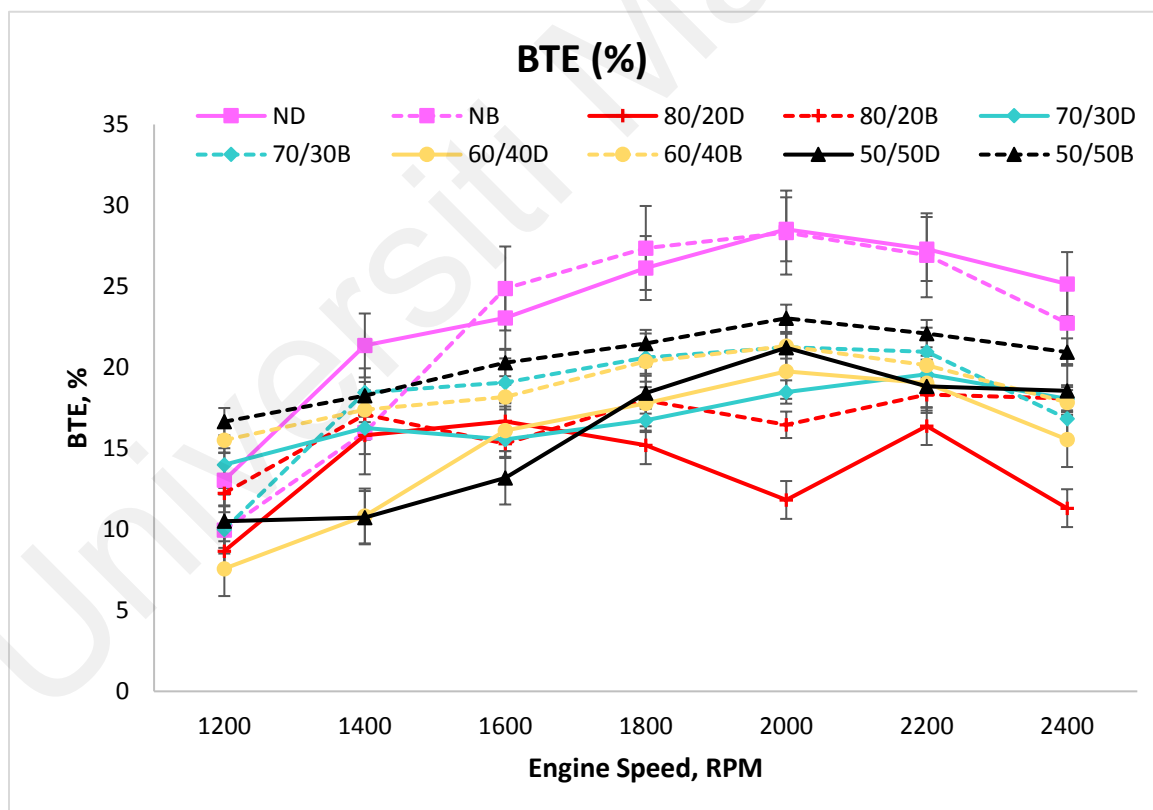


Figure 4.17: BTE percentage at various engine speed

During the maximum load of 1200 rpm for the diesel fuel, for BTE effect against the variable speed for all coated pistons tested with diesel fuel, the 70/30D recorded the highest BTE

(13.99 %), followed by 50/50D (10.51 %), 80/20D (8.66 %), and 60/40D (7.58%). As for the engine operation with biodiesel, the 50/50B recorded the highest BTE (16.65 %), followed by 60/40B (15.51 %), 80/20B (12.24 %), and 70/30B (9.99 %). Thus, the gained results at the maximum load of 1200 rpm revealed that the coated 70/30D and 50/50B yielded the highest BTE. From the results of the coated piston, the 70/30D did not manage to sustain the TBC for the durability test due to poor blended coating material characteristics. Henceforth, the next inline piston coated 50/50D was chosen to yield the highest BTE for the diesel fuelled engine. It was concluded that at speeds of 1200 rpm, the piston coated with 50% $Y_2O_3.ZrO_2$ + 50% $Al_2O_3.SiO_2$ (50/50D and 50/50B) yielded the highest BTE.

Following this was the maximum torque of 1600 rpm for the diesel fuelled engine, where the 80/20D recorded the highest BTE (16.67 %), followed by 60/40D (16.10 %), 70/30D (15.56 %), and 50/50D (13.18 %). As for the engine operation with biodiesel fuel, 50/50B recorded the highest BTE (20.30 %), followed by 70/30B (19.07 %), 60/40B (18.17 %), and 80/20B (15.30 %). Thus, the gained results at the maximum torque of 1600 rpm revealed that the 80/20D and 50/50B yielded the highest BTE.

As can be seen, at the maximum speed of 2400 rpm, the 50/50D recorded the highest BTE (18.56 %), followed by the 70/30D (18.07 %), 60/40D (15.54 %), and 80/20D (11.31 %). As for the biodiesel fuelled engine, the 50/50B recorded the highest BTE (20.95 %), followed by the 80/20B (18.09%), 60/40B (17.83 %), and 70/30B (16.83 %). The gained results at the maximum speed of 2400 rpm revealed that the 50% $Y_2O_3.ZrO_2$ + 50% $Al_2O_3.SiO_2$ (50/50D and 50/50B) yielded the highest BTE.


Overall, biodiesel contributed to a higher BTE than diesel. At all speeds, the 50% $Y_2O_3.ZrO_2$ + 50% $Al_2O_3.SiO_2$ (50/50D and 50/50B) maintained a good stability, and produced the highest BTE for the diesel & biodiesel test fuels. The BTE can be defined as the percentage of chemical energy from the fuel which is converted into kinetic energy in the engine (Masera and Hossain, 2019).

The selection of the right coating mixture is vital, as the TBC plays a significant role in converting chemical energy to kinetic energy. In addition, the excess oxygen content in the biodiesel generally contributes toward achieving a higher thermal efficiency (Kumar, Varun and Chauhan, 2015). Thus, the BTE of the biodiesel recorded a higher value compared to diesel.

4.3.3 Condition of piston crown after 6 hours engine operation

Table 4.6 represents a comparison between the conditions of the piston crown after running continuously for 6 hours to test the durability of the coated pistons. Five series of tests were conducted to evaluate the engine performance of the TBC of the samples of 90% $Y_2O_3.ZrO_2$ + 10% $Al_2O_3.SiO_2$, 80% $Y_2O_3.ZrO_2$ + 20% $Al_2O_3.SiO_2$, 70% $Y_2O_3.ZrO_2$ + 30% $Al_2O_3.SiO_2$, 60% $Y_2O_3.ZrO_2$ + 40% $Al_2O_3.SiO_2$ and 50% $Y_2O_3.ZrO_2$ + 50% $Al_2O_3.SiO_2$. The surface of the piston crown was observed to identify any abnormalities such as cracks or damage on the TBC coated on the piston crown.

Table 4.6: Comparison between conditions of piston crown after running 6 hours

Piston crown	Observation
<p>a) Coated Piston 90% $Y_2O_3.ZrO_2$ + 10% $Al_2O_3.SiO_2$</p> 	<p>The surface of the top and toroidal coated piston crown of 90% $Y_2O_3.ZrO_2$ + 10% $Al_2O_3.SiO_2$, was seen to have severe scaling (feel off)/damaged effect of coated TBC, observed based on visual inspection after 6 hours of engine running condition. There was no abnormality at the remaining uncoated parts of the combustion chamber. However, the engine suffers high vibration while operating with this coating, which is overaged. Overall, the piston coated with 90% $Y_2O_3.ZrO_2$ + 10% $Al_2O_3.SiO_2$ has the worst coating durability and integrity to protect the piston aluminium alloy substrate effectively. This blend is coated with 90% $Y_2O_3.ZrO_2$ + 10% $Al_2O_3.SiO_2$ is not recommended for engine testing and to believe having poor bonding morphological characteristics between $Y_2O_3.ZrO_2$ and $Al_2O_3.SiO_2$.</p>

b) Coated Piston 80% $Y_2O_3.ZrO_2$ +
20% $Al_2O_3.SiO_2$



The surface of the piston crown coated with TBC of 80% $Y_2O_3.ZrO_2$ + 20% $Al_2O_3.SiO_2$. There were no abnormalities other than a few traces of carbon deposits on the surface, observed based on visual inspection on the coated layer on piston crown part after 6h of engine running condition. Besides, the surface of the piston crown was seen to have minor cracks on the top surface. There was no abnormality at the remaining uncoated parts of the combustion chamber. Overall, no failure was detected after 6 hours of engine running condition. This shows that the TBC coated piston is 80% $Y_2O_3.ZrO_2$ + 20% $Al_2O_3.SiO_2$ can effectively protect by reducing the temperature of the piston aluminium alloy substrate.

The surface of the piston crown coated with TBC of 70% $Y_2O_3.ZrO_2$ + 30% $Al_2O_3.SiO_2$. The surface of the piston crown was seen to have a scaling (peel off) effect of coated TBC on the top surface and at the toroidal, observed based on visual inspection after 6 h of engine running condition. There was no abnormality at

c) Coated Piston 70% $Y_2O_3.ZrO_2$ +
30% $Al_2O_3.SiO_2$



the remaining uncoated parts of the combustion chamber. Overall, the piston coated with 70% $Y_2O_3.ZrO_2$ + 30% $Al_2O_3.SiO_2$ has poor coating durability and integrity to protect the piston aluminium alloy substrate effectively.

d) Coated Piston 60% $Y_2O_3.ZrO_2$ +
40% $Al_2O_3.SiO_2$



The surface of the piston crown coated with TBC of 60% $Y_2O_3.ZrO_2$ + 40% $Al_2O_3.SiO_2$. There were no abnormalities other than a few traces of carbon deposits on the surface, observed based on visual inspection on the coated layer on piston crown part after 6h of engine running condition. There was no abnormality at the remaining uncoated parts of the combustion chamber. Overall, no failure was detected after 6 hours of engine running condition. This shows that the TBC coated piston is 60% $Y_2O_3.ZrO_2$ + 40% $Al_2O_3.SiO_2$ can effectively protect by reducing the temperature of the piston aluminium alloy substrate.

e) Coated Piston 50% $Y_2O_3.ZrO_2$ +
50% $Al_2O_3.SiO_2$



The surface of the piston crown coated with TBC of 50% $Y_2O_3.ZrO_2$ + 50% $Al_2O_3.SiO_2$. There were no abnormalities other than a few traces of carbon deposits on the surface, observed based on visual inspection on the coated layer on piston crown part after 6 h of engine running condition. There was no abnormality at the remaining uncoated parts of the combustion chamber. Overall, no failure was detected after 6 hours of engine running condition. This show that the TBC of the blend coated 50% $Y_2O_3.ZrO_2$ + 50% $Al_2O_3.SiO_2$ can effectively protect by reducing the temperature of the piston aluminium alloy substrate. Furthermore, TBC of blend coated 50% $Y_2O_3.ZrO_2$ + 50% $Al_2O_3.SiO_2$ shows overwhelming coating durability without any minor cracks as good as coated 100% $Y_2O_3.ZrO_2$. This blend coat proved that blend between TBC is possible and without compromising its performance but subjected to the best match of blending composition, which coated 50% $Y_2O_3.ZrO_2$ + 50% $Al_2O_3.SiO_2$.

Based on Table 4.6, by comparing all variations of the TBC blends, for the samples of 90% $Y_2O_3.ZrO_2$ + 10% $Al_2O_3.SiO_2$, 80% $Y_2O_3.ZrO_2$ + 20% $Al_2O_3.SiO_2$, 70% $Y_2O_3.ZrO_2$ + 30% $Al_2O_3.SiO_2$, 60% $Y_2O_3.ZrO_2$ + 40% $Al_2O_3.SiO_2$ and 50% $Y_2O_3.ZrO_2$ + 50% $Al_2O_3.SiO_2$, the 150% $Y_2O_3.ZrO_2$ + 50% $Al_2O_3.SiO_2$ showed an overwhelming coating durability without any minor cracks. Secondly, the blended coating of 60% $Y_2O_3.ZrO_2$ + 40% $Al_2O_3.SiO_2$ and 80% $Y_2O_3.ZrO_2$ + 20% $Al_2O_3.SiO_2$ showed a positive result in terms of having very minor cracks. The blend coating of sample 90% $Y_2O_3.ZrO_2$ + 10% $Al_2O_3.SiO_2$ and 70% $Y_2O_3.ZrO_2$ + 30% $Al_2O_3.SiO_2$ were not recommended for engine testing, and to believe to have poor bonding morphological characteristics between the $Y_2O_3.ZrO_2$ and $Al_2O_3.SiO_2$. Therefore, by considering both the positive effects of with the blends between $Al_2O_3.SiO_2$ and $Y_2O_3.ZrO_2$ in the second phase of the experiment work, the blend coat's material characteristics achieved a possible stable condition and performance. Furthermore, by introducing the TBC in the piston crown, this will enhance the durability and life span of the piston.

The high temperature increase inside the piston attacks the surface of the uncoated piston as thermal fatigue loads. After engine operation, carbon gets accumulated (fouling) over the piston crown's surface. With the TBC, no cracks due to thermal fatigue were reported. The high strength and dense microstructure found on the coated piston's surface reduces the maintenance cost, and prolongs the piston's life span.

4.3.4 Summary

In this second phase test series, for the piston blend coated with 90% $Y_2O_3.ZrO_2$ + 10% $Al_2O_3.SiO_2$, 80% $Y_2O_3.ZrO_2$ + 20% $Al_2O_3.SiO_2$, 70% $Y_2O_3.ZrO_2$ + 30% $Al_2O_3.SiO_2$, 60% $Y_2O_3.ZrO_2$ + 40% $Al_2O_3.SiO_2$ and 50% $Y_2O_3.ZrO_2$ + 50% $Al_2O_3.SiO_2$ with test fuels of diesel and B100 palm biodiesel, which were evaluated for engine performance, emission, and combustion characteristics, these have been experimentally investigated in a DI diesel engine. The following main findings can be drawn from this test series. The engine performance measurement for the blend coated with 90% $Y_2O_3.ZrO_2$ + 10% $Al_2O_3.SiO_2$, 80% $Y_2O_3.ZrO_2$ + 20% $Al_2O_3.SiO_2$, 70% $Y_2O_3.ZrO_2$ + 30% $Al_2O_3.SiO_2$, 60% $Y_2O_3.ZrO_2$ + 40% $Al_2O_3.SiO_2$ and 50% $Y_2O_3.ZrO_2$ + 50% $Al_2O_3.SiO_2$ for both conventional diesel (as a baseline), and B100 palm biodiesel, can be concluded as shown in Table 4.7.

Table 4.7: Summary of the second phase of the engine performance

Blend TBC	Performance			
	BTE	BSFC	Power	Torque
Diesel Fuel				
90% $Y_2O_3.ZrO_2$ + 10% $Al_2O_3.SiO_2$	Very Poor	Very Poor	Very Poor	Very Poor
80% $Y_2O_3.ZrO_2$ + 20% $Al_2O_3.SiO_2$	Fair	Fair	Good	Good
70% $Y_2O_3.ZrO_2$ + 30% $Al_2O_3.SiO_2$	Very Good	Very Good	Fair	Fair
60% $Y_2O_3.ZrO_2$ + 40% $Al_2O_3.SiO_2$	Poor	Poor	Poor	Poor
50% $Y_2O_3.ZrO_2$ + 50% $Al_2O_3.SiO_2$	Good	Good	Very Good	Very Good

Biodiesel Fuel				
90% Y ₂ O ₃ .ZrO ₂ + 10% Al ₂ O ₃ .SiO ₂	Very Poor	Very Poor	Very Poor	Very Poor
80% Y ₂ O ₃ .ZrO ₂ + 20% Al ₂ O ₃ .SiO ₂	Fair	Fair	Fair	Fair
70% Y ₂ O ₃ .ZrO ₂ + 30% Al ₂ O ₃ .SiO ₂	Poor	Poor	Good	Good
60% Y ₂ O ₃ .ZrO ₂ + 40% Al ₂ O ₃ .SiO ₂	Good	Good	Poor	Poor
50% Y ₂ O ₃ .ZrO ₂ + 50% Al ₂ O ₃ .SiO ₂	Very Good	Very Good	Very Good	Very Good

Based on the analysis, the blend coated with 90% Y₂O₃.ZrO₂ + 10% Al₂O₃.SiO₂ (P4B & P4D) will not be evaluated, as the value of the BTE was poor, and the engine was underperforming under abnormal vibration. Thus, the 90% Y₂O₃.ZrO₂ + 10% Al₂O₃.SiO₂ coating mixture was not a good coating to be considered for TBC. Substantially, the coated 50% Y₂O₃.ZrO₂ + 50% Al₂O₃.SiO₂ demonstrated a better engine performance for both the diesel and biodiesel fuels. The rest of the coated piston for the 80% Y₂O₃.ZrO₂ + 20% Al₂O₃.SiO₂, 70% Y₂O₃.ZrO₂ + 30% Al₂O₃.SiO₂, 60% Y₂O₃.ZrO₂ + 40% Al₂O₃.SiO₂ depicted an average engine performance for both diesel, and biodiesel fuels.

The engine emission analysis for the blend coated with 90% Y₂O₃.ZrO₂ + 10% Al₂O₃.SiO₂, 80% Y₂O₃.ZrO₂ + 20% Al₂O₃.SiO₂, 70% Y₂O₃.ZrO₂ + 30% Al₂O₃.SiO₂, 60% Y₂O₃.ZrO₂ + 40% Al₂O₃.SiO₂ and 50% Y₂O₃.ZrO₂ + 50% Al₂O₃.SiO₂ for both the conventional diesel (as a baseline), and B100 palm biodiesel, can be concluded as shown in Table 4.8.

Table 4.8: Summary of the second phase of the emission analysis

Blend TBC	Emission			
	CO	CO ₂	HC	NO
Diesel Fuel				
90% Y ₂ O ₃ .ZrO ₂ + 10% Al ₂ O ₃ .SiO ₂	Very Poor	Very Poor	Very Poor	Very Poor
80% Y ₂ O ₃ .ZrO ₂ + 20% Al ₂ O ₃ .SiO ₂	Fair	Very Good	Fair	Good
70% Y ₂ O ₃ .ZrO ₂ + 30% Al ₂ O ₃ .SiO ₂	Good	Fair	Good	Fair
60% Y ₂ O ₃ .ZrO ₂ + 40% Al ₂ O ₃ .SiO ₂	Very Good	Good	Very Good	Very Good
50% Y ₂ O ₃ .ZrO ₂ + 50% Al ₂ O ₃ .SiO ₂	Poor	Poor	Poor	Poor
Biodiesel Fuel				
90% Y ₂ O ₃ .ZrO ₂ + 10% Al ₂ O ₃ .SiO ₂	Very Poor	Very Poor	Very Poor	Very Poor
80% Y ₂ O ₃ .ZrO ₂ + 20% Al ₂ O ₃ .SiO ₂	Poor	Very Good	Poor	Good
70% Y ₂ O ₃ .ZrO ₂ + 30% Al ₂ O ₃ .SiO ₂	Good	Poor	Fair	Poor
60% Y ₂ O ₃ .ZrO ₂ + 40% Al ₂ O ₃ .SiO ₂	Fair	Fair	Very Good	Very Good
50% Y ₂ O ₃ .ZrO ₂ + 50% Al ₂ O ₃ .SiO ₂	Very Good	Good	Good	Fair

Considerably, the coated 50% $Y_2O_3.ZrO_2$ + 50% $Al_2O_3.SiO_2$ demonstrated a slightly better value for emissions for both the diesel and biodiesel fuels, compared to the 60% $Y_2O_3.ZrO_2$ + 40% $Al_2O_3.SiO_2$. The remaining of the coated piston of the 80% $Y_2O_3.ZrO_2$ + 20% $Al_2O_3.SiO_2$ and 70% $Y_2O_3.ZrO_2$ + 30% $Al_2O_3.SiO_2$ performed an average engine performance for both the diesel and biodiesel fuels. The poor engine emission analysis logged for the blend coated with 90% $Y_2O_3.ZrO_2$ + 10% $Al_2O_3.SiO_2$ was due to the poor bond material characteristics between the $Y_2O_3.ZrO_2$ and $Al_2O_3.SiO_2$. It was observed that the use of the $Al_2O_3.SiO_2$ coating had an excellent result on the engine emission. This study produced an overwhelming result for reducing the NO emission using the blend coating. The correlation of other effects on the variation of the NO emissions when using the TBC can be evaluated much more comprehensively. Conclusively, in the second phase of the research, there was an opportunity to identify the optimum blend between the $Al_2O_3.SiO_2$ and $Y_2O_3.ZrO_2$ and enhance the gap between both materials, to achieve the lower emission value which is released to the environment.

The durability studies for the blend coated with 90% $Y_2O_3.ZrO_2$ + 10% $Al_2O_3.SiO_2$, 80% $Y_2O_3.ZrO_2$ + 20% $Al_2O_3.SiO_2$, 70% $Y_2O_3.ZrO_2$ + 30% $Al_2O_3.SiO_2$, 60% $Y_2O_3.ZrO_2$ + 40% $Al_2O_3.SiO_2$ and 50% $Y_2O_3.ZrO_2$ + 50% $Al_2O_3.SiO_2$ for both the conventional diesel (as a baseline), and B100 palm biodiesel, can be concluded as shown in Table 4.9.

Table 4.9: Summary of the second phase of the durability studies

Blend TBC	DURABILITY
Diesel	
90% Y ₂ O ₃ .ZrO ₂ + 10% Al ₂ O ₃ .SiO ₂	Very Poor
80% Y ₂ O ₃ .ZrO ₂ + 20% Al ₂ O ₃ .SiO ₂	Fair
70% Y ₂ O ₃ .ZrO ₂ + 30% Al ₂ O ₃ .SiO ₂	Poor
60% Y ₂ O ₃ .ZrO ₂ + 40% Al ₂ O ₃ .SiO ₂	Good
50% Y ₂ O ₃ .ZrO ₂ + 50% Al ₂ O ₃ .SiO ₂	Very Good
Biodiesel	
90% Y ₂ O ₃ .ZrO ₂ + 10% Al ₂ O ₃ .SiO ₂	Very Poor
80% Y ₂ O ₃ .ZrO ₂ + 20% Al ₂ O ₃ .SiO ₂	Fair
70% Y ₂ O ₃ .ZrO ₂ + 30% Al ₂ O ₃ .SiO ₂	Poor
60% Y ₂ O ₃ .ZrO ₂ + 40% Al ₂ O ₃ .SiO ₂	Good
50% Y ₂ O ₃ .ZrO ₂ + 50% Al ₂ O ₃ .SiO ₂	Very Good

Conversely, by comparing for the blend coated with 90% Y₂O₃.ZrO₂ + 10% Al₂O₃.SiO₂, 80% Y₂O₃.ZrO₂ + 20% Al₂O₃.SiO₂, 70% Y₂O₃.ZrO₂ + 30% Al₂O₃.SiO₂, 60% Y₂O₃.ZrO₂ + 40% Al₂O₃.SiO₂ and 50% Y₂O₃.ZrO₂ + 50% Al₂O₃.SiO₂ for both the conventional diesel and palm biodiesel, the 50% Y₂O₃.ZrO₂ + 50% Al₂O₃.SiO₂ showed an overwhelming coating durability without any minor cracks on the top surface of the piston crown. Hence, with the blend between the Al₂O₃.SiO₂ and Y₂O₃.ZrO₂, Y₂O₃.ZrO₂ material characteristics, this helped to strengthen the TBC material properties and characteristics. The overall criteria of the selection between the blend coated with 90% Y₂O₃.ZrO₂ + 10% Al₂O₃.SiO₂, 80% Y₂O₃.ZrO₂ + 20% Al₂O₃.SiO₂, 70% Y₂O₃.ZrO₂ + 30% Al₂O₃.SiO₂, 60% Y₂O₃.ZrO₂ + 40% Al₂O₃.SiO₂ and 50% Y₂O₃.ZrO₂ + 50% Al₂O₃.SiO₂ for both the conventional diesel and palm biodiesel for the piston crown evaluation is shown in Table 4.10.

Table 4.10: Piston selection of the second phase of the research work

TBC	Performance	Emission	Durability	Overall
90% Y ₂ O ₃ .ZrO ₂ + 10% Al ₂ O ₃ .SiO ₂	Very Poor	Very Poor	Very Poor	Very Poor
80% Y ₂ O ₃ .ZrO ₂ + 20% Al ₂ O ₃ .SiO ₂	Fair	Good	Fair	Fair
70% Y ₂ O ₃ .ZrO ₂ + 30% Al ₂ O ₃ .SiO ₂	Good	Fair	Poor	Poor
60% Y ₂ O ₃ .ZrO ₂ + 40% Al ₂ O ₃ .SiO ₂	Poor	Very Good	Good	Good
50% Y ₂ O ₃ .ZrO ₂ + 50% Al ₂ O ₃ .SiO ₂	Very Good	Poor	Very Good	Very Good

The coating mixture of 60% Y₂O₃.ZrO₂ + 40% Al₂O₃.SiO₂ produced an overwhelming result in terms of reducing the NO and CO emission, but is not promising in terms of performance. On the other hand, the 50% Y₂O₃.ZrO₂ + 50% Al₂O₃.SiO₂ showed a much better performance and slightly higher NO compared to the 60% Y₂O₃.ZrO₂ + 40% Al₂O₃.SiO₂. The overall criteria of the selection between the blend coats of different percentages of Y₂O₃.ZrO₂ and Al₂O₃.SiO₂ for the piston crown was evaluated. As per the conclusion, the coated piston with 50% Y₂O₃.ZrO₂ + 50% Al₂O₃.SiO₂ showed a promising result for higher engine performance, lower emission, and higher durability (TBC coated with longer lifespan) during the diesel and biodiesel fuelled engine testing. Further comparisons were extended between the uncoated and coated pistons with 50% Y₂O₃.ZrO₂ + 50% Al₂O₃.SiO₂ as shown in Table 4.11.

Table 4.11: Comparison between uncoated and selected blend coated piston

TBC	Performance	Emission	Durability	Overall
Uncoated piston	Very Good	Good	Good	Good
50% Y ₂ O ₃ .ZrO ₂ + 50% Al ₂ O ₃ .SiO ₂	Good	Very Good	Very Good	Very Good

Conclusively, the coated piston with 50% $Y_2O_3.ZrO_2$ + 50% $Al_2O_3.SiO_2$ showed a promising result for low emission, and higher durability during diesel and biodiesel fuelled engine testing. Despite slightly lower engine performance for the 50% $Y_2O_3.ZrO_2$ + 50% $Al_2O_3.SiO_2$ coated piston compared to the uncoated piston, the 50% $Y_2O_3.ZrO_2$ + 50% $Al_2O_3.SiO_2$ coated piston was expected to extend the maintenance downtime intervals (major overhaul; change piston). The RT125 is generally used in agricultural industries, whereby in general practices, the engine will be used for farming activities over extensive durations, and with high loads on a daily basis.

4.4 Cost Compression Analysis

Based on the selection criteria of the selected blended coatings of 50% $Y_2O_3.ZrO_2$ + 50% $Al_2O_3.SiO_2$, the potential cost saving was calculated and evaluated compared to the commonly used TBC coat of 100% $Y_2O_3.ZrO_2$. This analysis indicated the advantage in terms of cost compression, comparing the blend coating of the 50% $Y_2O_3.ZrO_2$ + 50% $Al_2O_3.SiO_2$ with the existing commercialized TBC coat in the market. For the purpose of this research study, the value or pricing were derived from the raw material cost purchased through a local supplier. Hence, further studies for the market survey with extensive business development and marketing strategy is required to produce practical and realistic cost saving values.

Table 4.12: Raw material cost of $Al_2O_3.SiO_2$ and $Y_2O_3.ZrO_2$

TBC	Raw material cost
$Y_2O_3.ZrO_2$	RM157.20/lbs.
$Al_2O_3.SiO_2$	RM72.00/lbs.

Based on the selected blend coats of 50% $Y_2O_3.ZrO_2$ + 50% $Al_2O_3.SiO_2$, the calculation was derived based on the composition of the percentage blend coat as follows:

$$\begin{aligned}
 \text{The cost of } 50\% Y_2O_3.ZrO_2 + 50\% Al_2O_3.SiO_2 &= (50\% \times RM157.20) + (50\% \times RM 72.00) \\
 &= (0.5 \times 157.20) + (0.5 \times 72.00) \\
 &= 78.6 + 36 \\
 &= RM 114.60
 \end{aligned}$$

Referring to the cost computed for the coated TBC of 50% $Y_2O_3.ZrO_2$ + 50% $Al_2O_3.SiO_2$, this cost will then be compared to the coated TBC of 100% $Y_2O_3.ZrO_2$ to help compute the potential cash generation as below:

$$\begin{aligned}
 \text{Potential cash generation} &= \text{Cost of } Y_2O_3.ZrO_2 - \text{Cost of } 50\% Y_2O_3.ZrO_2 + 50\% Al_2O_3.SiO_2 \\
 &= RM157.20 - RM 114.60 \\
 &= RM 42.60/lbs.
 \end{aligned}$$

Based on the computed potential cash generation of RM 42.60/lbs. using the TBC of 50% $Y_2O_3.ZrO_2$ + 50% $Al_2O_3.SiO_2$, the percentage of saving is defined as follows:

$$\begin{aligned}
 \text{Percentage of saving} &= \frac{\text{Cash saving from TBC } 50\% Y_2O_3.ZrO_2 + 50\% Al_2O_3.SiO_2}{\text{Cost of } Y_2O_3.ZrO_2} \\
 &= RM 42.60 / RM 157.20 \\
 &= \mathbf{27\%}
 \end{aligned}$$

Mathematically, by using a blend coat of 50% $Y_2O_3.ZrO_2$ + 50% $Al_2O_3.SiO_2$, this can help to generate cash savings, and commercial benefits of up to 27% compared to the purchase of a 100% $Y_2O_3.ZrO_2$. Hence, the coated piston with 50% $Y_2O_3.ZrO_2$ + 50% $Al_2O_3.SiO_2$ will be one of the most reliable TBC options to be considered, for commercialization due to its capacity to enhance the product's features.

CHAPTER 5

CONCLUSION & RECOMMENDATION

5.1 Conclusions

A series of experiment were conducted in this research to gauge the use of diesel and biodiesel fuels in internal combustion engines for engines operating with various TBCs. An experimental diesel engine system was built for this research study. With this system, a variety coating were tested and characterized to achieve the research objectives. The TBC coating of 50% $Y_2O_3.ZrO_2$ + 50% $Al_2O_3.SiO_2$ was capable to provide an optimal performance and reduce engine-out emissions.

In the case of the study of diesel and palm biodiesels on variable engine speeds for the coated pistons with a TBC of $Y_2O_3.ZrO_2$, and for the coated and uncoated pistons with $Al_2O_3.SiO_2$, the first objective of this research study managed to characterize the piston's surface coating using the thermal barrier $Y_2O_3.ZrO_2$ and $Al_2O_3.SiO_2$. In general, all diesel and biodiesel fuels showed a prominent result for the coated piston with 100% $Y_2O_3.ZrO_2$ for low emission producers, and had a higher durability (TBC coated longer lifespan) during the diesel engine's testing. Despite slightly lower engine performance for the 100% $Y_2O_3.ZrO_2$ coated piston compared to the uncoated piston, the 100% $Y_2O_3.ZrO_2$ coated piston was expected to extend the maintenance downtime intervals.

In the case of the study of the diesel and palm biodiesels on the variable engine speeds for the coated pistons with blend coatings of 90% $Y_2O_3.ZrO_2$ + 10% $Al_2O_3.SiO_2$, 80%

$Y_2O_3.ZrO_2 + 20\% Al_2O_3.SiO_2$, $70\% Y_2O_3.ZrO_2 + 30\% Al_2O_3.SiO_2$, $60\% Y_2O_3.ZrO_2 + 40\% Al_2O_3.SiO_2$ and $50\% Y_2O_3.ZrO_2 + 50\% Al_2O_3.SiO_2$ for both conventional diesel and palm biodiesel for piston crowns, the second objective of this research study managed to evaluate the engine's thermal efficiency and emission characteristics of the palm biodiesel with uncoated and coated $Y_2O_3.ZrO_2$ and $Al_2O_3.SiO_2$ materials with different percentages. Coating mixtures of $60\% Y_2O_3.ZrO_2 + 40\% Al_2O_3.SiO_2$ produced an overwhelming result for reducing the NO and CO emissions but was not promising in terms of the performance. On the other hand, the $50\% Y_2O_3.ZrO_2 + 50\% Al_2O_3.SiO_2$ showed a better performance and slightly higher NO compared to the $60\% Y_2O_3.ZrO_2 + 40\% Al_2O_3.SiO_2$. Additionally, the piston coated with a TBC of $50\% Y_2O_3.ZrO_2 + 50\% Al_2O_3.SiO_2$ was compared to the uncoated piston. Despite slightly lower engine performance for the $50\% Y_2O_3.ZrO_2 + 50\% Al_2O_3.SiO_2$, the TBC of the $50\% Y_2O_3.ZrO_2 + 50\% Al_2O_3.SiO_2$ produced a substantially overwhelming result in terms of its low emission and high durability TBC and is expected to extend the maintenance downtime intervals for the RT 125 diesel engine.

Based on selection criteria of the selected blended coating of $50\% Y_2O_3.ZrO_2 + 50\% Al_2O_3.SiO_2$, it generated a 27% cash saving and commercial benefits, compared to the purchase of a $100\% Y_2O_3.ZrO_2$. Additionally, the third objective of this research study managed to analyse the cost-effectiveness for the industrial commercial CI Engine's application coating materials. Ultimately, the results from this study suggested that the TBC of the $50\% Y_2O_3.ZrO_2 + 50\% Al_2O_3.SiO_2$ has a high potential as a substitution material for the $Y_2O_3.ZrO_2$ for engines operating with current and future combustion strategies.

5.2 Recommendations

This research work is a stepping stone for long term goals for creating sustainable and eco-friendly, cost affordable, and resources friendly security alignments with The Energy Trilemma. More considerations will be required for the advancement of this technology and studies in the future. The following recommendations for future works are suggested:

- Due to limited available facilities, it is suggested that the variation of thickness of the blend coats should be studied.
- The blend between $Y_2O_3.ZrO_2$ and other competitive TBCs in the market need to be compared and studied.
- To enhance the engine's performance, a complete study should apply coatings across the entire system (piston crown, valves, combustion liner, cylinder head).

REFERENCES

- Abbas, M.R., Uday, M.B., Mohd Noor, A., Ahmad, N. & Rajoo, S. (2016). Microstructural evaluation of a slurry based Ni/YSZ thermal barrier coating for automotive turbocharger turbine application. *Materials & Design*, 109, 47 – 56.
- Aydin, S., Sayin, C., Altun, S. & Aydin, H. (2016). Effects of thermal barrier coating on the performance and combustion characteristics of a diesel engine fueled with biodiesel produced from waste frying cottonseed oil and ultra-low sulfur diesel. *International Journal of Green Energy*, 13(11), 1102 – 1108.
- Aydin, S., & Sayin, C. (2014). Impact of thermal barrier coating application on the combustion, performance and emissions of a diesel engine fuelled with waste cooking oil biodiesel-diesel blends. *Fuel*, 136, 334 – 340.
- Ahmaniemi, S. et al. (2004). Characterization of modified thick thermal barrier coatings', *Journal of Thermal Spray Technology*, 13(3), 361–369.
- Ali, O. M. et al. (2015). Analysis of blended fuel properties and engine performance with palm biodiesel-diesel blended fuel. *Renewable Energy*. Elsevier Ltd, 86, 59-67.
- Azadi, M. et al. (2013). A review of thermal barrier coating effects on diesel engine performance and components lifetime. *International Journal of Automotive Engineering*, 3(1), 305-317.
- Abdelrahman Hegab, Kamal Dahuwa, Reza Islam, Alasdair Cairns, Ankit Khurana, Suman Shrestha, & Robin Francis. (2021). Plasma electrolytic oxidation thermal barrier coating for reduced heat losses in IC engines. *Applied Thermal Engineering*, 196, 117316.
- Arka Roychoudhury, Ayan Banerjee, Prakash Chandra Mishra, & Fuad Khoshnaw. (2021). An FEA material strength modelling of a coated engine piston. *Materials Today: Proceedings*, 44(1), 1320-1325.
- Akshay Maruti Narad, & Mahesh P. Joshi. (2020). Experimental analysis of CI engine using titanium oxide and aluminum oxide alloy coated piston fuelled with biofuel made up of agricultural waste. *Results in Materials*, 8, 100140.

- Ali Şanlı, İlker Turgut Yılmaz, & Metin Gümüş. (2021). Investigation of combustion and emission characteristics in a TBC diesel engine fuelled with CH₄-CO₂-H₂ mixtures. *International Journal of Hydrogen Energy*, 46(47), 24395-24409.
- Aydin, S., Sayin, C., Aydin, H. (2015). Investigation of the usability of biodiesel obtained from residual frying oil in a diesel engine with thermal barrier coating. *Applied Thermal Engineering*, 80, 212-219.
- Aydin, H. (2013). Combined effects of thermal barrier coating and blending with diesel fuel on usability of vegetable oils in diesel engines. *Applied Thermal Engineering*, 51, 623-629.
- Ayat, Gharehghania, Hossein, & Pourrahmani. (2019). Performance evaluation of diesel engines (PEDE) for a diesel-biodiesel fueled CI engine using nano-particles additive. *Energy Conversion and Management*, 198, 111921.
- A. J. Modi & D. C. Gosai. (2010). Experimental Study on Thermal Barrier Coated Diesel Engine Performance with Blends of Diesel and Palm Biodiesel. *SAE International*, 1519.
- Behçet, R., Oktay, H., Çakmak, A. & Aydın, H. (2015). Comparison of exhaust emissions of biodiesel-diesel fuel blends produced from animal fats. *Renewable and Sustainable Energy Review*, 46, 157 – 165.
- Buyukkaya, E. (2010). Effects of biodiesel on a DI diesel engine performance, emissions and combustion characteristics. *Fuel*, 89, 3099 – 3105.
- Behçet, R. et al. (2015). Comparison of exhaust emissions of biodiesel-diesel fuel blends produced from animal fats. *Renewable and Sustainable Energy Reviews. Elsevier*, 46, 157-165.
- Buyukkaya, E. (2010). Effects of biodiesel on a di diesel engine performance, emission and combustion characteristics. *Fuel Elsevier Ltd*, 89(10), 3099–3105.

- Bahattin İŞCAN. (2016). Application of ceramic coating for improving the usage of cottonseed oil in a diesel engine. *Journal of the Energy Institute*, 89(1), 150-157.
- BloombergNEF (BNEF), 2019. *Better Batteries*.
- Cerit, M., & Coban, M. (2014). Temperature and thermal stress analyses of a ceramic-coated aluminum alloy piston used in a diesel engine. *International Journal of Thermal Sciences*, 77, 11-18.
- Clarke, D.R., Oechner, M. & Padture, N.P. (October 2012). Thermal-barrier coatings for more efficient gas-turbine engines. *MRS Bulletin*, 37, 10.
- Charles E. Baukal, Jr. 2014. The John Zink Hamworthy Combustion Handbook, Second Edition. *CRC Press, Tulsa*, 1184.
- C.P. Abdul Gafoor, & Rajesh Gupta. (2015). Numerical investigation of piston bowl geometry and swirl ratio on emission from diesel engines. *Energy Conversion and Management*, 101, 541-551.
- da Silva, M.A.V., Ferreira, B.L.G., Marques, L.G. d. C., Murta, A. L. S. & de Freitas, M. A. V. (2017). Comparative study on NO_x emissions of biodiesel-diesel blends from soybean, palm and waste frying oils using methyl and ethyl transesterification routes. *Fuel*, 194, 144-156.
- Devarajan, Y., Munuswamy, D. B., Mahalingam, A. & Arunkumar, T. (2018). Combustion, performance and emission study of a research diesel engine fueled with palm oil biodiesel and its additive. *Energy Fuel*, 32, 8447 – 8452.
- Devarajan, Y., Munuswamy, D. B., Mahalingam, A. & Nagappan, B. (2017). Performance, combustion and emission analysis of pure palm oil biodiesel and higher alcohol blends in a diesel engine. *Energy Fuel*, 31 (12), 13796 – 13801.
- Demirbas, A. (2007). Progress and recent trends in biofuels. *Progress in Energy and Combustion Science*, 33(1), 1–18.

- Dhinesh B, Maria Ambrose Raj Y, Kalaiselvan C & KrishnaMoorthy R. (2018). A numerical and experimental assessment of a coated diesel engine powered by high- performance nano biofuel. *Energy Convers Manag*, 171, 815-824.
- Dhinesh, B, Bharathi, RN, Lalvani, JIJR, Parthasarathy, M & Annamalai, K. (2017). An experimental analysis on the influence of fuel borne additives on the single cylinder diesel engine powered by *Cymbopogon flexuosus* biofuel. *Journal of the Energy Institute*, 90 (4), 634-645.
- Daniel Monzon, Augusto Kinbaum, Rodolfo Guzman, Stephen Rogers, & Alexandre Lavelle. (2018). The Oil Company of the Future. World Energy Council (WEC), 2019. New Hydrogen Economy – Hope or Hype? World Bank. Carbon Pricing Dashboard.
- Engin Özçelik, A., Aydoğan, H. & Acaroğlu, M. (2015). Determining the performance, emission and combustion properties of camelina biodiesel blends. *Energy Conversion and Management*, 96, 47 – 57.
- Ekrem Buyukkaya. (2008). Thermal analysis of functionally graded coating AlSi alloy and steel pistons. *Surface and Coatings Technology*, 202(16), 3856-3865.
- Ekrem Buyukkaya, & Muhammet Cerit. (2007). Thermal analysis of a ceramic coating diesel engine piston using 3-D finite element method. *Surface and Coatings Technology*, 202(2), 398-402.
- Elumalai, P.V., Annamalai, K., & Dhinesh, B. (2019). Effects of thermal barrier coating on the performance, combustion and emission of DI diesel engine powered by biofuel oil–water emulsion. *J Therm Anal Calorim* 137, 593-605.
- Focus Applied Technologies, 2017. Standard Procedure for Dyno Test, 2017.
- Gad, M.S., El-Araby, R., Abed, K.A., El-Ibiari, N.N., El Morsi, A.K. & El-Diwani, G.I. (2018). Performance and emissions characteristics of C.I. engine fueled with palm oil/palm oil methyl ester blended with diesel fuel. *Egyptian Journal of Petroleum*, 27 (2), 215 – 219.
- Ganapathy, T., Gakkhar, R. P. & Murugesan, K. (2011). Influence of injection timing on performance, combustion and emission characteristics of *Jatropha* biodiesel engine. *Applied Energy. Elsevier Ltd*, 88(12), 4376–4386.

- G. Vidyasagar Reddy, R.L. Krupakaran, Hariprasad Tarigonda, D. Raghurami Reddy, & N. Govindha Rasu. (2021). Energy balance and emission analysis on diesel engine using different thermal barrier coated pistons. *Materials Today: Proceedings*, 43(1), 646-654.
- G. G. Sivakumar, & S. Senthil Kumar. (2014). Investigation on effect of Yttria Stabilized Zirconia coated piston crown on performance and emission characteristics of a diesel engine. *Alexandria Engineering Journal*, 53(4), 787-794.
- Gnanamoorthi Venkadesan, & Jayaram Muthusamy. (2019). Experimental investigation of $\text{Al}_2\text{O}_3/8\text{YSZ}$ and $\text{CeO}_2/8\text{YSZ}$ plasma sprayed thermal barrier coating on diesel engine. *Ceramics International*, 45(3), 3166-3176.
- Godiganur VS, Nayaka S & Kumar GN. (2021). Thermal barrier coating for diesel engine application. A review. *Mater Today Proc*, 45, 133–7.
- Hasimuglu, C., Ciniviz, M., Özsert, I., Icingür, Y., Parlak, A. & Salman, M.S. (2008). Performance characteristics of a low heat rejection diesel engine operating with biodiesel. *Renewable Energy*, 33, 1709 – 1715.
- Hazar, H. (2011). Characterization and effect of using cotton methyl ester as fuel in a LHR engine diesel. *Energy Conversion and Management*, 52 (1), 258 – 263.
- Haşimoğlu, C. et al. (2008). Performance characteristics of a low heat rejection diesel engine operating with biodiesel. *Renewable Energy*, 33(7), 1709–1715.
- Hazar, H. (2010). Characterization of MoN coatings for pistons in a diesel engine. *Materials and Design. Elsevier Ltd*, 31(1), 624–627.
- Heywood, J. B. (1988). *Internal combustion engine fundamentals*. New York: Mcgraw-hill.
- Hossain, A. K. & Davies, P. A. (2010). Plant oils as fuels for compression ignition engines: A technical review and life-cycle analysis. *Renewable Energy. Elsevier Ltd*, 35(1), 1–13.

- H.R. Amriya Tasneem, K.P. Ravikumar, H.V. Ramakrishna, & B. Kuldeep. (2021). Ceramic Material for Thermal Barrier Coatings in Compression Ignition Engine for its Performance Evaluation with Biodiesel. *Materials Today: Proceedings*, 46(17), 7745-7751.
- Hoseinia, S.S., Najafia, G., Ghobadiana, B., Ebadia, M.T., Mamat, T., Yusaf, T. (2020). Performance and emission characteristics of a CI engine using graphene oxide (GO) nano-particles additives in biodiesel-diesel blends. *Renewable Energy*, 145, 458-465.
- Iscan, B. (2016). Applications of ceramic coating for improving the usage of cottonseed oil in a diesel engine. *Journal of the Energy Institute*, 89, 150-157.
- Işcan, B. (2016). Application of ceramic coating for improving the usage of cottonseed oil in a diesel engine. *Journal of the Energy Institute*, 89(1), 150–157.
- Imdat Taymaz. (2007). The effect of thermal barrier coatings on diesel engine performance. *Surface and Coatings Technology*, 201(9–11), 5249-5252.
- International; Energy Agency (IEA), 2019. Oil 2019. Analysis & Forecast to 2024. Organisation of Petroleum Exporting Countries (OPEC), 2019, World Oil Outlook 2040, BP, 2019. BP Energy Outlook Technical Intelligence, 2019. TI Analysis.
- Johari, A., Nyakuma, B.B., Mohd Nor, S.H., Mat, R., Hashim, H., Ahmad, A., Zakaria, Z.Y. & Tuan Abdullah, T.A. (2015). The challenges and prospects of palm oil biodiesel in Malaysia. *Energy*, 81, 255 – 261.
- Johari, A. et al. (2015). The challenges and prospects of palm oil based biodiesel in Malaysia. *Energy. Elsevier*, 81, 255–261.
- Jai Kumar Sharma, Ritu Raj, Sateesh Kumar, Ratan Kumar Jain, & Mukesh Pandey. (2021). Finite element modelling of Lanthanum Cerate ($\text{La}_2\text{Ce}_2\text{O}_7$) coated piston used in a diesel engine. *Case Studies in Thermal Engineering*, 25, 100865.
- Jami Paparao, Krishna Kumar Pandey, & S. Murugan. (2021). Experimental studies on the effect of TBC piston in a dual-fueled diesel engine. *Fuel*, 306, 121700.

- J Hemanandh, K.V. Narayanan, Kondraganti Venkatesh, K. Rahul Sai Balaji, Lokireddy Charan & Tejeswar Reddy. (2018). Comparative Analysis of Stellite-6 Coated and Uncoated Piston using Pongamia Biodiesel. *Materials Today: Proceedings*, 5(11), 24323-24329.
- Janardhan, N., Krishna, M., Ushasri, P., Murthy & P.V.K. (2013). Control of exhaust emissions of jatropha oil in crude form and biodiesel from high grade low heat rejection diesel engine. *Int. J. Mech. Prod. Eng. Res. Dev.* 3, 199-212.
- Janakiraman, S., Lakshmanan, T., Chandran, V, & Lingesan, Subramani. (2020). Comparative behavior of various nano additives in a DIESEL engine powered by novel Garcinia gummi-gutta biodiesel. *Journal of Cleaner Production*, 245, 118940.
- Karthickeyan, V., Balamurugan, P. & Senthil, R. (2017). Environmental effects of thermal barrier coating with waste cooking palm oil methyl ester blends in a diesel engine. *Biofuels*, 10(2), 227 – 220.
- Karthickeyan, V. & Balamurugan, P. (2017). Effect of thermal barrier coating with various blends of pumpkin seed oil methyl ester in DI diesel engine. *Heat Mass Transfer*, 53, 3141 – 3154.
- Krishnamoorthi, T. & Vinayagasundram, G. (2019). Performance and emission characteristics analysis of thermal barrier coated diesel engine using palm biodiesel. *Environmental Science and Pollution Research*, 26 (11), 11438 – 11451.
- Karthickeyan, V. & Balamurugan, P. (2017). Effect of thermal barrier coating with various blends of pumpkin seed oil methyl ester in DI diesel engine', Heat and Mass Transfer/Waerme- und Stoffuebertragung. *Heat and Mass Transfer*, 53(10), 3141–3154.
- Krishna, M. V. S. M. et al. (2016). Experimental investigations on direct injection diesel engine with ceramic coated combustion chamber with carbureted alcohols and crude jatropha oil. *Renewable and Sustainable Energy Reviews. Elsevier*, 53, 606–628.
- Kumar, N., Varun & Chauhan, S. R. (2015). Evaluation of endurance characteristics for a modified diesel engine runs on jatropha biodiesel. *Applied Energy. Elsevier Ltd*, 155, 253–269.

- K. Manjunatha, Hiregoudar Yerrennagoudaru, KG. Prakash, Suhas Bhat, Shadab Khan, & Mohammed Saifuddin. (2021). Investigation of effect of ceramic material over which platinum coated piston crown and alcohols mixed with vegetable oils and its performance evaluation in Twin cylinder CRDI diesel engine. *Materials Today: Proceedings*.
- Karthickeyan Viswanathan, Wei Wu, Muhammad Ikhsan Taipabu, & Walairat Chandra-Ambhorn. (2021). Effects of antioxidant and ceramic coating on performance enhancement and emission reduction of a diesel engine fueled by Annona oil biodiesel. *Journal of the Taiwan Institute of Chemical Engineers*, 125, 243-256.
- Karthickeyan V. (2018). Effect of thermal barrier coating on performance and emission characteristics of kapok oil methyl ester in diesel engine. *Australian Journal of Mechanical Engineering*, 18(3), 467-480.
- Karthickeyan V. (2018). Experimental analysis on thermally coated diesel engine with neem oil methyl ester and its blends. *Heat Mass Transfer*, 54, 1961-1974.
- Karthickeyan V. (2019). Effect of cetane enhancer on Moringa oleifera biodiesel in a thermal coated direct injection diesel engine. *Fuel*, 235, 538-550.
- Karthickeyana, V., Thiyagarajan, S., Ashok, B., Edwin Geob, V., & Azadd, A.V. (2020). Experimental investigation of pomegranate oil methyl ester in ceramic coated engine at different operating condition in direct injection diesel engine with energy and exergy analysis. *Energy Conversion and Management*. 205, 112334.
- Kumaravel, S.V., Murugesan, A., Vijayakumar, C., & Thenmozhi, M. (2019). Enhancing the fuel properties of tyre oil diesel blends by doping nano additives for green environments. *Journal of Cleaner Production*, 240, 118128.
- List of GHGs and their global warming potential (source: Table TS2 page 33-34. Climate change 20017. The physical Sciences. Working Group 1 Contribution to the Fourth Assessment Report of the Intergovernmental Panel on Climate Changes).
- Mahalingam, A., Munuswamy, D., Devarajan, Y. & Radhakrishnan, S. (2018). Investigation on the emission reduction technique in acetone-biodiesel aspirated diesel engine. *Journal of Oil Palm Research*, 30(2), 345 – 349.

- MohamedMusthafa, M., Sivapiraksam, S.P. & Udayakumar, M. (2010). A comparative evaluation of Al₂O₃ coated low heat rejection diesel engine performance and emission characteristics using fuel as rice bran and pongamia methyl ester. *Journal of renewable and sustainable energy*, 2, 053105-1 – 053105-15.
- MohamedMusthafa, M., Sivapirakasam, S.P. & Udayakumar, M. (2011). Comparative studies on fly ash coated low heat rejection diesel engine on performance and emission characteristics fueled by rice bran and pongamia methyl ester and their blend with diesel. *Energy*, 36, 2343 – 2351.
- Murali Krishna, M.V.S., Ohm Prakash, T., Ushasri, P., Janardhan, N. & Murthy, P.V.K. (2016). Experimental investigation on direct injection diesel engine with ceramic coated combustion chamber with carbureted alcohols and crude jatropa oil. *Renewable and Sustainable Energy Reviews*, 53, 606-628.
- Masera, K. and Hossain, A. K. (2019). Combustion Characteristics of Cottonseed Biodiesel and Chicken Fat Biodiesel Mixture in a Multi-Cylinder Compression Ignition Engine. *SAE Technical Papers*, 1–14.
- Mohamed Musthafa, M. (2016). Synthetic lubrication oil influences on performance and emission characteristic of coated diesel engine fuelled by biodiesel blends. *Applied Thermal Engineering. Elsevier Ltd*, 96, 607–612.
- Mohamed Musthafa, M. (2019). A comparative study on coated and uncoated diesel engine performance and emissions running on dual fuel (LPG – biodiesel) with and without additive. *Industrial Crops and Products. Elsevier*, 128(x), 194–198.
- Manoj Babu, C.G. Saravanan, M. Vikneswaran, V. Edwin Geo, J. Sasikala, J.S. Femilda Josephin, & Debasish Das. (2021). Analysis of performance, emission, combustion and endoscopic visualization of micro-arc oxidation piston coated SI engine fuelled with low carbon biofuel blends. *Fuel*, 285, 119189.
- M. Kalyana Kumar, & P.D. Sudersanan. (2021). A study on thermomechanical properties of zirconium di oxide coated piston material of various thickness and its comparison with uncoated material. *Materials Today: Proceedings, Volume 45(1)*, 294-298.

- Muhammet Cerit, & Mehmet Coban. (2014). Temperature and thermal stress analyses of a ceramic-coated aluminum alloy piston used in a diesel engine. *International Journal of Thermal Sciences*, 77, 11-18.
- Mohanraj Shanmugam, S. Sathiyamurthy, G. Rajkumar, S. Saravanakumar, S. Tamil Prabakaran, & V.S. Shaisundaram. (2021). Effect of thermal Barrier coating in CI engines fueled with Citrus Medica (Citron) peel oil biodiesel dosed with cerium oxide nanoparticle. *Materials Today: Proceedings*, 37(2), 1943-1956.
- Mohamed Abbas, S., & Elayaperumal, A. (2019). Experimental investigation on the effect of ceramic coating on engine performance and emission characteristics for cleaner production. *Journal of Cleaner Production*, 214, 506-513.
- Mohamed Musthafa, M. (2019). A comparative study on coated and uncoated diesel engine performance and emissions running on dual fuel (LPG – biodiesel) with and without additive. *Industrial Crops and Products*, 128, 194-198.
- Mangesh, VL, Padmanabhan, S, Tamizhdurai, P, Narayanan, S, & Ramesh, A.(2020). Combustion and emission analysis of hydrogenated waste polypropylene pyrolysis oil blended with diesel. *Journal of Hazardous Materials*, 386, 121453.
- M.G. Gok, G. Goller. (2019). State of the Art of Gadolinium Zirconate Based Thermal Barrier Coatings: Design, Processing and Characterization. *IntechOpen, London-United Kingdom*, 1-23.
- M.M. Dokur, G. Goller. (2014). Processing and characterization of CYSZ/Al₂O₃ and CYSZ/Al₂O₃+YSZ multilayered thermal barrier coatings. *Surface and Coatings Technology*, 258, 804-813.
- M.G. Gok, G. Goller. (2016). Production and characterisation of GZ/CYSZ alternative thermal barrier coatings with multilayered and functionally graded designs. *Journal of the European Ceramic Society*, 36 (7), 1755-1764.
- Ömer Cihan, İlker Temizer, Mustafa Güven Gök, & Muhammet Karabaş. (2020). Investigation of the effect of rare earth doped La₂Zr₂O₇ based thermal barrier coating on performance and combustion characteristics of DI diesel engine. *Surface and Coatings Technology*, 403, 126437.

- Öztürk, U., Hazar, H. & Yilmaz, F. (2019). Comparative performance and emission characteristics of peanut seed oil methyl ester (PSME) on thermal isolated diesel engine. *Energy*, 167, 260 -268.
- Oguma, M., Lee, Y. J., & Goto, S. (2011). An overview of biodiesel in Asian countries and the harmonization of quality standards. *International Journal of Automotive Technology*, 13(1), 33–41.
- Ozturk U, Hazar H, & Yılmaz F. (2019). Comparative performance and emission characteristics of peanut seed oil methyl ester (PSME) on a thermal isolated diesel engine. *Energy*, 8, 167-260.
- Oerlikon Metco. (2014). Material product data sheet; Premium EBC-grade aluminium silicate (mullite) powder [brochure]. *Oerlikon Metco: Westbury, NY, USA*.
- Oerlikon Metco. (2014). Material product data sheet; 8% Yttria Stabilized Zirconia Agglomerated and HOSP™ thermal spray powders [brochure]. *Oerlikon Metco: Westbury, NY, USA*.
- Pandian, A.K., Ramakrisnan, R.B.B. & Devarajan, Y. (2017). Emission analysis on the effect of nanoparticles on pure biodiesel in unmodified diesel engine. *Environmental Science and Pollution Research*, 24(29), 23273 – 23278.
- Prabhakar, M. & Rajan, K. (2013) .Performance and combustion characteristics of a diesel engine with titanium oxide coated piston using Pongamia methyl ester. *Journal of Mechanical Science and Technology*, 27(5), 1519–1526.
- Parvati Ramaswamy, V. Shankar, V.R. Reghu, Nikhil Mathew, & S. Manoj Kumar. (2018). A Model to Predict the Influence of Inconsistencies in Thermal Barrier Coating (TBC) Thicknesses in Pistons of IC Engines. *Materials Today: Proceedings*, 5(5), 12623-12631.
- Ping Wang, Jianping Li, Yongchun Guo, Jianli Wang, Zhong Yang, & Minxian Liang. (2016). Effect of zirconia sol on the microstructures and thermal-protective properties of PEO coating on a cast Al–12Si piston alloy. *Journal of Alloys and Compounds*, 657, 703-710.

- P. Balu, P. Saravanan, & V. Jayaseelan. (2021). Effect of ceramic coating on the performance, emission, and combustion characteristics of ethanol DI diesel engine. *Materials Today: Proceedings*, 39(4), 1259-1264.
- P.V. Elumalai, Dhinesh Balasubramanian, M. Parthasarathy, A.R. Pradeepkumar, S. Mohamed Iqbal, J. Jayakar, & M. Nambiraj. (2021). An experimental study on harmful pollution reduction technique in low heat rejection engine fuelled with blends of pre-heated linseed oil and nano additive. *Journal of Cleaner Production*, 283, 124617.
- Prabhakar, M., & Rajan, K. (2013). Performance and combustion characteristics of a diesel engine with titanium oxide coated piston using Pongamia methyl ester. *J Mech Sci Technol* 27, 1519-1526.
- Perumala, Varatharaju & Ilangkumara, M. (2018). The influence of copper oxide nano particle added pongamia methyl ester biodiesel on the performance, combustion and emission of a diesel engine. *Fuel*, 232, 791-802.
- Rahiman M.K, Venkatachalam R. & Nedunchezian N. (2013). Experimental investigation on thermal barrier coated diesel engine fueled with diesel-biodiesel-ethanol-diethyl ether blends. *Journal of Renewable and Sustainable Energy*, 5(3).
- Rashed, M.M., Kalam, M.A., Masjuki, H.H., Mofijur, M., Rasul, M.G. & Zulkifli N.W.M (2016). Performance and emission characteristics of a diesel engine fueled with palm, jatropha, and moringa oil methyl ester. *Industrial Crops and Products*, 79, 70-76.
- Ramalingam, S., Rajendran, S. & Ganesan, P. (2016). Performance improvement and emission control in a direct injection diesel engine using nano catalyst coated pistons. *Biofuels. Taylor & Francis*, 7(5), 529–535.
- R. Thirunavukkarasu, M. Mahendran, R. Tamilselvan, & S. Periyasamy. (2018). Investigation on Single, Four And Five Holes Fuel Injector Nozzle on Performance And Emission Characteristic of Diesel on A VCR Engine by Using Ceramic Coating Material on The Piston Crown. *Materials Today: Proceedings*, 5(2), 7577-7585.
- Senthikumar, S., Sivakumar, G. & Manoharan, S. (2015). Investigation of palm methyl ester biodiesel with additive on performance and emission characteristics of a diesel engine under 8 mode testing cycle. *Alexandria Engineering Journal*, 54(3), 423 – 428.

- Senthil, R., Sivakumar, E., Silambarasan, R., & Pranesh, G. (2016). Performance and emission characteristics of using sea lemon biodiesel with thermal barrier coating in a direct-injection diesel engine. *Biofuels*, 8(2), 235–241.
- Sivakumar, G. & Senthil Kumar, S. (2014). Investigation on effect of Ytria Stabilized Zirconia coated piston crown on performance and emission characteristics of a diesel engine. *Alexandria Engineering Journal*, 53, 787-794.
- Sakthivel, A., Selvakumar, P. & Gopalakrishnan, A. (2014). Effect of mineral deposition on shrimp *litopenaeus vannamei* in high alkaline water of pennar river, Andhra Pradesh of southeast coast of India. *Journal of Aquaculture Research and Development*, 5(4), 5–10.
- Sharon, H. et al. (2012). A test on DI diesel engine fueled with methyl esters of used palm oil. *Renewable Energy. Elsevier Ltd*, 47, 160–166.
- Sabino Caputo, Federico Millo, Giulio Boccoardo, Andrea Piano, Giancarlo Cifali & Francesco Concetto Pesce, (2019). Numerical and experimental investigation of a piston thermal barrier coating for an automotive diesel engine application. *Applied Thermal Engineering*, 162. 1359-4311.
- S. Prakash, M. Prabhahar, O.P. Niyas, Safavanul Faris, & C. Vyshnav. (2020). Thermal barrier coating on IC engine piston to improve efficiency using dual fuel. *Materials Today: Proceedings*, 33 (1), 919-924.
- S. Mohamed Abbas, A. Elayaperumal, & G. Suresh. (2021). A study on combustion and performance characteristics of ceramic coated (PSZ/Al₂O₃) and uncoated piston – D.I engine. *Materials Today: Proceedings*, 45(2), 1328-1333.
- S. Aravindha Balaji, S. Lakshmana kumar, & S.N. Saranya. (2020). Study of combustion characteristics on single cylinder direct injection diesel engine with plasma and HVOF coated ceramic powders on piston crown. *Materials Today: Proceedings*, 33(1), 989-994.
- S. Saravanan, C. Ramesh Kumar, Arivalagan Pugazhendhi, & Kathirvel Brindhadevi. (2020). Role of thermal barrier coating and porous medium combustor for a diesel engine: An experimental study. *Fuel*, 280, 118597.

- Salih Özer, Erdinç Vural, & Serkan Özel. (2021). Effects of fuel oil use in a thermal coated engine. *Fuel*, 306, 121716.
- S. Mohamed Abbas, & A. Elayaperumal. (2019). Experimental investigation on the effect of ceramic coating on engine performance and emission characteristics for cleaner production. *Journal of Cleaner Production*, 214, 506-513.
- Serkan Özel, Erdinç Vural, & Murat Binici. (2020). Optimization of the effect of thermal barrier coating (TBC) on diesel engine performance by Taguchi method. *Fuel*, 263, 116537.
- S. Vedharaj, R. Vallinayagam, W.M. Yang, S.K. Chou, K.J.E. Chua, & P.S. Lee. (2014). Experimental and finite element analysis of a coated diesel engine fueled by cashew nut shell liquid biodiesel. *Experimental Thermal and Fluid Science*, 53, 259-268.
- Selman Aydin, Cenk Sayin, & Hüseyin Aydin. (2015). Investigation of the usability of biodiesel obtained from residual frying oil in a diesel engine with thermal barrier coating. *Applied Thermal Engineering*, 80, 212-219.
- Suresh, G., Kamath, H.C., & Banapurmath, N.R. (2014). Studies on the use of low-volatile non-edible oils in a thermal barrier-coated diesel engine. *International Journal of Sustainable Engineering*, 7(4), 341-351.
- Srithar, K.K., Arun, Balasubramanian, Vivar, M., & Skryabin, I. (2013). An Experimental Investigation on Diesel and Low Heat Rejection Engines with Dual Biodiesel Blends. *International Journal of Green Energy*, 10(10), 1041-1055.
- Syed Aalam, C. (2020). Investigation on the combustion and emission characteristics of RDI diesel engine fuelled with nano Al_2O_3 and Fe_3O_4 particles blended biodiesel, Materials. *Today: Proceedings*, 33, 2540-2546.
- S. Ahmaniemi, P. Vuoristo, T. Mantyla, F. Cernuschi, & L. Lorenzoni. (2004) Modified thick thermal barrier coatings: Thermophysical characterization. *Journal of the European Ceramic Society*, 24(9), 2669-2679.
- Schalk Cloete. (2019). International Energy Agency (IEA). World Energy Outlook 2019. An Independent Global Energy Forecast to 2050, to compare with the IEA's.

- Thiruselvam, K. & Ganesh, V. (2019). Performance and emission of diesel engine using thermal barrier coating and addition of cerium oxide nanoparticles to palm biodiesel. *Journal of Oil Palm Research*, 31(1), 138 – 145.
- Traon, N., Schnieder, J., Vilalba, A., Tonnesen, T., Telle, R., Huger, M. & Chotard, T. (2014). Influence of Andalusite, $\text{Al}_2\text{O}_3\cdot\text{ZrO}_2\cdot\text{SiO}_2$ and $\text{Al}_2\text{O}_3\cdot\text{ZrO}_2$ Addition on Elastic and Mechanical Properties of High Aluminum Castables. *Interceram-Refractories Manual II/2014*.
- Tüccar, G., Tosun, E., Özgür, T. & Aydın, K. (2014). Diesel engine emissions and performance from blends of citrus sinesis biodiesel and diesel fuel. *Fuel*, 132, 7 -11.
- T. Fukuchi, N. Fuse, T. Fujii, M. Okada, K. Fukunaga, & M. Mizuno. (2013). Measurement of topcoat thickness of thermal barrier coating for gas turbines using terahertz waves. *Electrical Engineering in Japan (English Translation of Denki Gakkai Ronbunshi)*, 183(4), 166-172.
- V.R. Reghu, Nikhil Mathew, Pramod Tilleti, V. Shankar, & Parvati Ramaswamy. (2020). Thermal Barrier Coating Development on Automobile Piston Material (Al-Si alloy). *Numerical Analysis and Validation*, 22, (4), 1274-1284.
- V.R Reghu, V Shankar, & Parvati Ramaswamy. (2018). Challenges in Plasma Spraying of 8% $\text{Y}_2\text{O}_3\text{-ZrO}_2$ Thermal Barrier Coatings on Al Alloy Automotive Piston and Influence of Vibration and Thermal Fatigue on Coating Characteristics, *Materials Today: Proceedings*, 5(11), 23927-23936.
- V. Dananjayakumar, Mallesh B. Sanjeevannavar, Shailesh M. Golabhanvi, & M.A. Kamoji. (2021). Experimental analysis of CI engine using zirconia ceramic powder coated piston fuelled with Karanja biodiesel. *Materials Today: Proceedings*, 42(2), 1387-1392.
- V. Dananjayakumar, Mallesh B. Sanjeevannavar, Shailesh M. Golabhanvi, & M.A. Kamoji. (2021). Experimental analysis of CI engine using zirconia ceramic powder coated piston fuelled with Karanja biodiesel. *Materials Today: Proceedings*, 42(2), 1387-1392.

- V. Dattatreya, B.R. Ramesh Babu, & B. Durga Prasad. (2019). Study of Combustion Characteristics on Single Cylinder Direct Injection Diesel Engine with Plasma and HVOF Coated Ceramic Powders on Piston Crown. *Materials Today: Proceedings*, 16(2), 621-628.
- V.R. Reghu, Kevin Lobo, Arhan Basha, Pramod Tilleti, V. Shankar, & Parvati Ramaswamy. (2019). Protection offered by thermal barrier coatings to Al-Si alloys at high temperatures – A microstructural investigation. *Materials Today: Proceedings*, 19(2), 676-681.
- Viswanathan K, Balasubramanian D, Subramanian T, & Varuvel EG. (2019). Investigating the combined effect of thermal barrier coating and antioxidants on pine oil in DI diesel engine. *Environ Sci Pollut*, 26, 15573-15599.
- Wang, P., Li, Y., Guo, Y., Wang, J., Yang, Z. & Liang, M. (2016). Effect of zirconia sol on the microstructure and thermal-protective properties of PEO coating on a cast Al-12Si piston alloy. *Journal of Alloys and Compounds*, 657, 703-710.
- Wang, P. et al. (2016). Effect of zirconia sol on the microstructures and thermal-protective properties of PEO coating on a cast Al-12Si piston alloy. *Journal of Alloys and Compounds. Elsevier B.V*, 657, 703–710.
- Wellington Uczak de Goes, Nicolaie Markocsan, Mohit Gupta, Robert Vaßen, Taishi Matsushita, & Kseniya Illkova. (2020). Thermal barrier coatings with novel architectures for diesel engine applications. *Surface and Coatings Technology*, 396, 125950.
- World Energy Outlook 2020, International Energy Agency (IEA), Petronas Internal Analysis.
- World Energy Council (WEC), 2019. World Energy Trilemma Index 2019.
- Yilmaz, I. T. & Gumus, M. (2017). Investigation of the effect of biogas on combustion and emissions of TBC diesel engine. *Fuel. Elsevier Ltd*, 188, 69–78.

Zhimin Yao, Kunsheng Hu, & Rong Li. (2019). Enhanced high-temperature thermal fatigue property of aluminum alloy piston with Nano PYSZ thermal barrier coatings. *Journal of Alloys and Compounds*, 790, 466-479.

Zhimin Yao, & Wengui Li. (2020). Microstructure and thermal analysis of APS nano PYSZ coated aluminum alloy piston. *Journal of Alloys and Compounds*, 812, 152162.

Zhimin Yao, & Zuoqin Qian. (2018). Thermal analysis of Nano ceramic coated piston used in natural gas engine. *Journal of Alloys and Compounds*, 768, 441-450.

Ziming Yan, Brian Gainey, James Gohn, Deivanayagam Hariharan, John Saputo, Carl Schmidt, Felipe Caliari, Sanjay Sampath, & Benjamin Lawler. (2021). A comprehensive experimental investigation of low-temperature combustion with thick thermal barrier coatings. *Energy*, 222, 119954.

Universiti Malaysia